Double (Iron and Zinc) Fortified Black Tea: Assessing the Bioaccessibility and Bioavailability using Spray Drying Microencapsulation Technology

by

Alejandro Leiva Arrieta

A THESIS SUBMITTED IN PARTIAL FULFILLMENT OF

THE REQUIREMENTS FOR THE DEGREE OF

MASTER OF SCIENCE

in

THE FACULTY OF GRADUATE AND POSTDOCTORAL STUDIES

(Food Science)

THE UNIVERSITY OF BRITISH COLUMBIA

(Vancouver)

October 2020

The following individuals certify that they have read, and recommend to the Faculty of Graduate and Postdoctoral Studies for acceptance, a thesis entitled:

Double (Iron and Zinc) Fortified Black Tea: Assessing the Bioaccessibility and Bioavailability using Spray Drying Microencapsulation Technology

submitted by Jorge Alejandro Leiva Arrieta in partial fulfillment of the requirements for the degree of Master of Science in Food Science

Examining Committee:

Dr. Anubhav Pratap-Singh, Assistant Professor, Food Science
Supervisor

Dr. Yvonne Lamers, Associate Professor, Human Nutrition
Supervisory Committee Member

Dr. David Kitts, Associate Dean, Food Science
Supervisory Committee Member

Dr. Feng Jiang, Assistant Professor, Wood Science
Additional Examiner

Abstract

Fortification of black tea with iron and zinc has the potential to reduce the prevalence of iron and zinc deficiency in the developing world. Tea is an ideal vehicle for food fortification because it is the second most consumed beverage globally, aside from water, and is consumed throughout the world independent of socioeconomic strata. Unfortunately, polyphenolic compounds present in tea form complexes with iron, which cause colour changes. The formation of this intensely blue-purple non-bioavailable iron-polyphenol complex is a barrier to consumer acceptance and the public health effectiveness of iron-fortified tea.

The objective of this study was to develop and assess the fortification of tea with microencapsulated iron and zinc to increase their absorption, and that could prevent the formation of the iron-polyphenol complex in tea. Whey protein isolate and Eudraguard® that either provide gastric and intestinal protection and increase bioaccessibility of iron and zinc in the human body, were used as coating materials for the development of the microencapsulated iron and zinc. A response surface design was used to optimize the encapsulation efficiency of iron and zinc in the microcapsules. The microcapsules were subjected through a simulated gastric and intestinal digestion, whereas the microcapsules showed higher resistance to intestinal conditions.

Absorption studies performed using a Caco-2 cell model revealed that the iron delivered through the microcapsules increased cellular absorption by 73%. Zinc from the microcapsules also increased cellular absorption by 81%. The iron-polyphenol complex is dependent on the pH, therefore, the use of MES and PIPES buffers was investigated for the measurement of the iron-polyphenol complex formation. The results show that MES buffer at 0.2M and pH 5.5 can be used

to quantify the iron-polyphenol complex in a polyphenolic model system (gallic acid), closely resembling tea. The prevention of the iron-polyphenol complex formation was further investigated with the microencapsulated iron and zinc using a gallic acid and brewed tea. The microcapsules slowed down the formation of iron-polyphenol complex in tea by 60% within 30 minutes of tea brewing. The results of this thesis have the potential to guide the path to reduce micronutrient deficiencies, through fortification of commonly consumed tea with iron and zinc.

Lay Summary

Tea is known and consumed by a large segment of the population, making tea the second most consumed beverage in the world. Overall, more than 2 billion people in the world are affected by iron and zinc micronutrient deficiency that can lead to a range of severe medical conditions and economic development impact. Iron and zinc deficiencies are also prevalent in developed nations like Canada, particularly in marginalized communities. Despite the benefits of tea, iron and zinc become unavailable for absorption by the human body when taken with a polyphenol-rich beverage such as tea. Therefore, this thesis was aimed at developing iron and zinc fortified tea using a microencapsulation technique in which it reduced the prevalence of iron and zinc from becoming unavailable for absorption. The results of this thesis help guide the development of a new food vehicle for fortification to prevent iron and zinc deficiencies in the world.

Preface

Iron and zinc content analysis was performed using equipment from the analytical chemistry laboratory from the Faculty of Chemistry, with training from Dr. Robin Stoodley and Christina Wong on using the atomic absorption spectroscopy. The iron and zinc content data analysis was done with guidance from Dr. Anubhav Pratap-Singh. Cell culture experiments performed in Chapter 3 were done with the help of Ph.D. candidate Yigong Guo. The rest of the literature review and experimental work in this thesis was designed and conducted by the author, Alejandro Leiva, under the guidance of Dr. Anubhav Pratap-Singh.

Part of Chapter 3 has been prepared for peer review submission. Leiva, A., & Singh, A.P. (2020). Release kinetics of microencapsulated iron and zinc using whey proteins and Eudraguard®

The studies in Chapter 2,3, and 4 have been prepared for peer review submission. Leiva, A., & Singh, A.P. (2020). Iron and zinc fortified tea: Development and *in-vitro* bioaccessibility and bioavailability assessment using gastrointestinal digestion and Caco-2 cells.

Table of Contents

List of Tables

List of Figures

List of Abbreviations

AAS	Atomic absorption spectroscopy
EE Fe	Encapsulation efficiency of iron
EE Zin	Encapsulation efficiency of zinc
FeS	Ferrous sulphate
GA	Gallic acid
GAE	Gallic acid equivalents
GRAS	Generally recognized as safe
mM	Millimolar
TF	Theaflavins
TR	Thearubigins
WPI	Whey protein isolate
ZnS	Zinc sulphate

Acknowledgements

First and foremost, I would like to thank my supervisor, Dr. Anubhav Pratap-Singh, for allowing me to pursue my studies and research at The University of British Columbia Food Processing Engineering Laboratory. I also thank Dr. Singh for his guidance and encouragement to perform high-quality scholastic work.

Secondly, I would like to thank my committee members, Dr. Yvonne Lamers and Dr. David Kitts, for their research and academic support. Their guidance helped me get unstuck in some parts of my research work.

I would also like to thank my lab members for their support. Thank you, Yigong Guo, for your help in the cell culture experiments. Thank you, Ronit Mandal, for your support in ordering supplies and reagents, so my experiments were never delayed. Above all, thank you, Philip Pui-Li Yen, for teaching me the inner works of academia, for providing a roadmap to success in graduate school, for helping me in some classwork and for keeping the lab organized and safe for all of us.

Also, I would like to thank Peter Hoffman for his support in operating and finding equipment and materials in FNH. Also, thank you, Barbara Wakal; it is very comforting to see someone smile after a long day at the lab.

Dedication

"*Not everyone decides to leave the comforts and safety of home*." This is what my father told me before I left Mexico to pursue a higher degree in Canada. The unknown and the unexpected is highly avoided by most people, including myself. Yet, I knew, and I still know that on the other side of the unknown lies infinite possibilities for growth.

Perhaps I was naive at first. I thought that it was not going to be that hard, so maybe I jumped blindly into the unknown. Around halfway into my degree, I seriously doubted my capabilities to the point where I was on the verge of giving it all up. The one and a half years of preparation to come to Canada and one year of research work. Most graduate students can relate to this experience, and we colloquially call it the 'holy crap stage.' On top of that, a new coronavirus emerged that disrupted all aspects of normal life. Will I ever finish?

If it wasn't for my parents moral and unconditional support, I do not think I could have. The support of my partner also deserves merit. I remember calling her frustrated one day after a series of failed experiments. She tried to comprehend what I was trying to do, and she sent me a protocol from one of her chemistry classes in high school. The protocol was of no use, but her intention made the whole difference to me.

It is not enough to say thank you to my parents and to all the people I met during these two years that remained in the good and the bad moments. Thank you to all my friends in Mexico and Canada. A special mention goes to my friend Omar and my friend Philip. Thank you to my mother and father for motivating me and for being an essential part of my personal growth. Life will never

be free of problems; the problems just change context. It all depends on the attitude that *you* decide to face them.

I hope that you, the reader, can learn something from my thesis or even guide you in some parts of your research work.

Overall, I am thankful I jumped blindly into the unknown.

Chapter 1: Introduction

1.1 Food Fortification to Decrease the Prevalence of Iron and Zinc Deficiencies

Micronutrient deficiencies are a significant global public health problem that can affect all age groups in both developed and developing countries; however, micronutrient deficiencies in the latter are far more severe. Depending on the micronutrient deficiency, it can cause a range of health disorders such as reduced brain development, decreased immunity against disease, poor pregnancy outcome, impaired work capacity, blindness, and in some cases, death (Venkatesh Mannar & Hurrell, 2018).

Iron is a micronutrient with essential functions in the human body such as oxygen transport, DNA synthesis and muscle metabolism. Iron deficiency is the leading cause of anemia, the most prevalent nutritional deficiency in the world, which affects 33% of non-pregnant women, 40% of pregnant women and 42% of children worldwide. In total, iron deficiency affects more than two billion people (Stoltzfus et al., 2018). Besides the high prevalence of this micronutrient deficiency, iron deficiency can have long-term side effects because iron deficiency in children under two years of age can have significant and irreversible effects on brain development, which can lead to negative consequences on learning and performance later in life (WHO, 2020).

Zinc is another essential micronutrient for the human body involved in growth and development, immune function, neurotransmission, vision, and reproduction systems. Zinc deficiency affects about one-third of the world's population (Branca et al., 2014), approximately 2.3 billion people.

Notably, zinc deficiency has been associated with impaired growth and development in children, pregnancy complications, and immune dysfunction (Maxfield & Crane, 2019).

Iron and zinc deficiencies mainly affect southeast Asian countries (WHO, 2020); India and Pakistan being the most affected. In these countries, women and children from economically stable households are often anemic, thus suggesting a problem with common cultural dietary patterns. Commonly, countries from this region share cultural practices involving vegetarianism and frequent fasting (Pratap-Singh et al., 2018). A diet that predominantly lacks animal sources and has a high quantity of phytates is known to affect iron and zinc absorption (Health Canada, 2018; Venkatesh Mannar & Hurrell, 2018; Zijp, Korver, M Tijburg, et al., 2000). Furthermore, iron deficiency leads to a decreased absorption of iodine and vitamin A, which adds to the burden of diseases caused by nutritional deficiencies (Diosady et al., 2002).

Iron and zinc deficiencies are readily preventable via three main strategies: medical supplementation, dietary diversification and food fortification (Akhtar et al., 2011; Allen et al., 2006). Medical supplementation is the periodic administration of pharmacological preparations in the form of injections, capsules, and tablets. Dietary diversification involves increasing the content of the micronutrient that is deficient through the daily diet. For example, in the case for iron and zinc, this involves consuming more animal foods, increasing green leafy vegetables that are rich in iron and consuming more fruits and vegetables rich in vitamin C. Finally, fortification is the addition of one or more micronutrients to a staple food or a food that is consumed by the majority of a population (Huma et al., 2007).

Out of the three prevention strategies, dietary diversification is preferred. However, it is challenging to implement because it requires that the target population is educated on nutrition. Essentially, the target population needs to change the daily foods they consume. It also requires a substantial amount of financial resources. Nonetheless, medical supplementation and fortification strategies have also been effective, yet they both have limitations. For example, the main challenge with medical supplementation is the often prohibitive cost of the supplements for low-income families, and the difficulty of maintaining a medical infrastructure that reaches nutritionally challenged communities in developing countries (Huma et al.,2007). Even in developed countries like Canada, an Evaluation of Health Canada's First Nations Health Facilities Program (2017) recognized limitations in the extent of health care outreach in remote Canadian communities (Galloway, 2017).

Food fortification is considered the best approach against micronutrient deficiencies because it is the most cost-effective strategy in the long term, and can be as effective as dietary diversification (Mehansho, 2006). Common foods that can be fortified, often referred to as food vehicles, include wheat and wheat products, maize, rice, milk and milk products, cooking oils, salt, sugar, and condiments or spices (Allen et al., 2006). However, food fortification requires effective distribution channels for the fortified food and proper selection of a food vehicle that is consumed by the majority of the target population. Also, the micronutrient that is used to fortify has to be well absorbed by the body, and that it does not change the sensory characteristics of the food vehicle (Huma et al., 2007) such as flavour or appearance. In food fortification strategies, iron and zinc fortification is of central focus, and fortification strategies have been successful.

1.2 Iron

Iron is a metal that exists in different oxidation forms from Fe^{6+} to Fe^{2+}; however, only oxidation states Fe^{3+} (ferric) and Fe^{2+} (ferrous) are found in food and in the human body. Iron in food is found in two distinct forms; heme and non-heme iron. Heme iron is iron found at the center of a porphyrin ring, while non-heme iron is mainly iron salts (See Section 1.2.6). Heme iron is found in the myoglobin and hemoglobin from animal meat products, accounting for 50% to 60% of the iron found in animal foods. The rest is non-heme iron. Non-heme iron is also found in dark green leafy vegetables. Some non-heme iron can be found in dairy products, although they are generally considered poor sources of non-heme iron due to their insufficient quantity of iron present (Hooda et al., 2014).

1.2.1 Iron in the Human Body

Iron is a mineral essential for human life. Its primary biological function is that of oxygen transport in hemoglobin and myoglobin. Additionally, iron plays a role in more than 200 enzymatic systems such as energy utilization, DNA, RNA and protein synthesis, all of which are essential for normal cellular function. Iron also plays a role in cholesterol and neurotransmitter metabolism, collagen catabolism, vitamin D activation, among others (Blanco-Rojo & Vaquero, 2019).

Iron content in the human body is between 20-50 mg Fe/kg of body weight, depending on gender. Men usually retain higher iron in their bodies than women, whereas women require more iron than men for good health. About 65% of total iron in the body is found in hemoglobin (an oxygen carrier protein found the blood) and 10% as myoglobin (an iron and oxygen-binding protein in the muscles). The remaining is distributed among other proteins found in the blood, such as enzymes

that play an essential role as electron carriers aiding in energy production during aerobic respiration. These proteins are mainly stored in the liver as ferritin and hemosiderin (Benz et al., 2018).

Iron is lost from the body through sloughing off death cells (from the skin, gastrointestinal tract, and urinary tract) and through the loss of blood. The recommended intake of iron in men is 8 mg per day, while for women, it is 18 mg of iron per day. Women require more than double the iron requirement for men because there is additional iron loss during menstruation and more iron requirement during pregnancy (O'Brien & Ru, 2017).

1.2.2 Iron Digestion and Absorption

Two separate pathways absorb heme and non-heme iron. However, both types of iron are absorbed in the small intestine, particularly in the duodenum and proximal jejunum (Gropper et al., 2008; Moll & Davis, 2017).

Before heme iron can be absorbed across the brush border of the mucosal cell wall (enterocyte) in the small intestine, it must be hydrolyzed from the globin portion of hemoglobin or myoglobin, which is accomplished by proteases in both the stomach and the small intestine. Heme iron is highly bioavailable and easily absorbed (Hurrell et al., 2006). On the other hand, non-heme iron is less bioavailable than heme iron.

Non-heme iron is usually bound to food components; therefore, like heme iron, it must also be hydrolyzed in the gastrointestinal tract before being absorbed. Once released from food

components, iron then mixes with alkaline juices secreted into the intestine from the pancreas. While in the alkaline fluids, some of the iron is transformed into ferric hydroxide ($Fe(OH)_3$), which is less soluble, therefore minimizing its absorption in the intestine (Wallace, 2016).

Iron absorption is directly related to the body's iron storage. There is an inverse logarithmic relationship between iron stores and iron absorption rate (Zijp, Korver, & Tijburg, 2000); for example, iron absorption may range between 10% in an individual with normal iron status and up to 35% for an individual with iron deficiency (Zijp, Korver, & Tijburg, 2000). In other words, iron absorption can rise to 3 to 6 mg daily when the body is depleted of iron and can fall to 0.5 mg or less daily when iron stores are high (Wallace, 2016).

1.2.3 Enhancers and Inhibitors of Iron Absorption

The absorption of heme and non-heme varies significantly among the two. Absorption of heme iron ranges from 15% to 35%, while the absorption of non-heme iron can range between 3% and 20% (Zijp, Korver, & Tijburg, 2000). Iron absorption is enhanced with the help of acids such as ascorbic, lactic, citric and tartaric acid. Acids act as reducing agents at low pH to form a highly soluble chelate complex with iron, thus, increasing iron absorption in the body. In the case of ascorbic acid, absorption can be increased by two- to three-fold (Venkatesh Mannar & Hurrell, 2018). Proteins are also enhancers of iron absorption. The exact mechanism is unknown, although it’s been hypothesized that the amino acids present in the protein, such as cysteine, act as a ligand to iron, facilitating iron absorption in the intestine (Gropper et al., 2008; Hurrell et al., 2006; Venkatesh Mannar & Hurrell, 2018). Another possible explanation is that proteins also protect

iron from redox reactions due to the presence of sulfhydryl groups; hence it prevents iron from being converted to ferric iron, a form of iron that is less absorbed (Gropper et al., 2008).

Non-heme iron absorption is inhibited by polyphenols, phytates and some divalent cations. Polyphenols are found in high concentrations in tea and coffee as well as in many vegetables, legumes and condiments. Phytates are mostly found in cereals, nuts, and legumes. Divalent cations such as manganese, nickel and calcium compete for iron absorption, therefore minimizing its absorption in the small intestine (Lopez et al., 2016)

1.2.4 RDA of Iron in Different Age Groups

Iron requirement changes in growth and development. The recommended dietary allowances (RDAs) are summarized in Table 1-1 and for vegetarians in Table 1-2. Health Canada recommends an RDA for this group, which is almost two times higher compared to individuals with a non-vegetarian diet. This is because a vegetarian diet is high in polyphenols and phytates, which inhibit iron absorption (Health Canada, 2018).

The tolerable upper limit or TUL for iron is 40 mg/day based on recommendations of either the United States FNB/IOM or the Scientific Committee for Food of the European Community (Allen et al., 2006).

Age (years)	Male	Female
1-3	7 mg	7 mg
4-8	10 mg	10 mg
9-13	8 mg	8 mg

Age (years)	Male	Female
14-18	11 mg	15 mg
19-49	8 mg	18 mg
Over 50	8 mg	8 mg
Pregnancy	N.A	27 mg

N.A = Not applicable

*This table is a copy of the version available at [https://www.healthlinkbc.ca/healthlinkbc-files/iron-health]

Table 1-1: RDA for Daily Iron Intake. Modified from (Health Canada, 2018)

Age (years)	Male	Female
14-18	20 mg	27 mg
19-49	14 mg	33 mg
Over 50	14 mg	14 mg
Pregnancy	N.A	49 mg

N.A = Not applicable

*This table is a copy of the version available at [https://www.healthlinkbc.ca/healthlinkbc-files/iron-health]

Table 1-2: RDA for Daily Iron Intake in Vegetarians (Modified from (Health Canada, 2018)

1.2.5 Iron Deficiency

Iron deficiency remains one of the most common nutritional deficiencies worldwide (Gropper et al., 2008). Iron deficiency occurs when physiological demands are not met due to inadequate dietary intake or excessive iron losses (Peña-Rosas et al., 2015). Iron deficiency anemia occurs when iron deficiency is severe. Anemia is a medical condition characterized by a severely low amount of red blood cells or hemoglobin concentration in the blood (Gropper et al., 2008). Iron deficiency, as a result of insufficient intake of iron through diet, is responsible for 50% of anemia

cases globally (Petry et al., 2016). Different portions of the population are affected differently; children and women, in general, are at higher risk of iron deficiency anemia. In 2011, it was estimated that roughly 43% of children (0-5 years), 38% of pregnant women, and 29% of nonpregnant women and 29% of all women of reproductive age (all ages 15-49 years) had anemia globally. As shown in Figure 1-1, iron deficiency anemia is prevalent worldwide.

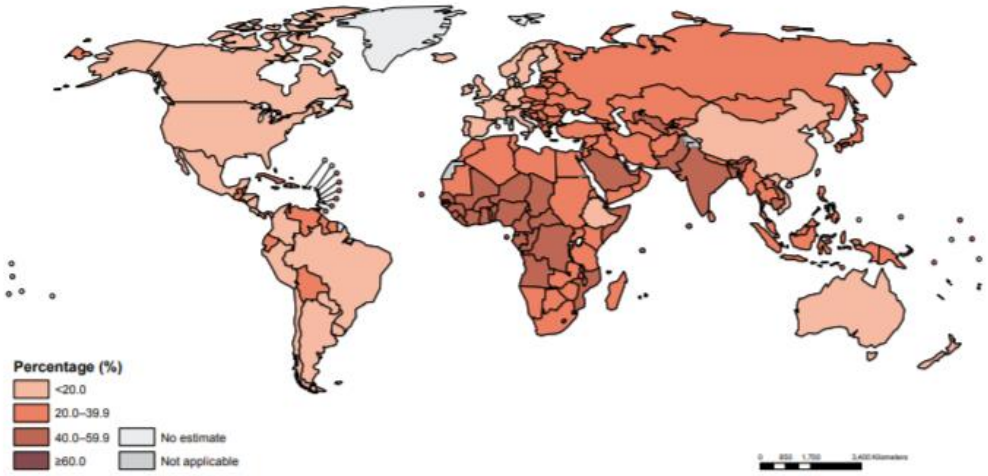

Figure 1-1: Global Estimates of the Prevalence of Anemia in Women of Reproductive Age between 15-49 Years in 2011 (WHO, 2011). Licence: CC BY-NC-SA 3.0 IGO.

Symptoms of iron deficiency anemia include impaired physical and cognitive performance and increased maternal and child mortality. Iron deficiency anemia, from decreased physical and mental performance, translates in 2.5% to 4% reduced GDP earnings (depending on the country) every year (Horton, 2006; Venkatesh Mannar & Hurrell, 2018). Therefore, it is of high interest for developing nations to combat iron deficiency.

1.2.6 Iron Fortification Compounds

There are four types of iron compounds used in fortification strategies: ferrous iron salts, ferric iron salts, elemental iron and chelated iron. The least expensive iron sources are elemental iron, followed by iron salts and finally chelated iron sources (McGee, 2017). Ferrous iron salts can include ferrous sulphate and ferrous fumarate. Some ferric iron salts include ferric orthophosphate and ferric pyrophosphate. Lastly, chelated iron includes ferrous bisglycinate and sodium iron EDTA. The solubility of the type of iron compound is essential because it is linked to bioavailability; therefore, the more soluble an iron compound is, the more bioavailable it is.

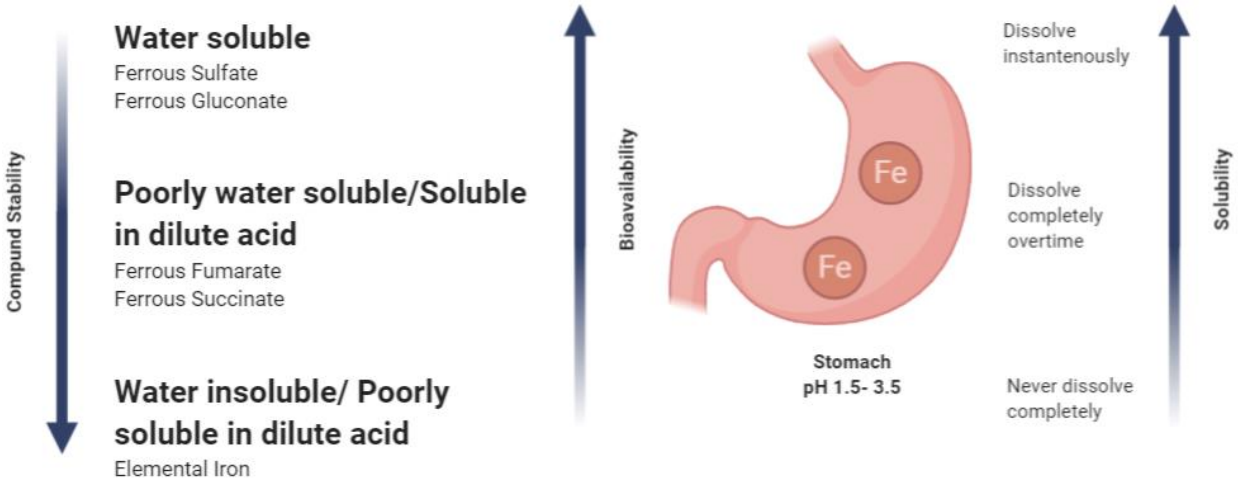

Figure 1-2: Stability, Bioavailability and Solubility Relationship of Iron Compounds used in Food Fortification.

The most common iron compound used is ferrous sulphate because it is the least expensive and most bioavailable due to its high solubility. Ferrous fumarate has good bioavailability but is poorly water-soluble unless it is dissolved in dilute acid. Ferric pyrophosphate is water-insoluble, so it causes no sensory changes in the food vehicle but has very poor bioavailability (Venkatesh Mannar

& Hurrell, 2018). Sodium iron ethylenediaminetetraacetic acid (NaFeEDTA) and ferrous bisglycinate (FBG) are chelated iron sources that effectively protect iron from absorption inhibitors like phytates and polyphenols. Nonetheless, they are not commonly used in food due to their very high cost (Dary, 2002). Despite having seemingly high bioavailability, soluble iron salts are susceptible to reactions with polyphenols and phytates by forming complexes that are not absorbable; therefore, they need to be protected from these components (Livney, 2015). Table 1-3 shows the most common iron compounds (non-heme iron or iron salts) used in food fortification and classified according to their solubility.

	Iron compound	Iron Content (%)	Bioavailability (%)	Relative cost to ferrous sulphate
Freely water soluble	Ferrous sulphate ($7H_2O$)	20	100	1.0
	Ferrous gluconate	12	89	5.1
	Ferrous lactate	19	106	4.1
	Ferric saccharate	3-35	92	4.1
	Ferric ammonium citrate	18	107	5.2
	Ferrous ammonium sulphate	14	99	2.1
	Ferric choline citrate	14	102	11.0
Slowly soluble	Dried ferrous sulphate	33	100	0.65
	Ferric glycerophosphate	15	93	10.5
	Ferric citrate	17	31	4.8
	Ferric sulphate	22	34	1.1
Poorly soluble	Ferrous fumarate	33	101	1.3
	Ferrous succinate	35	123	4.1
	Ferrous tartrate	22	62	3.9
	Ferrous citrate	24	74	3.9
Insoluble	Ferric pyrophosphate	25	45	2.3
	Ferric orthophosphate	28	31	4.1
	Sodium iron pyrophosphate	15	15	3.5
	Reduced elemental iron	97	13-90	0.1-1.0

Table 1-3: Common Iron Compounds Used in Food Fortification. Modified from (Clydesdale, 2016)

1.3 Zinc

Zinc is a mineral that is mostly found as ion Zn^{2+} in animal food products. Red meats are an excellent source of zinc. Around 40% to 70% of zinc is from animal products. Dairy, whole grains and leafy and plant sources are also excellent sources of zinc. Like iron, zinc from plant sources is less bioavailable due to the presence of phytates and polyphenols that bind to zinc and inhibit intestinal absorption (Gropper et al., 2008).

1.3.1 Zinc in the Human Body

Zinc is an essential mineral for the human body. It is used as a cofactor for over 300 metalloenzymes. Zinc is required for the regular functioning of the immune, gastrointestinal, dermatologic, neurologic, and reproductive systems (Gibson, 2012a; Mayo-Wilson et al., 2014). Total zinc in the human body is between 1.5 to 2.5 g of zinc, depending on gender. Men usually have higher zinc in the body than women. Zinc is found primarily in muscles and bones (85%), 11% in the skin and liver and 0.1% in plasma and other tissues (Gropper et al., 2008; King et al., 2000). Zinc is stored in most tissues as part of the protein thionein, which, when bound to zinc, it is known as metallothionein. Unlike iron, the body does not have a functional reservoir of zinc; therefore, a daily intake of zinc is required to maintain zinc balance in the body (Tang & Skibsted, 2016). Alternatively, when dietary zinc intake is insufficient to meet the body's needs, plasma zinc-containing enzymes and metallothionein are broken down to provide zinc (Gropper et al., 2008).

1.3.2 Zinc Digestion and Absorption

Zinc must be first be freed from amino acids to be absorbed. This is achieved by the presence of proteases in the stomach. Zinc is absorbed in the proximal small intestine, mostly by the jejunum and duodenum, like in iron (Gropper et al., 2008).

Zinc is absorbed into the enterocyte by various protein carriers such as ZIP4 and ZIP2, among others. They are known as carrier-mediated transport proteins. At RDA zinc intakes, this is the predominant pathway of absorption, which is more efficient. On the other hand, zinc can also be absorbed by passive diffusion in the cells at this RDA and at higher inake (Gropper et al., 2008).

Studies have generally shown that zinc absorption varies from 10% to 59%; at higher intake, absorption diminishes, and at lower intake, absorption increases, like in iron. Also, like iron, the amount of zinc absorbed depends on whether it comes from animal or plant sources (Gibson, 2012a; Gropper et al., 2008).

1.3.3 Enhancers and Inhibitors of Zinc Absorption

Citric acid, picolinic acid, proteins and amino acids enhance zinc absorption. Among amino acids, cysteine and histidine serve as ligands for zinc as well as for iron (Hurrell et al., 2006).

Zinc absorption is inhibited by phytate (phytic acid) and oxalate (oxalic acid) found in plant foods and polyphenols found primarily in tea and coffee. Other divalent cations like $Fe^{2+,}$ Cu^{2+}, Ca^{2+}, if present in concentrations higher than zinc, diminish zinc absorption because they compete for ligands in the intestine. For example, according to a study, ferrous sulphate and zinc sulphate

ingested together in a ratio of 2:1 (50 mg:25 mg) and 3:1 (75 mg:25 mg) decreased zinc absorption. It is worth mentioning that iron from heme does not affect zinc absorption (Gropper et al., 2008).

1.3.4 RDA of Zinc in Different Age Groups

Zinc requirements change depending on the life cycle, when the physiological requirement is high like during infancy and pregnancy. The recommended dietary allowances (RDAs) are summarized in Table 1-4. The estimated TUL for zinc is 40 mg/day for adults (Brown et al., 2010). Unlike iron, Health Canada has not specified an RDA of zinc for vegetarians, even though vegetarians usually require as much as 50% more of the RDA for zinc than non-vegetarians (NHS, 2020).

Age (years)	Male	Female
1-3	3 mg	3 mg
4-8	5 mg	5 mg
9-13	8 mg	8 mg
14-18	11 mg	9 mg
19-49	11 mg	8 mg
Over 50	11 mg	8 mg
Pregnancy	N.A	12 mg

N.A = Not applicable

*This table is a copy of the version available at [https://www.canada.ca/en/health-canada/services/food-nutrition/healthy-eating/dietary-reference-intakes/tables/reference-values-elements-dietary-reference-intakes-tables-2005.html]

Table 1-4: RDA for Daily Zinc Intake. Modified from (Health Canada, 2006)

1.3.5 Zinc Deficiency

Zinc deficiency has high mortality rates and is one of the five leading risk factors that contribute to the burden of disease in developing countries; despite this, zinc deficiency has not received sufficient public health attention as compared to iron or iodine. Inadequate intakes of dietary zinc and reduced bioavailability, or a combination of these nutritional factors are the main contributors to zinc deficiency (Gibson, 2012b).

Zinc deficiency causes growth retardation (stunting) and delayed sexual maturation in children, skeletal abnormalities from impaired development of cartilage, defective collagen synthesis, poor wound healing, dermatitis, alopecia and impaired immune function and protein synthesis as well as diarrhea and pneumonia (WHO, 2018).

As with other micronutrient deficiencies, zinc deficiency is more likely during pregnancy and in children, but seniors and vegetarians are also vulnerable to zinc deficiency (Allen et al., 2006; Venkatesh Mannar & Hurrell, 2018)

In 2011, it was estimated that the proportion of deaths of children under the age of 5 years due to zinc deficiency alone was 1.7%. The global estimate of zinc deficiency is 20% of the world's population based on stunted growth statistics in developing countries (Venkatesh Mannar & Hurrell, 2018). Fortification strategies with foods that contain both iron and zinc could have the potential to reduce the double public health burden of iron and zinc deficiencies.

1.3.6 Zinc Fortification Compounds

In food supplements and fortified foods, zinc can be found as either zinc oxide, zinc sulphate, zinc acetate, zinc chloride, and zinc gluconate. Zinc oxide has the least bioavailability because of its high insolubility in water (Zhang et al., 2018). Nevertheless, cereals fortified with zinc oxide have been proven to be as good as that from those fortified with zinc sulphate, a more soluble compound (Venkatesh Mannar & Hurrell, 2018). Zinc sulphate is the most widely used compound in fortification due to its balance between low price and high bioavailability because of its high water solubility (Allen et al., 2006). Table 1-5 shows the most common zinc compounds used in food fortification.

Zinc Compound	Zinc Content (%)	Cost ($US/kg)
Zinc oxide	80	3.4
Zinc sulphate	23-32	4.2
Zinc gluconate	14	-
Zinc chloride	48	-

Table 1-5: Common Zinc Compounds Used in Zinc Fortification (Horton, 2006)

1.4 Tea as a Food Vehicle for Fortification

The concept of tea as a food vehicle for fortification is not new. Fortification of tea was first suggested in 1943 as a carrier for vitamin A in Pakistan, India, and Tanzania (FAO, 2014). Tea fortified with iron has not been successfully developed, although attempts to fortify tea using chelated iron compounds have been attempted (McGee & Diosady, 2018b).

As previously mentioned, the fortification of foods is the most effective strategy to alleviate micronutrient deficiencies. For the fortification of foods to be successful, a staple food, or a food that is consumed by the majority of the population needs to be selected. Successful food vehicles that have been fortified are wheat and milk products and salt, among others. Salt is among the food vehicles that have been very successful because of its universal use in food preparation; therefore, food consumption patterns do not change. Additionally, salt also has an established distribution supply chain. All of these characteristics are key role players in successful food fortification strategies (Neufeld et al., 2017).

Tea could potentially be an excellent choice as a food vehicle for fortification strategies because it is the second most consumed beverage in the world, aside from water, and has established central processing facilities and distribution channels (FAO, 2018; Fernando & Soysa, 2015; McGee & Diosady, 2018a; Van Der Burg-Koorevaar et al., 2011). The estimated amount of 18–20 billion tea cups consumed daily worldwide evokes its economic and social interest as well (Fernando & Soysa, 2015).

The three major types of tea are black, green, and oolong tea (Xiong et al., 2015). Around 83% of total tea consumption happens in developing countries (McGee & Diosady, 2018a). Therefore, tea could be an excellent option for populations at risk in developing countries.

Black tea is the most produced variety of tea (FAO, 2014; McGee, 2017). Most of the tea produced worldwide is black tea, which represents 76–78% of the tea produced and consumed worldwide (Fernando & Soysa, 2015). World production of black tea is projected to rise annually by 2.2%;

this is driven by a combination of overall higher income in developing economies as well as the health benefits associated with the consumption of tea (FAO, 2018). In terms of black tea consumption by country, India is the largest consumer, with 32.2% of total black tea consumption (FAO, 2014).

It is worthwhile to mention that while tea is highly consumed in developed countries, the degree of consumption is highly dependent on many cultural factors. Black tea was chosen to be the food vehicle in this study because it is the most produced variety of tea globally and could easily reach those in both developed and underdeveloped countries. Of the latter, India is of paramount interest. The challenges posed by iron and zinc fortification in black tea are very similar for all other varieties of tea; therefore, the technology developed for black tea applies to other tea varieties.

There have not been many studies attempting to fortify tea with iron, despite meeting all essential requirements of a food vehicle. The main reason to explain this is that tea imposes a formidable technological challenge for iron and zinc, given that they are both profoundly affected by the excellent source of polyphenols in tea.

1.4.1 Black Tea Production and Processing

Black tea accounts for 80% of total tea production. The remaining 20% of production is distributed between green tea, oolong tea, and other types of tea (Preedy, 2013). The process for making black tea consists of withering, crushing/rolling, fermentation, drying, and sorting of the *Camellia sinensis* leaves (Liang Chen et al., 2013; Preedy, 2013; Zheng, 2002). During withering, the moisture content is reduced by 25%, in consequence, this allows to increase cell membrane

permeability and to increase the formation of aroma compounds (Liang Chen et al., 2013; Preedy, 2013). During the crushing/rolling process, the leaves are broken into small pieces allowing internal cell constituents such as polyphenol oxidase and polyphenols to leak out during the fermentation process (Liang Chen et al., 2013; Preedy, 2013). During fermentation, the polyphenols are oxidized with the aid of polyphenol oxidase to produce a diverse range of phenolic compounds. Some manufacturers of black tea carefully control this part of the process to ensure the correct ratio of theaflavins (TF) to thearubigins (TR) (1:10 to 1:12) and to maximize the theaflavin amount (to above 0.8%) (Preedy, 2013). The final step in black tea processing is drying, where the moisture content is reduced to approximately 3%, which enables the black tea to have high shelf stability (Preedy, 2013).

1.4.2 Black Tea Chemistry

Tea leaves and shoots have naturally high levels of polyphenols. The largest group of polyphenolic compounds in leaves of black tea are catechins (Figure 1-4), which are a type of phenolic compound belonging to the family of flavanols) (Preedy, 2013). Catechins are water-soluble pigments and are the primary reducing agents of the leaves (Preedy, 2013). The catechin content depends on how the leaves are processed before drying, as well as environmental conditions in which the tea plant is cultivated (Preedy, 2013).

During the production of black tea, green tea leaves are anaerobically fermented (Preedy, 2013). During fermentation, some of the tea catechins are polymerized by the endogenous polyphenol oxidase enzyme into theaflavins and thearubigins (Figure 1-3). Theaflavin content of tea increases during fermentation and starts declining after reaching a peak; on the other hand, thearubigin

content increases continuously throughout the fermentation process (Preedy, 2013). Compared to unfermented green tea, the catechin content of black tea is reduced by approximately 85% (Liang Chen et al., 2013; Preedy, 2013)

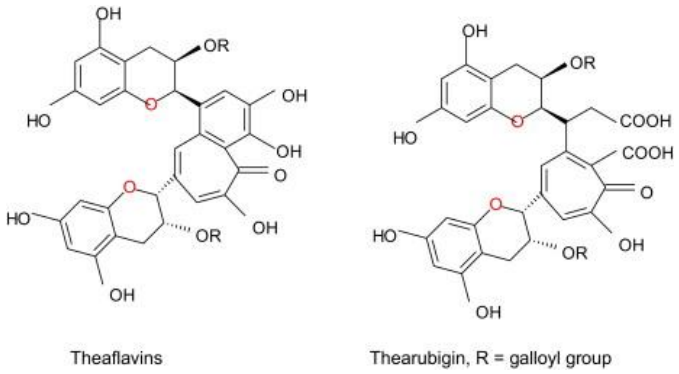

Figure 1-3: Structures of Major Black Tea Polyphenols After Fermentation (Preedy, 2013)

Theaflavins are yellow/orange/red compounds that give colour, briskness, and strength to the tea (Liang Chen et al., 2013; Preedy, 2013). On the other hand, thearubigins are red/brown and also play an essential role in providing the sensory characteristics of black tea (Liang Chen et al., 2013; Preedy, 2013; Zheng, 2002). After fermentation of black tea, the main phenolic compounds in black tea based on the total polyphenol content are catechins (10%-12%), theaflavins (3%-6%), thearubigins (12%-18%), phenolic acids (10%-12%), flavonols (6%-8%), and methylxanthines (8%-11%) (e.g. caffeine) (Preedy, 2013).

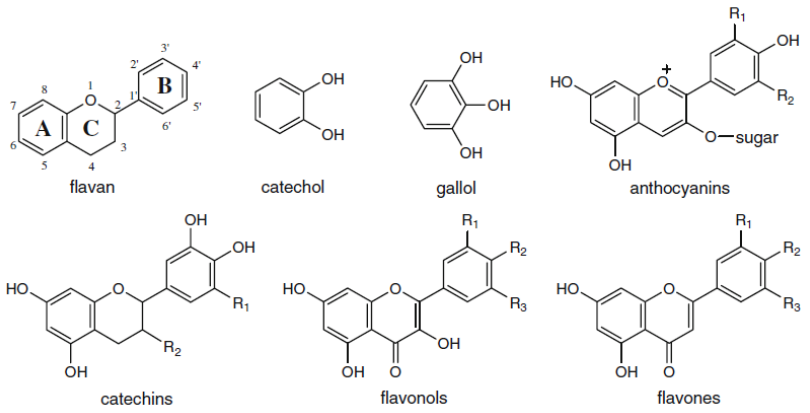

Figure 1-4: Major Polyphenol Compounds found in Tea. R Groups can be either H, OH, OCH_3 or Galloyl Esters (Perron & Brumaghim, 2009).

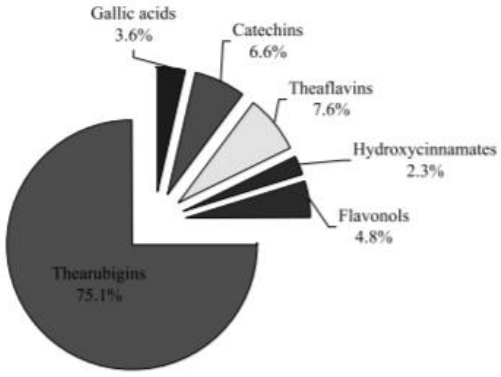

Figure 1-5: Average Polyphenol Composition in Black Tea (Rechner et al., 2009).

1.4.3 Iron Absorption in the Presence of Tea

Polyphenols in tea are known to form chelation complexes that inhibit iron absorption and could potentially contribute to iron and zinc deficiencies, especially in high-risk populations (Preedy, 2013). Polyphenols affect the absorption of non-heme iron, while heme iron remains mostly unaffected (Reddy et al., 2006). The major polyphenolic compounds in tea are catechins and, in

black tea, polymerized catechins called theaflavins and thearubigins, which are potent metal cation chelators (Preedy, 2013).

Iron chelation by polyphenols in the small intestine depends on the type of polyphenols present and their degree of protonation; thus, it is highly dependent on pH. As the pH increases, the formation of metal-polyphenol complexes increases. The pH effect on iron-polyphenol complex formation is particularly significant in the small intestine because the pH is close to neutral (Preedy, 2013).

In-vitro models of digestion (pH adjustment followed by enzymatic digestion) indicate that tea decreases iron absorption by 30% or more. Iron absorption decreases as the pH increases. The effect is observed when iron is given as a solute in the tea solution or a meal consumed with tea (Preedy, 2013). Another study using a Caco-2 cell culture model, which is considered to be predictive of human absorption, found that tea polyphenols decrease iron absorption by 73% (Lei et al., 2008). A study by Disler et al. (1975) performed with iron and black tea in rats; concluded that iron malabsorption was caused by the tannins naturally present in black tea. This study showed a decrease in iron absorption in rats that consumed tea, tannin extract, and tannic acid by up to 50%, compared to the control, in which tannins were not present (Disler et al., 1975).

One of the methods to avoid iron from being chelated by polyphenols is with the addition of ascorbic acid. Ascorbic acid is the most potent enhancer of non-heme iron absorption: it reduces Fe^{3+} to Fe^{2+} (the absorbable form of iron). Ascorbic acid loosely binds to iron, thereby decreasing chelation by polyphenols (Preedy, 2013).

1.5 Metal Polyphenol Complex Chemistry

Protonated phenolic groups (phenols) found in tea do not have a high affinity for metal cations; however, once deprotonated, phenols have a strong affinity to them. The typical pH range of polyphenol deprotonation is 9.0-10.0, but in the presence of certain cations, such as Fe^{3+} and Fe^{2+}, it is lowered to pH 5.0-8.0 (Hider et al., 2001). Thus, polyphenols are easily deprotonated at or below physiological pH in the presence of certain metal cations and form very stable complexes (Perron & Brumaghim, 2009).

Once deprotonated, phenols form oxygen centers with a high charge density, so they become high-affinity ligands for metal cations. The oxygen centers form coordinate covalent bonds with metal cations resulting in the formation of metal:phenol complexes (Hider et al., 2001) or, in this case, an iron:phenol complex. The term "iron-polyphenol" is used to refer to both iron-phenol and iron-polyphenol complexes.

A coordinate covalent bond is a type of covalent bond in which both electrons in the bonding pair originate from one species (McGee, 2017). Polyphenolic compounds are often bidentate, meaning they can form two coordinate covalent bonds (see Figure 1-6A) with a metal cation. As a result, bidentate ligands are more powerful scavengers of metal cations (Hider et al., 2001). Additionally, polyphenols with multiple attached rings have less affinity for metal cations than polyphenols with single rings. (Hider et al., 2001). For example, the affinity of the molecule in Figure 1-6C and D is lower than the molecule in Figure 1-6A and B.

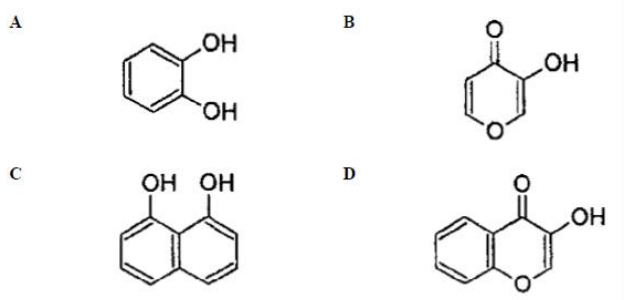

Figure 1-6: Chemical Structures with Chelation Centers; (A) catechol, (B) pyromeconic acid (3-hydroxy-4-pyrone), (C) 1,8-dihydroxy naphthalene, (D) 3-hydroxychromone. Modified from (Hider et al., 2001)

Polyphenols can form 1:1, 1:2, and 1:3, iron:polyphenol complexes. The ratio of interaction depends on the concentration of the metal, the concentration of the ligand, the pH of the solution, and the natural structure of the polyphenol compounds (Hider et al., 2001; Perron & Brumaghim, 2009). For example, in the latter, some polyphenols possess multiple metal-binding sites, and thus are capable of oligomerization and polymerization (see Figure 1-3) (Hider et al., 2001).

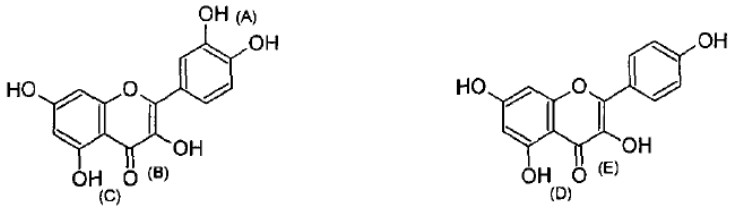

Figure 1-7: Quercetin (left) has three potential metal-binding sites depicted by (A), (B) and (C). Kaempferol (right) has two potential binding sites illustrated by (E) and (D). Modified from (Hider et al., 2001)

In general, tribasic cations are preferred to dibasic cations (see Figure 1-8). For example, Fe^{3+} (ferric iron) is preferred to Fe^{2+} (ferrous iron) due to the electronegativity of the oxygen electron donor (O-) of the phenol compounds (Crichton, 2016; Hider et al., 2001). Polyphenols firmly

stabilize Fe^{3+} over Fe^{2+} because catecholate and gallate complexes of Fe^{2+} rapidly oxidize in the presence of O_2 to form a Fe^{3+} -polyphenol complexes, a process called autoxidation (Figure 1-9). Fe^{2+} autoxidation occurs very slowly in the presence of O_2. Still, when Fe^{2+} is bound to a polyphenol, the rate of iron autoxidation occurs much faster. Therefore, close to neutral pH, there is rapid oxidization of Fe^{2+}-polyphenol complexes into Fe^{3+}-polyphenol complexes (Hider et al., 2001).

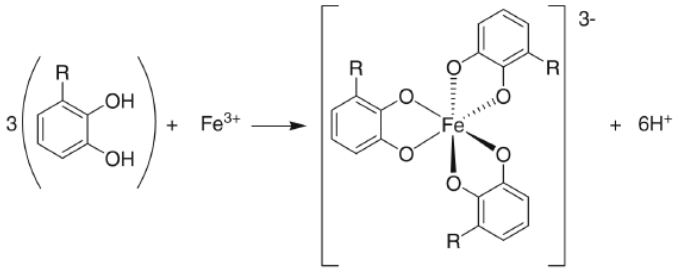

Figure 1-8: Iron-Polyphenol Complex Formation Requires Deprotonation of the Polyphenol Ligand (Perron & Brumaghim, 2009).

Iron autoxidation rate varies for polyphenol complexes. Polyphenols with gallol groups have faster autooxidation rates for iron. The reaction rates are first order with respect to the ligand concentration and Fe^{2+} concentration, meaning that the reaction rate increases in proportion to increases in polyphenol concentration or Fe^{2+} concentration. Additionally, the reaction rate of iron oxidation decreases as pH decreases as well (Perron et al., 2010).

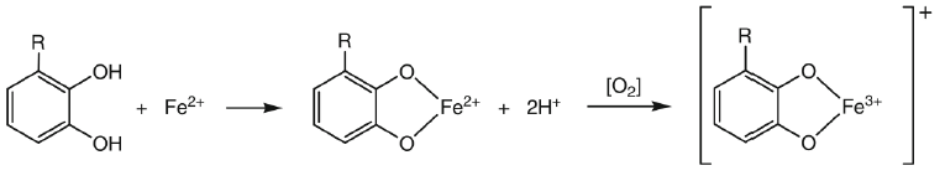

Figure 1-9: Fe^{2+} Iron-Polyphenol Complex and Subsequent Autoxidation. Modified from (Perron & Brumaghim, 2009)

The ratio of iron:polyphenol upon complexation is pH-dependent. Between pH 5.0 and pH 7.0, polyphenols complex with iron in a 1:2 iron:polyphenol ratio. Complexes at this pH are blue-purple (Perron & Brumaghim, 2009). At pH < 4.0, polyphenols bind iron in a 1:1 ratio, forming complexes that are blue-green. Between pH 5.0 to 7.2, a mixture of both 1:2 and 1:3 iron:polyphenol complexes form (Perron & Brumaghim, 2009). At pH > 8 and above, the 1:3 iron:polyphenol complexes dominate, which are red (Perron & Brumaghim, 2009; Templeton, 2002).

The colour formation indicates that the amount of complex can be quantified using a spectrophotometric method. The absorption wavelength of each iron:polyphenol ratio (1:1, 1:2, 1:3) is different. At a 1:1 iron:polyphenol ratio, the complex is blue-green and absorbs at about 670 nm; at a 1:2 ratio, the complex is blue-purple and absorbs between 542 to 561 nm for gallates, or 561 to 586 nm for catecholate.; and at a 1:3 ratio the complex is red and absorbs between 490 and 520 nm. Fe^{2+} complexes of polyphenol ligands are colourless in the absence of oxygen (Perron & Brumaghim, 2009).

1.6 Prevention of the Metal-Polyphenol Complex Formation in Foods

The effectiveness of fortified food products in preventing diseases depends on preserving the stability and bioavailability of the micronutrient. Stability refers to the effective prevention of the micronutrient from interacting with the food system. If the fortified food vehicle has low stability, the micronutrient could interact with other components in the food system, which could potentially cause off-flavours, off-colours, and severely impact its shelf-life. Changes in stability can happen in two ways, either by (1) food processing conditions such as changes in temperature, oxygen or light and (2) after being orally administered due to changes in pH, presence of enzymes and other food components that could interact (Đorđević et al., 2014).

Bioavailability refers to how much the micronutrient is available for absorption in the body, which is directly related to the stability of the protected micronutrient. Both stability and bioavailability are critical parameters for successful incorporation into food systems and products (Đorđević et al., 2014).

Amongst the different fortification technologies, microencapsulation is considered a suitable technology that provides controlled release and thermal protection of the micronutrient to increase bioavailability and stability; therefore, it could also provide a robust delivery method of the micronutrient (Dwyer & Bailey, 2017). At the same time, sensory changes of the food vehicle can be effectively avoided (Đorđević et al., 2014; Livney, 2015).

1.6.1 Microencapsulation

Encapsulation is defined as "a process to entrap one substance within another substance, thereby producing particles with diameters of a few nanometers to a few millimetres, depending on the encapsulation technique used" (Đorđević et al., 2014). In other words, encapsulation enables the protection of a compound of interest by incorporating it within a protective coating material that releases its components at controlled rates in a defined period (Abbasi & Azari, 2011).

From a technological point of view, an efficient encapsulation system suitable for industrial-scale food production must comply with the following:

(a) it must be formulated with food-grade (natural ingredients are preferred) using solvent-free production methods (Acosta, 2009),

(b) should be able to incorporate bioactive compounds into food matrices with high physicochemical stability and minimal impact on the organoleptic properties of the product,

(c) should be able to protect the encapsulated compounds from interaction with other food ingredients and degradation due to physical and chemical conditions like temperature, light, or pH,

(d) should maximize the bioavailability of the compound,

(e) ensure controlled release in response to specific gastrointestinal conditions, and

(f) should be easily scalable for industrial production characteristics (McClements et al., 2007).

The binding of iron to the polyphenols can be mitigated by adding ligands that form complexes with iron that increase its absorption. Such ligand can be ascorbic acid (Butt et al., 2014; Widlansky et al., 2005). Tea with ferrous sulphate had 33% ± 6% of iron remaining bioavailable,

while fortified tea had 81% ± 18% iron bioavailable. When iron is added to tea, and it is not protected by a matrix or with the addition of a reducing agent like ascorbic acid, more than 90% of the iron could be complexed with polyphenols, thus significantly reducing bioavailability (Dueik et al., 2017). It is estimated that supplying 30% of the recommended daily allowance (RDA) of iron for a pregnant woman in two cups of fortified tea (4 mg/cup, 0.0175 mg/ml, or 0.3 mmol/L of iron) could help to mitigate iron deficiency (McGee & Diosady, 2018a).

For the purpose of this research project, special attention is given to a cost-effective material that improves a functional characteristic in delivery, can encapsulate the core material successfully and is in widespread use in the food industry or is certified as GRAS (generally recognized as safe).

1.6.2 Microencapsulation Techniques

There are several microencapsulation techniques with different cost efficiency and coating quality. The most common microencapsulation techniques are pan coating, air suspension and spray drying.

Pan coating is the oldest microencapsulation technique initially developed in the pharmaceutical industry. It involves tumbling the micronutrients in a pan while slowly adding coating agents. Fluidized bed coating is an improved version of pan coating, which allows a more robust coating mechanism. It involves suspending the micronutrients in an airstream while the coating agent is also added to the airstream. This process is repeated until the micronutrient is effectively encapsulated (Venkatesh Mannar & Hurrell, 2018).

Amongst the microencapsulation technologies, spray drying is the most used because it is easy to operate, provides a high production rate and requires low operating costs. These advantages have established spray drying as one of the few unit operations that can be easily scalable and employed in industrial proportions (Shishir & Chen, 2017). As a result, it is estimated that 90% of microencapsulates are prepared using a spray dryer (Nedović et al., 2013).

1.6.2.1 Spray Drying

Spray drying is a process in which liquids are transformed into stable and soluble powders (Đorđević et al., 2014; Xin Huang et al., 2010). Spray drying has been used since the 1930s to encapsulate flavours and as of today,

Spray drying can also be used with heat-sensitive compounds because the drying process lasts a few milliseconds to a few seconds (Đorđević et al., 2014) and for encapsulating hydrophobic compounds (de Vos et al., 2010). Furthermore, if a compound is prone to oxidation, nitrogen can be used as the drying gas instead of air. Some disadvantages of spray drying include non-uniform size and shape of the obtained particles, as well as particles tending to aggregate (Nedović et al., 2013)

The spray drying process (see Figure 1-10) starts with a (1) feed solution that contains in suspension our core or material to encapsulate and our polymer or coating material; both are homogeneously mixed in the same solution. The feed solution is then pumped through a (2) atomizer that disperses the liquid feed solution into a fine spray. Due to surface tension and amphipathic properties of the coating material and core, the liquid forms micelles, which are then

rapidly dried using a hot gas (usually air) that is above the boiling temperature of the solvent (Gharsallaoui et al., 2007). Finally, the liquid spray, which has now become a dry powder, is collected using a (3) cyclone. Figure 1-10 shows a diagram of the spray drying process.

The efficiency of microencapsulation in spray drying is dependent on both physical process parameters and chemical characteristics of the coating material and compound of interest to encapsulate. The two main parameters determining the efficiency of encapsulation are coating/core mass ratio and the inlet air temperature in a spray dryer (Đorđević et al., 2014). Due to the high number of factors influencing the microencapsulation process, the encapsulation efficiency (EE) of spray drying varies from 10% to 90% (Đorđević et al., 2014).

Ideally, a coating material for spray drying should have the following properties: be an excellent emulsifier, form a stable emulsion, be readily soluble in water, possess network-forming abilities, and form low-viscosity solutions at high concentrations (Gharsallaoui et al., 2007). Gums such as gum arabic and guar gum and proteins such as sodium caseinate, whey protein, and gelatin exhibit the previous characteristics mentioned; therefore, they are commonly used in spray-drying encapsulation (Gharsallaoui et al., 2007).

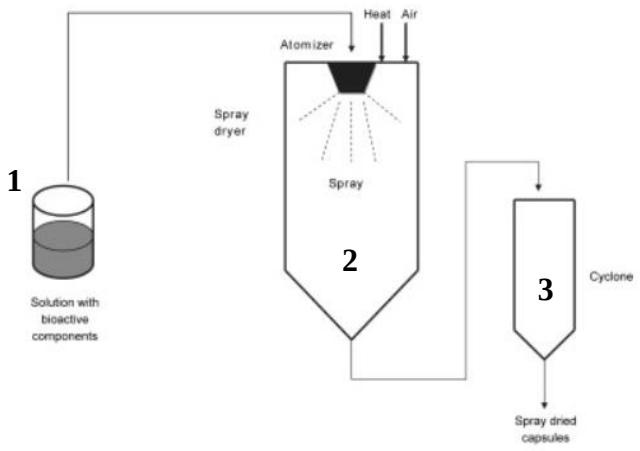

Figure 1-10: Simplified Schematic Representation of Spray Drying.

In a spray drying process, (1) the feed solution is passed (2) through the atomizer and into the spray dryer tank. The microcapsules formed flow through a (3) cyclone that collects the microcapsules into a collection tank. Modified from (de Vos et al., 2010)

1.6.3 Common Coating Materials for Microencapsulation in the Food Industry

The most commonly used wall materials are gum arabic, maltodextrins, modified starches, other polysaccharides and whey proteins (Krokida, 2018). The selection of the proper coating material is based on the micronutrient to be delivered, the microencapsulation technique used, and the food vehicle for micronutrient delivery.

For this research project, whey proteins from whey protein isolate (WPI) and Eudraguard® are selected as the coating materials to be used for microencapsulating iron and zinc with spray drying.

Category of Coating Material	Coating Material	Microencapsulation Technique Used
Carbohydrate	Starch, modified starch, maltodextrins, chitosan, cyclodextrins	Spray drying, freeze-drying, coacervation, extrusion
Cellulose	Carboxymethylcellulose, methylcellulose, ethylcellulose	Spray drying, coacervation
Gum	Gum arabic, acacia, agar, sodium alginate, carrageenan	Spray drying
Protein	Whey proteins, casein, gelatin, albumin	Emulsion, spray drying

Table 1-6: Common Coating Materials Used for Microencapsulation in the Food Industry. Modified from (Goud et al., 2005)

1.6.3.1 Whey Proteins

Whey proteins are by-products of cheese manufacturing with significant commercial potential. Whey contains 0.6% protein and 93% water. Separation techniques allow to produce whey protein concentrates with 25% to 80% protein, and whey protein isolate with over 90% protein (Foegeding et al., 2002). Whey proteins have the highest possible protein digestibility corrected amino acid score (PDCAAS) of 1.0, which is an indicator of their ability to supply all essential amino acids. The inherent properties of whey protein make it widely used in foods because they have high nutritional value and is GRAS certified (Lingyun Chen et al., 2006; Ramos et al., 2012).

The main proteins found in whey are β-lactoglobulin (β-Lg), α-lactalbumin (α-La), representing approximately 50% and 20% of the whey fraction, respectively. According to some studies, bovine β-lactoglobulin is highly stable at acidic pH, resisting denaturation at pH values as low as 1, and is easily denatured at alkaline pHs (above pH 9) (Diarrassouba et al., 2013; Taulier & Chalikian,

2001). In other studies, native β-lactoglobulin is almost entirely resistant to pepsin degradation at low pH and also that the protein remained intact in simulated gastric fluids (Barbosa et al., 2017). Thus, WPI could be an interesting material to investigate, given its reported functional characteristics. Furthermore, **s**everal studies have reported that whey proteins enhance the bioavailability of iron and zinc in *in-vitro* models (Gandhi, Banjare, et al., 2019; Nakano et al., 2007; Shilpashree et al., 2018).

1.6.3.2 Eudragard Natural®

Gastro-resistant coatings have been widely researched and employed in the pharmaceutical industry. However, most of these polymers are not regarded as natural ingredients or do not possess GRAS status (Barbosa et al., 2017). On the other hand, most natural coating materials are not formulated as gastro-resistant and can, therefore, lack efficacy (Barbosa et al., 2017). Hence, there is a need for natural polymers to offer sufficient enteric protection for the nutraceutical industry.

Polysaccharide based polymers are among the most used as coating materials in microencapsulation technologies. Recently, a starch-based aqueous coating has been commercialized by Evonik Industries under the brand name of Eudraguard® Natural (Evonik, 2018). This coating is a GRAS substance and has been licensed to be used for nutraceutical formulations in the United States and Europe (Barbosa et al., 2017). It is claimed that this coating provides taste-masking and acid-resistant properties (pH-sensitive) (Barbosa et al., 2017; Demetriades & Williams, 2016). However, information such as the type of starch and other composition of the coating system is not disclosed.

1.7 Outline and Objectives

In raw numbers, iron and zinc affect more than one-third of the world's population. In particular, Southeast Asian countries such as India and Pakistan are mostly affected in part due to shared cultural practices such as vegetarianism and frequent fasting; however, iron and zinc deficiencies are also present in more industrialized countries, and it can affect people of all age groups.

Given that the best approach to prevent iron and zinc deficiencies is food fortification, the selection of a proper food vehicle is essential for the success of a food fortification strategy. As such, it could be hypothesized that tea could be an excellent food vehicle; however, it imposes a tremendous technological challenge because polyphenols in tea are known to form chelation complexes that inhibit iron and zinc absorption that could potentially contribute to iron and zinc deficiencies, especially in high-risk populations.

Previous studies have focused on encapsulating tea polyphenols, thus avoiding their interactions with other food components like metal cations. Until recently, two studies have been made attempting to fortify tea with iron; nevertheless, the microencapsulation of iron or zinc to avoid their interaction with tea polyphenols has not been attempted. We hypothesize that iron and zinc interaction with tea polyphenols could be reduced by coating iron and zinc with appropriate encapsulants with a target release profile. The general objective of this research project is to microencapsulate iron and zinc with cost-effective materials that provide functional characteristics in delivery and is in widespread use in the food industry or are certified as GRAS. This research project is divided into three specific objectives in different chapters of this thesis. Description of Chapters 2-5 are presented in the following paragraphs.

The specific objective presented in Chapter 2 was to develop an optimized formulation based on the capability of WPI and Eudraguard® to encapsulate both iron and zinc in the same formulation. This objective was achieved using a Box-Behnken response surface experimental design. The efficiency of microencapsulation was further assessed using atomic absorption spectroscopy. The yield was also determined to give insight into the upscale industrial capability. Lastly, the physical characteristics of the microcapsules were assessed, such as colour, morphology and size.

Chapter 3 addresses the specific objective of determining the bioaccessibility of the microencapsulated iron and zinc in a simulated gastric and intestinal digestion as well as cellular uptake using an *in-vitro* Caco-2 cell model. Furthermore, the release behaviour was characterized by estimating the kinetics of release using different mathematical models commonly used in the pharmaceutical industry that can be applied to food systems.

The last specific objective is presented in Chapter 4. In this chapter, the objective was to quantify the iron-polyphenol complex formation from the developed microencapsulated iron and zinc (Chapter 2). This objective was based on a newly developed spectrophotometric method which allows for measurement at pH representative of tea, the small intestine and the stomach. Because the iron-polyphenol complex is pH-dependent, the use of buffers with minimal reported interaction with metals was assessed because this was an unknown left to investigate in a previously developed method for iron-polyphenol complex quantification. Finally, the microencapsulated iron and zinc was tested to assess its ability to slow-down the iron polyphenol complex formation in tea and gallic acid, a polyphenol model system

These chapters are followed by Chapter 5. This chapter summarizes and concludes the main findings in the previous chapters. Lastly, recommendations on scientific advancement for further development are suggested.

Chapter 2: Development and Optimization of Microencapsulated Iron and Zinc

The goal of microencapsulation strategies for food fortification relies on the protection of the micronutrients against other food components. In the context of iron and zinc fortification, these micronutrients need to be protected against absorption inhibitors such as phytates and polyphenols. Iron also needs to be protected because it is a highly oxidizing agent affecting sensory characteristics and food quality of the food vehicle. In this chapter, two GRAS substances, whey protein isolate and Eudraguard®, a new starch-based aqueous coating agent, were used to microencapsulate ferrous and zinc sulphate in the same premix using a spray dryer. The colour of the microcapsules was assessed using a HunterLab colorimeter and revealed that the higher the iron loading, the darker the premix. Morphology and size of the microcapsules were assessed using a scanning electron microscope (SEM). The size of the microcapsules ranged between 1 - 20 μm.

Encapsulation efficiency was found to be most affected by the initial iron and zinc loading. The encapsulation efficiency of iron ranged from 57% to 96.5%, while for zinc ranged from 6% to 47%. The yield of the premixes was between 65 - 75%. A Box-Behnken response surface design was used to maximize the encapsulation efficiency and yield of the premix, obtaining an R^2-adj of 87%. Three optimized formulations were selected where iron and zinc encapsulation efficiency was maximized to 100% and 52%, respectively. The optimized formulations were found to fit the response surface model. The results of this study show that iron and zinc can be encapsulated in

the same premix; however, the encapsulation efficiency of zinc might be improved if they are encapsulated in separate premixes.

2.1 Introduction

Food fortification is the best strategy to alleviate micronutrient deficiencies. The selection of a proper food vehicle is essential to the success of a fortification strategy. Nevertheless, the proper selection of a food vehicle needs to be accompanied with the right delivery technology for iron and zinc. In the context of tea, polyphenols inhibit the absorption of iron and zinc, thereby reducing its effectiveness in a food fortification strategy.

Previous studies have focused on encapsulating tea polyphenols, thus avoiding their interactions with other food components like metal cations (Massounga Bora et al., 2018). Nevertheless, the microencapsulation of iron or zinc to avoid their interaction with tea polyphenols has not been attempted. Other studies have focused on encapsulated iron or zinc in different food vehicles such as milk (Abbasi & Azari, 2011) and bread (Bryszewska et al., 2019). However, none have investigated a form of microencapsulation in tea as a food vehicle. An attempt to fortify tea with iron has been made by McGee & Diosady (2018a) and by Dueik (2017). However, these studies investigated the effectiveness of chemically chelated iron to avoid the metal:polyphenol complex in tea and not microencapsulated iron; thus, this is an unknown to be investigated.

Microencapsulation is one of the few technologies that could be very effective in tackling current issues in food fortification (Livney, 2015; Murugesan & Orsat, 2012). Spray drying is the technology primarily used in microencapsulation that can process material very rapidly while

being robust (Obón et al., 2009). It is estimated that 90% of microencapsulates are prepared using a spray dryer (Nedović et al., 2013). Spray drying is also a relatively inexpensive process, although this mostly depends on the coating material to be used. Among coating materials, whey protein is commonly used and is GRAS (Gharsallaoui et al., 2007; Krokida, 2018). Furthermore, several studies have reported that whey proteins enhance iron absorption (Gandhi, Banjare, et al., 2019; Nakano et al., 2007; Shilpashree et al., 2018).

Recently, a starch-based aqueous coating has been commercialized by Evonik Industries under the brand name of Eudraguard® Natural (Evonik, 2018). This coating is a GRAS substance and has been licensed to be used for nutraceutical formulations in the United States and Europe (Barbosa et al., 2017). It is claimed that this coating provides taste-masking and acid-resistant properties (pH-sensitive) (Barbosa et al., 2017; Demetriades & Williams, 2016). There is little research on the study of Eudraguard® to microencapsulate micronutrients, in particular iron and zinc, and how they behave in a simulated gastrointestinal environment.

When selecting the coating materials, encapsulation efficiency is critical to decide on how well our coating materials can entrap the iron and zinc to avoid interactions with other food components in the stomach that could hinder the absorption of iron and zinc in the small intestine. Among other parameters essential to elucidate in a microencapsulation process is the yield because it can help determine its economic feasibility and scalability (Pratap-Singh et al., 2018). Therefore, yield and encapsulation efficiency are essential parameters to elucidate in an encapsulation process and that are beneficial to optimize.

The research question driving the development of this chapter is focused on determining the capability of these coating materials on encapsulating two essential minerals in the same formulation. To the best of our knowledge, there are no previous published studies on the simultaneous encapsulation of iron and zinc using these coating materials. Therefore, the objective of this chapter is to develop an optimized microencapsulation formulation that maximizes the yield and encapsulation efficiency of iron and zinc using whey proteins and Eudraguard®.

2.2 Materials

WPI was obtained from Canadian Protein (Canada). Eudraguard® was obtained from Evonik Industries (Switzerland). Iron and zinc standards (2%HNO_3) for the determination of iron and zinc were purchased from Ricca Chemical Company (U.S.A). 70% HNO_3 was purchased from Anachemia (Canada). Ferrous sulphate and zinc sulphate heptahydrate were purchased from Fisher Scientific (U.S.A). Distilled and deionized water was used for all experiments.

2.3 Methods

2.3.1 Experimental Design

Optimization aims at improving performance by adjusting the parameters of a process. Response surface methodology (RSM) was chosen as the statistical tool for the optimization of the microcapsule formulation based on the selected material composition. RSM is commonly applied in the optimization of microcapsules formed using a spray dryer (Shishir & Chen, 2017). Within RSM, Central Composite Design (CCD) and Box Behnken design are the most recommended (Shishir & Chen, 2017). The main advantage of a Box-Behnken design is the reduced number of tests runs with three factors. For example, in a Box-Behnken with three factors, there are 15

experimental runs. In comparison, a Central Composite Design (CCD) has 20 experimental runs with three factors.

Optimization of microencapsulation using the Box-Behnken design is determined by fitting the experimental data to a second-order polynomial equation that is used to model the effects of the factors on the response.

$$y = \beta_0 + \sum_{j=1}^{k} \beta_j X_j + \sum_{j=1}^{k} \beta_{jj} X_j^2 + \sum \sum_{i<j} \beta_{ij} X_i X_j$$

Equation 2-1: Second-order Polynomial Equation for Optimizing Iron and Zinc Microencapsulation

From the above equation, β_0, β_j, β_{jj}, β_{ij} are the regression coefficients for intercept, linear, quadratic and interaction coefficients respectively, and X_i, X_j are the factors or independent variables (Ba & Boyaci, 2007).

For the purpose of this research project, a Box-Behnken of three factors and three levels each was used. The factors were WPI concentration (A), Eudraguard® concentration (B), and iron and zinc loading (C). WPI protein concentration was set at 3%, 6%, 9% (w/v), Eudraguard® concentration at (2%, 4%, 6% (w/v) and iron and zinc loading at 10%, 25%, 40% (w/w) with respect to the amount of WPI added. The responses or outcomes to be optimized are (1) yield, (2) encapsulation efficiency of iron (EE Fe), and (3) encapsulation efficiency of zinc (EE Zn).

2.3.2 Preparation of Microencapsulated Iron and Zinc

2%, 4%, and 6% (w/v) of Eudraguard® (Evonik Industries, Switzerland) was dissolved in 200 ml of water. The mixture was heated to 90ºC for 10 minutes under agitation to allow Eudraguard® to dissolve completely. After heating, Eudraguard® was left to cool to 25ºC in ice. After cooling the Eudraguard®, 3%, 6%, and 9% (w/v) of WPI (Canadian Protein, Canada) was added and left for 5 minutes under agitation. Finally, 10%, 25%, and 40% of iron and zinc (w/w) was added. The mixed solution was then left to homogenize with agitation at 300 rpm for 5 minutes before spray drying.

2.3.3 Preparation of Microparticles by Spray Drying

The mixed solution containing WPI, Eudraguard®, iron and zinc was spray-dried using a B-290 Büchi Mini Spray Dryer (Buchi® Labortechnik AG, Switzerland), which employs a system of co-current drying via a two-fluid nozzle mechanism (Büchi, 2019). For all the experimental runs, aspiration was maintained at 100% ($35m^3/h$) to maximize the separation rate of the cyclone (Büchi, 2019), and spray gas flow rate or Q-flow was set to 40mm Hg or 473 L/h. The feed pump rate was set to 6 mL/min or 20% of the feed pump rate. The inlet temperature was set at 150˚C. After each run, the powder (microcapsules) was stored in airtight containers at 4˚C.

2.3.4 Determination of Iron and Zinc Content

The iron and zinc content of the microcapsules was measured using atomic absorption spectroscopy (AAS) using an Agilent 55B AA spectrometer (Agilent Technologies, U.S.A) available from the UBC Chemistry Department. Calibration curves for iron quantification were made by diluting a 1000 ppm iron standard in 2% HNO_3 (Ricca Chemical Company, U.S.A) to

concentrations of 0.2 ppm, 0.5 ppm, 1 ppm, 5 ppm, and 10 ppm. Similarly, calibration curves for zinc were made by diluting a 1000 ppm zinc standard in 2% HNO_3 (Ricca Chemical Company, U.S.A) to concentrations of 0.2 ppm, 0.5 ppm, 1 ppm, 1.5 ppm, 3 ppm, and 5 ppm for zinc. The calibration points were within the expected range of the maximum and minimum quantity of iron and zinc in the microcapsules.

2.3.5 Encapsulation Efficiency

Encapsulation efficiency is the percentage of a compound successfully entrapped inside the microcapsule. Encapsulation efficiency was determined with a two-step approach. First, total iron and zinc content was determined by adding 50 mg of microcapsules to 10 mL of concentrated (70%) HNO_3 (Anachemia, Canada). The microcapsules were left digesting for 24 hrs at 70ºC and 200 rpm using a C25KC incubator shaker (New Brunswick Scientific, U.S.A). This method is based on the work by McGee and Diosady (2011) and Clegg et al. (1981). Second, iron and zinc release from the microcapsules was determined by dissolving 50 mg of microcapsules in 10 mL of double deionized water. After 30 minutes, the solution was poured over a No.4 Whatman® (GE Healthcare Life Sciences, U.S.A). Lastly, 9.7 ml of the filtered supernatant was collected, and 0.3 ml of concentrated (70%) HNO_3 was added to make this solution into 2% HNO_3. The total iron and zinc in both steps were determined by AAS, as described above. This method is based on McGee and Diosady (2011) and Pratap-Singh et al. (2018) with some modifications. Encapsulation efficiency was calculated based on the following equation:

$$EE\ (\%) = \frac{Total\ Fe/Zn\ content - Fe/Zn\ released\ in\ water}{Total\ Fe/Zn\ content}\ x\ 100$$

Equation 2-2: Formula for Calculating Encapsulation Efficiency for Iron

2.3.6 Yield

The microcapsules were collected from the collection tank of the spray dryer. The weight of the collection tank was previously tared to avoid sample loss when transferring to a separate container is used. Yield is defined as the total amount of collected solids after spray drying over the total initial amount of solids added; therefore, the yield was calculated using the following equation:

$$Yield\ (\%) = \frac{Total\ amount\ of\ collected\ solids\ (g)}{Total\ amount\ of\ initial\ solids\ in\ the\ spray\ drying\ solution\ (g)}\ x\ 100$$

Equation 2-3: Formula for Calculating Yield

2.3.7 Colour Measurement of Microencapsules

A LabScan XE spectrophotometer (HunterLab, U.S.A) was used to measure the colour of the microencapsulated iron and zinc that was initially calibrated using a standard calibration black and white screen. The colour measurement was done in terms of L* [dark (0–50) and light (50–100)], a* [green (negative numbers) and red (positive numbers)] and b* [blue (negative numbers) and yellow (positive numbers)]. Samples were measured six times. This protocol was based on the work by Gandhi et al. (2019).

2.3.8 Morphology and Size of Microcapsules

Scanning electron microscopy was used to determine the morphology of the microcapsules using an S-4700 Field Emission SEM (Hitachi High-Technologies, Japan) available at the UBC Bioimaging Facility. The microcapsules were attached on an SEM stub by carbon conductive

double-coated adhesive tape. A blast of compressed air was used to remove any excess microparticles over the adhesive tape. The SEM micrographs were recorded at an acceleration voltage of 5 kV and a working distance of 12 mm, under a high vacuum. The size of the microcapsules was evaluated and calculated using image analysis with ImageJ software.

2.3.9 Statistical Analysis

The Box-Behnken was designed using Minitab 19® The goodness of fit of the model and significance of each regression coefficient was evaluated by response surface regression analysis, and ANOVA was also calculated using Minitab 19®. Microsoft Excel (version 1908, Microsoft) was used for calculating yield and fitting the calibration curves of iron and zinc for encapsulation efficiency determination. Student's t-test was conducted for comparing two sets of data to determine if they were significantly different from each other. All experimental results were expressed as mean ± standard deviation.

2.4 Results and Discussion

2.4.1 Encapsulation Efficiency and Yield

A total of 30 experimental runs (duplicates) were performed (Table 2-1). The encapsulation efficiency of iron ranged from 57% to 96.5%, while for zinc ranged from 6% to 47%. These results can be observed in Figure 2-1. Yield ranged from 53% to 73.5%. Similar studies performed by microencapsulating ferrous sulphate in chitosan or Eudragit® achieved a similar yield between 65 - 75% (Pratap-Singh et al., 2018). Although yield is mainly dependent on the properties of the coating material and spray drying conditions, a yield above 70% is typical when microencapsulating through spray drying (Büchi, 2019).

	Coded Levels			Uncoded Levels				
Run Order	**WPI**	**Eudraguard ®**	**Fe/Zn Loading**	**WPI (g)**	**Eudragard® (g)**	**Fe+Zn (g)**	**Fe (g)**	**Zn (g)**
1	-1	0	1	6	8	2.4	1.71	0.69
2	0	1	1	12	12	4.8	3.43	1.37
3	0	-1	1	12	4	4.8	3.43	1.37
4	1	0	1	18	8	7.2	5.14	2.06
5	0	0	0	12	8	3	2.14	0.86
6	1	1	0	18	12	4.5	3.21	1.29
7	0	0	0	12	8	3	2.14	0.86
8	1	-1	0	18	4	4.5	3.21	1.29
9	0	0	0	12	8	3	2.14	0.86
10	-1	0	-1	6	8	0.6	0.43	0.17
11	0	-1	-1	12	4	1.2	0.86	0.34
12	-1	1	0	6	12	1.5	1.07	0.43
13	1	0	-1	18	8	1.8	1.29	0.51
14	0	1	-1	12	12	1.2	0.86	0.34
15	-1	-1	0	6	4	1.5	1.07	0.43
16	0	1	-1	12	12	1.2	0.86	0.34
17	1	-1	0	18	4	4.5	3.21	1.29
18	0	0	0	12	8	3	2.14	0.86
19	0	1	1	12	12	4.8	3.43	1.37
20	-1	0	-1	6	8	0.6	0.43	0.17
21	0	0	0	12	8	3	2.14	0.86
22	-1	1	0	6	12	1.5	1.07	0.43
23	1	0	-1	18	8	1.8	1.29	0.51
24	-1	0	1	6	8	2.4	1.71	0.69
25	0	-1	1	12	4	4.8	3.43	1.37
26	1	1	0	18	12	4.5	3.21	1.29
27	-1	-1	0	6	4	1.5	1.07	0.43
28	0	-1	-1	12	4	1.2	0.86	0.34
29	1	0	1	18	8	7.2	5.14	2.06
30	0	0	0	12	8	3	2.14	0.86

Table 2-1: Experimental Runs for Development of Microencapsulated Iron and Zinc. WPI: Whey Protein Isolate.

The yield is highly variable because it depends on the type of material and spray drying conditions used (Bürki et al., 2011). Yield loss is mainly due to the microcapsules sticking to the instrument wall or passing through the air filter. The encapsulating or coating materials tend to stick to the glass wall of the instrument due to the electric charge of the microcapsules occurring during their formation (Pratap-Singh et al., 2018). Microparticles are lost in the air filter because they are very lightweight particles that are lost due to the suction force created by the vacuum pump (Pratap-Singh et al., 2018). Although these microparticles can be collected from the air filter, they are usually not considered when calculating yield. In terms of yield, the formulation with 2% Eudraguard® **requires ten times less** wall material per gram of iron and zinc (13:1, coating material: Fe/Zn added) than the formulation with 4% Eudraguard® (23:1, coating material: Fe/Zn added). In an industrial context, this is highly desirable because it translates into less production costs.

The highest encapsulation efficiency achieved for iron and zinc was 96.5% and 47%, respectively. This formulation resulted in Eudraguard® concentration of 2%, a WPI concentration of 6%, and a 10% Fe/Zn loading. This formulation also achieved the highest yield of 73.5%. A similar formulation of 4% Eudraguard and 3% WPI with 10% Fe/Zn loading resulted in the second-highest encapsulation efficiency of iron and zinc, 95.1% and 36.4%, respectively. Yield for this formulation was not among the highest (66.4%). Amongst these formulations, the difference in encapsulation efficiency of iron was not significant ($p > 0.05$).

An interesting finding is the low encapsulation efficiency of zinc compared to iron. According to some studies, iron is preferably bound to whey proteins. This phenomenon is not clearly

understood, although some studies suggest that the carboxylic groups of ionic amino acids are mainly involved in the mineral binding mechanism of whey proteins. At low pH, the reactive side chains of amino groups tend to become protonated, which decreases their affinity for cations, thus reducing their complexation with the protein. When the pH is increased, the side chains acquire a negative charge and tend to complex with cations. Hence, binding is generally higher at a more neutral pH (Shilpashree et al., 2016; Sugiarto et al., 2009). Another possible explanation can be the electronegativity of iron and zinc. By definition, electronegativity is an atom's tendency to attract electrons to itself, and it can explain the type and strength of a bond. Iron has an electronegativity of 1.83, while zinc has an electronegativity of 1.65, based on the Pauling electronegativity scale. The higher electronegativity of iron means that iron tends to attract electrons from other atoms and resist having its electrons taken away (Plietker, 2008); thus, in this context, iron tends to attract more to the atoms present in the amino acids of proteins.

Another possibility is the atomic size or radius. Iron has an atomic radius of 126 pm (picometers), while zinc has an atomic radius of 139 pm. Zinc is atomically bigger than iron (Krężel & Maret, 2016; Plietker, 2008); therefore, its bigger size could play a role in how it interacts with the proteins.

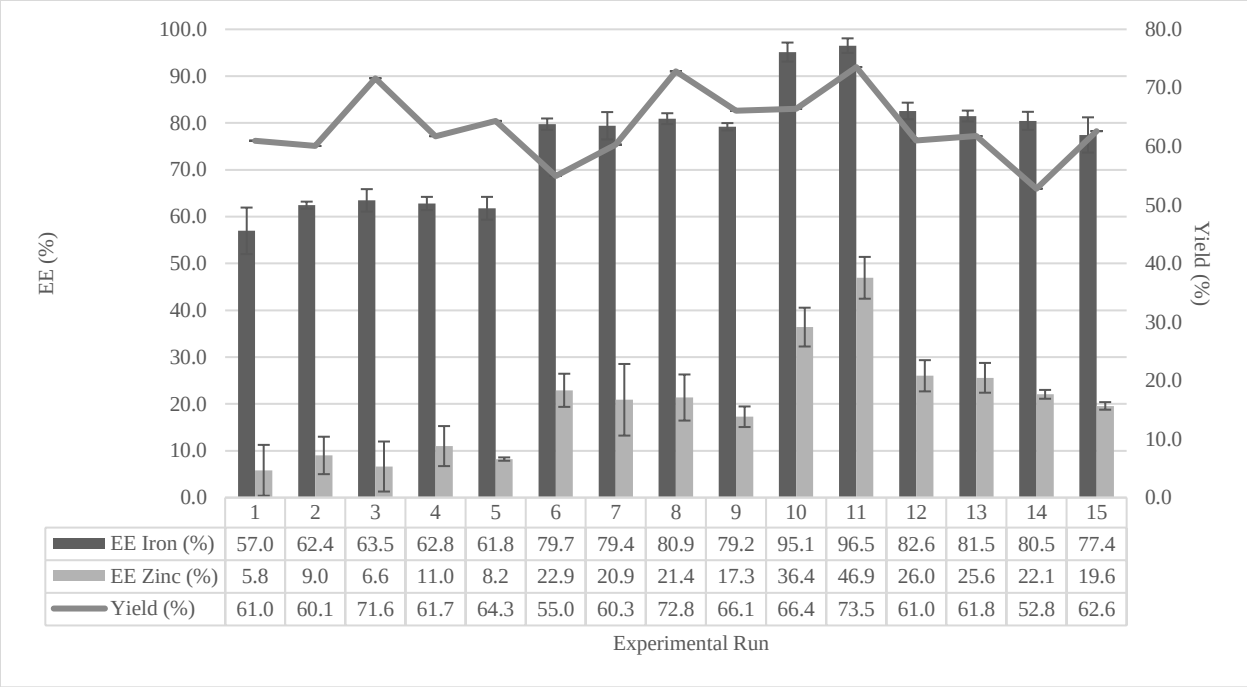

	1	2	3	4	5	6	7	8	9	10	11	12	13	14	15
EE Iron (%)	57.0	62.4	63.5	62.8	61.8	79.7	79.4	80.9	79.2	95.1	96.5	82.6	81.5	80.5	77.4
EE Zinc (%)	5.8	9.0	6.6	11.0	8.2	22.9	20.9	21.4	17.3	36.4	46.9	26.0	25.6	22.1	19.6
Yield (%)	61.0	60.1	71.6	61.7	64.3	55.0	60.3	72.8	66.1	66.4	73.5	61.0	61.8	52.8	62.6

Figure 2-1: Encapsulation Efficiency and Yield of Each Experimental Run. EE= Encapsulation Efficiency

2.4.2 Optimization of Microencapsulated Iron and Zinc

As mentioned earlier, the experimental data were fitted to a second-order polynomial equation, which was used to model the effects of the factors on the response. The goodness of fit of the model and significance of each regression coefficient was evaluated by response surface regression analysis and ANOVA (Table 2-2). From the statistical analysis, lack of fit was used as a measure of the failure of the optimization model to represent the experimental data. Lack of fit was not significant ($p > 0.05$), indicating that the data fit the model well. The adjusted coefficient of determination or R^2-adj was a second statistical measure considered to assess the goodness-of-fit of this experimental model. Based on the response surface regression models for each of the responses, the response yield obtained an R^2-adj of 87%, while for EE of iron and zinc were 82% and 87%, respectively. This is considered a good correlation

	EE Iron	EE Zinc	Yield
P-value of Model	0.166	0.080	0.086
P-value of Lack-of-fit	0.700	0.494	0.368
R^2-adj (%)	81.65	87.09	86.61

Table 2-2: ANOVA and Goodness-of-fit of the Models

The linear effect of Fe/Zn loading had a significant impact on EE Iron ($p<0.03$) and on EE Zinc ($p < 0.009$). Hence, the lower the concentration of iron and zinc in the formulation, the encapsulation efficiency is improved. This result is in agreement with the results of a similar study by Onsekizoglu et al. (2017). The linear effect of yield is also not significant ($p > 0.05$). Yield is mostly affected by spray drying process parameters, mainly inlet temperature. Because spray drying conditions were not varied in the Box-Behnken design, this could explain why yield was not significantly affected. Interaction effects between WPI, Eudraguard®, and Fe/Zn loading are not significant.

The empirical models of encapsulation efficiency based on the optimization model are shown below:

$$EE\ Fe\ (\%) = 97.2 + 4.91A - 3.54B - 24.85C - 0.0208A^2 + 0.245B^2 - 0.56C^2 - 0.196AB + 1.277AC + 0.522BC$$

Equation 2-4: Regression Equation for Encapsulation Efficiency of Iron

$$EE\ Zn\ (\%) = 44.6 + 5.29A - 4.08B - 27.34C - 0.157A^2 + 0.265B^2 + 0.181C^2 - 0.288AB + 0.877AC + 0.946BC$$

Equation 2-5: Regression Equation for Encapsulation Efficiency of Zinc

$$Yield\ (\%) = 56.9 + 3.00A - 0.00B - 3.04C - 0.0531A^2 + 0.026B^2 - 0.109C^2 - 0.2496AB + 0.099AC + 0.320BC$$

Equation 2-6: Regression Equation for Yield

Where A is the factor WPI, B is the factor Eudraguard®, and C is the factor Fe/Zn loading. The units of the coefficients A, B, and C are expressed in grams (g).

In RSM, the visualization of the predicted model equation can be obtained by the response surface plot; therefore, three-dimensional (3D) surface plots were generated by employing the fitted polynomial model. The 3D surface plots help illustrate the relationship among the responses of EE Iron EE Zinc and yield with the levels of each of the factors used in this experimental design. Figure 2-2A shows the 3D plot of EE Iron with varying concentrations of WPI and Fe/Zn Loading. An increase in encapsulation efficiency is observed as the iron loading decreases. Also, EE of iron is not affected by a change in WPI concentration. This is reflected in the non-significant interaction between these two factors on the ANOVA analysis. The effect of EE Zinc with varying concentrations of WPI and Fe/Zn loading is presented in Figure 2-2B. The surface plot also indicates that the encapsulation efficiency of zinc increases as the loading of zinc decreases.

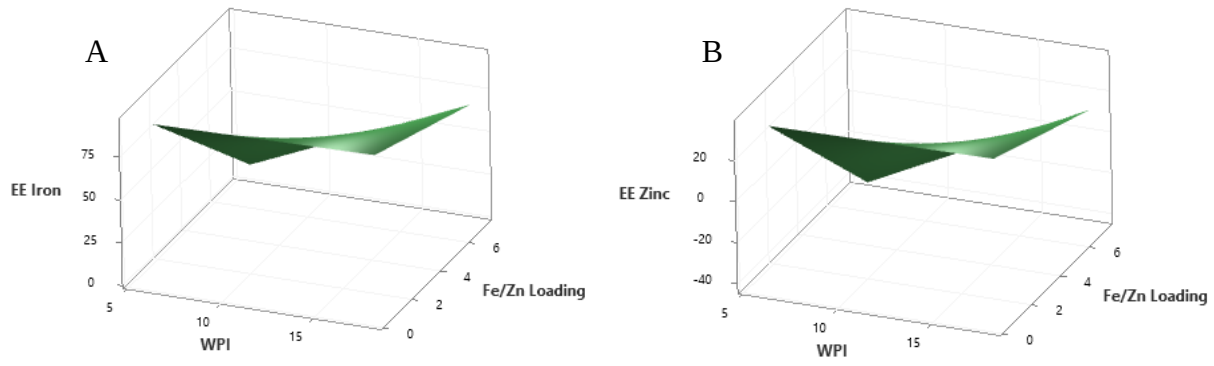

Figure 2-2: 3D Response Surface Plot of (A) EE Iron and (B) EE Zinc as a Function of WPI and Fe/Zn Loading

The response optimizer function in Minitab® 19 was used to obtain the optimal conditions for microencapsulating iron and zinc by using the above regression equations. Given that the formulation that achieved the highest encapsulation efficiency and yield was composed of Eudraguard® concentration of 2% (4.0 g), a WPI concentration of 6% (12.0 g), and a 10% Fe/Zn loading (1.2 g), it is expected that the response surface optimizer determines a very similar formulation within this range. The parameters set for the response optimizer were to maximize the encapsulation efficiency of iron and zinc and yield. Eight possible optimization solutions were obtained. The details of each solution are found in Table 2-3. To choose the optimized formulations, the composite desirability is a useful parameter.

Composite desirability assesses how well the combination of the independent variables or factors satisfies the target defined for the responses (Minitab, 2020). Composite desirability has a value from zero to one. One represents the ideal case where the factors achieve the desired response, while zero indicates that one or more responses are outside their cut-off limits (Minitab, 2020).

Given that the desired composite should approximate one, solutions one, two, and four are chosen as the best formulations to maximize EE Iron, EE Zinc, and yield. Solution one has a composite desirability of one, meaning that it achieves the maximum target of the responses. Based on the response optimizer, solution one achieves an encapsulation efficiency of iron and zinc of 100% and 52%, respectively. Yield is maximized to 73.62% in solution one. Solutions one, two and four in Table 2-3 were chosen as the optimized formulations to further study for bioaccessibility studies (see Chapter 3) and their ability to prevent the metal-polyphenol complex (see Chapter 4).

From Table 2-3, composite desirability decreases as the iron and zinc loading increases, regardless of an increase in the coating material. This result is also in agreement with other authors where an additional increase in the mass ratio over the optimum hardly improved the encapsulation efficiency (Onsekizoglu Bagci & Gunasekaran, 2017) because one of the main factors affecting encapsulation efficiency is the wall/core mass ratio (Đorđević et al., 2014). The 3D surface plots shown previously help visualize this same trend.

Solution	**WPI (g)**	**Eudraguard® (g)**	**Fe/Zn Loading (g)**	**EE Zn Fit**	**EE Fe Fit**	**Yield Fit**	**Composite Desirability**
1	12.42	4.00	0.60	52.09	101.74	73.62	1.00
2	12.69	4.01	1.27	44.13	96.52	73.30	0.97
3	13.20	4.05	1.32	43.96	96.19	73.55	0.97
4	17.95	4.64	1.29	42.67	90.54	73.50	0.91
5	17.97	4.63	1.41	41.91	90.42	73.54	0.91

Solution	WPI (g)	Eudraguard® (g)	Fe/Zn Loading (g)	EE Zn Fit	EE Fe Fit	Yield Fit	Composite Desirability
6	13.87	4.04	1.99	37.56	91.78	73.54	0.88
7	13.81	4.02	2.00	37.43	91.70	73.54	0.88
8	18.00	11.78	7.20	22.94	70.62	56.73	0.30

WPI: Whey Protein Isolate, EE Fe: Encapsulation Efficiency of Iron, EE Zn: Encapsulation Efficiency of Zinc

Table 2-3: Response Optimization for Microencapsulated Iron and Zinc

Formulation	WPI (g)	WPI % (w/v)	Eudraguard® (g)	Eudraguard® % (w/v)	Fe/Zn Loading (g)	Fe/Zn Loading (%)	EE Zn Fit	EE Fe Fit	Yield Fit	Composite Desirability
1 (A)	12.42	6	4.00	2	0.60	5	52.09	101.74	73.62	1.00
2 (B)	12.00	6	4.00	2	1.20	10	44.13	96.52	73.30	0.97
3 (C)	17.95	9	4.65	2	1.29	7	42.66	90.53	73.50	0.91

WPI: Whey Protein Isolate, EE Fe: Encapsulation Efficiency of Iron, EE Zn: Encapsulation Efficiency of Zinc

Table 2-4: Final Formulations to Assess in Bioaccessibility and Metal Polyphenol Complex Studies

At the optimal formulation conditions, new trials were performed to test the adequacy of second-order polynomial models. From this point on, solution one is referred to as formulation A, solution two as formulation B, and solution three as formulation C. The composition of each formulation is shown in the Table 2-5 on the next page.

Formulation A	(6% WPI, 2% Eudraguard®, 5% Fe/Zn loading)
Formulation B	(6% WPI, 2% Eudraguard®, 10% Fe/Zn loading)
Formulation C	(9% WPI, 2% Eudraguard®, 7% Fe/Zn loading)

Table 2-5: Composition of Optimized Formulations of Microencapsulated Iron and Zinc. Optimization was based using a Box-Behnken Response Surface Model.

Based on the results of Table 2-6, a good correlation was observed between the experimental and the predicted values, indicating that the optimization model is of good precision. This result is expected because the lack-of-fit of the regression model is non-significant, and the R^2-adjusted of the model is within the acceptable range.

Formulation	**EE Fe (%) Predicted**	**EE Fe (%) Actual**	**EE Zn (%) Predicted**	**EE Zn (%) Actual**	**Yield Predicted (%)**	**Yield (%) Actual**
A	101.74	97.30	52.09	51.82	73.62	73.00
B	96.52	96.48	44.13	45.00	73.30	73.50
C	90.54	95.14	42.67	44.15	73.50	72.97

Table 2-6: Experimental and Predicted values of the Optimized Microencapsulated Iron and Zinc

2.4.3 SEM Microscopy

Scanning electron microscopy (SEM) was used to evaluate particle morphology and size. Assessing the morphology can help us to evaluate how well the coating material can encapsulate the iron and zinc salt.

The SEM micrographs are shown in Figure 2-3. The microcapsules have better uniformity as the amount of coating material increases. In general, the microparticles showed a spherical shape, smooth surface, and variable sizes. Some microcapsules also showed surfaces with concavities. According to Rigon and Zapata (2016), concavities are typical of spray-dried samples due to the rapid water evaporation, which causes rapid shrinkage of the microcapsule followed by expansion of air bubbles trapped inside them (Rigon & Zapata Noreña, 2016).

As the concentration of a coating material decreases, the microparticles also tend to diminish in size. This tendency can be seen between Figure 2-3C and Figure 2-3D, where the latter has a lower concentration of Eudraguard®. Smaller microparticles between 0.3 – 0.8 μm tended to aggregate over the surface of microparticles of bigger size under these conditions. The smaller size of the microcapsules at a lower coating material concentration is indicative of probably insufficient coating material to provide a good film. Hence, there was no impedance to mass transfer resulting in the microparticles to keep shrinking further, resulting in smaller particles with imperfect morphology (non-smooth surface) (Pratap-Singh et al., 2018). Figure 2-3A and Figure 2-3B show similar results where the latter has a lower concentration of Eudraguard® that resulted in microparticles with a tendency to rupture.

The size of the microcapsules varied between 1- 20 μm. According to the spray dryer manufacturer, the size output of the microcapsules is between 2–25 μm (Büchi, 2019). In general, the size of the microcapsules is highly variable due to spray drying conditions, coating and core material properties (Rigon & Zapata Noreña, 2016).

The results of the SEM images indicate that a higher amount of coating material results in microparticles with a more spherical shape and less concavities on its surface. Nevertheless, the higher concentration of coating material does not result in a better encapsulation efficiency. As previously reported, the encapsulation efficiency is dependent on the amount of iron and zinc added. Thus, the lower the iron and zinc added, the better the encapsulation efficiency.

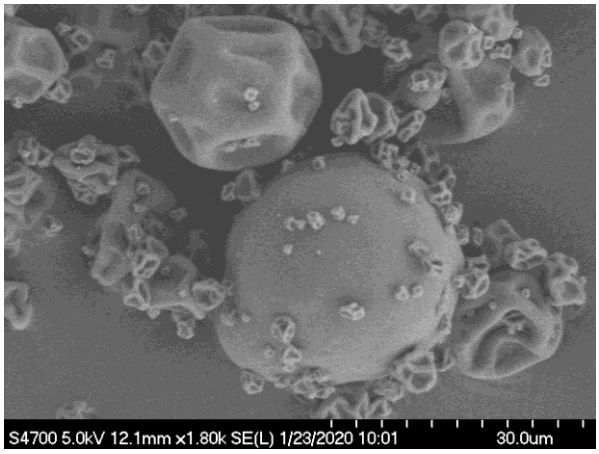

A

WPI 9%, Eudraguard® 6%, Fe/Zn Loading 25%

(Run 6)

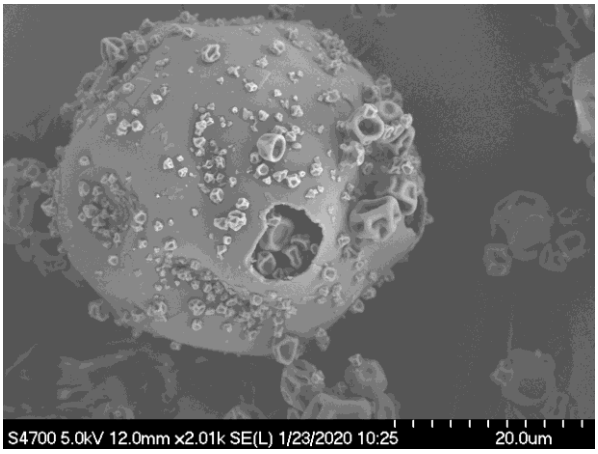

B

WPI 9%, Eudraguard® 2%, Fe/Zn Loading 25%

(Run 8)

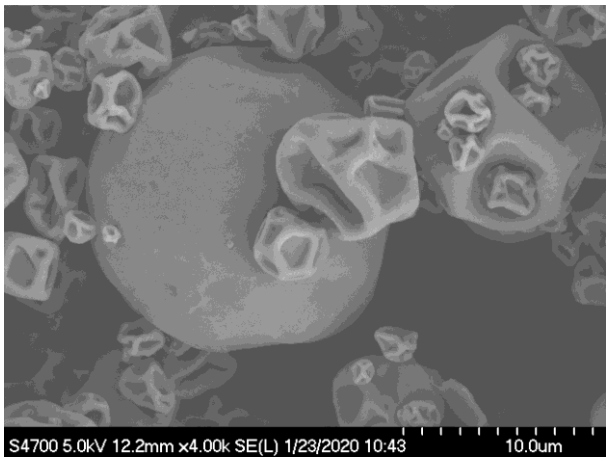

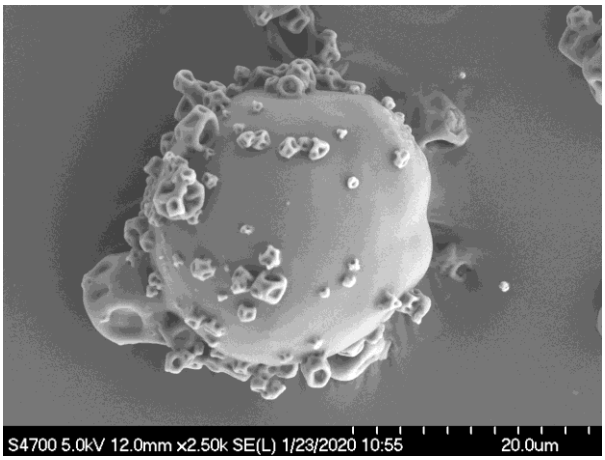

C

WPI 6%, Eudraguard® 4%, Fe/Zn Loading 25%

(Run 9)

D

WPI 6%, Eudraguard® 2%, Fe/Zn Loading 10%

(Run 11)

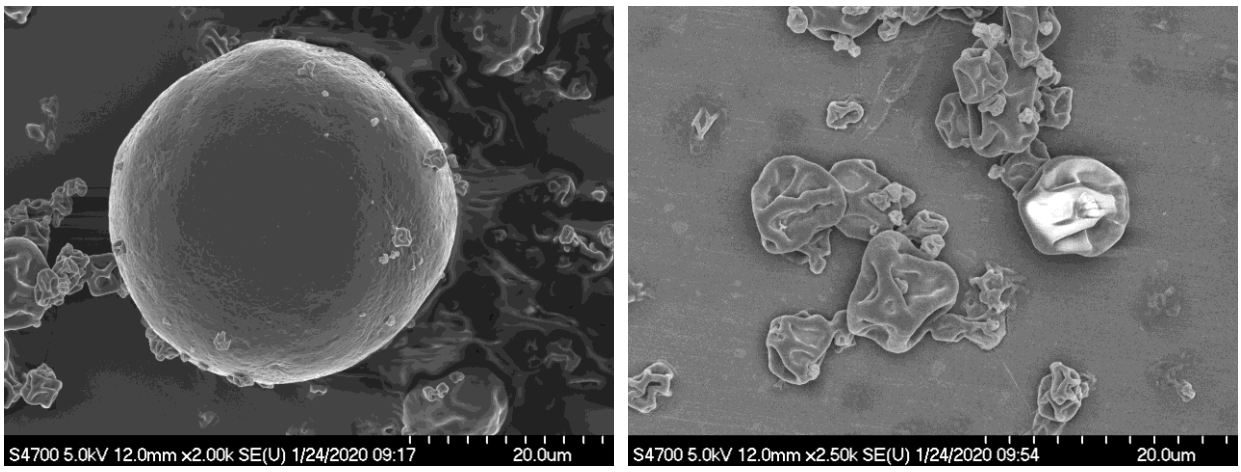

E

WPI 3%, Eudraguard® 6%, Fe/Zn Loading 25%

(Run 12)

F

WPI 3%, Eudraguard® 2%, Fe/Zn Loading 25%

(Run 15)

Figure 2-3: SEM Images of the Prepared Microcapsules (Magnification Shown in Image)

***For a reference on the composition of each Run, see* Table 2-1.**

2.4.4 Colour Parameters of Microencapsulated Iron and Zinc

Colour measurement is perfectly suited for the determination of colour difference and strength, as well as comparison of similar colours; therefore, colour measurement is very valuable for quality control and is primarily used in multiple stages of a manufacturing chain, depending on the product (Ramanathan, 2016).

In a food fortification context, colour measurement is essential because it allows for a robust measurement to quantify and control for customer acceptability and is dependent on the purpose

of the food vehicle to be used for fortification. For example, a lighter/whiter colour is preferred in salt, rice, or bread, but a darker/browner is preferred when fortifying tea and coffee. Colour measurements give guidance to the amount of colourants needed to change the colour of the vehicle to the desired target, if necessary (Pratap-Singh et al., 2018).

Table 2-7 presents the L*, a*, and b* of the prepared microcapsules after the spray drying process. The L* value for each scale, therefore, indicates the level of light or dark, where a low number (0-50) indicates dark, and a high number (51-100) indicates light. The a* value provides a scale red vs. green, where a positive number indicates red, and a negative number indicates green. Finally, the b* value gives the difference between a yellow and blue colour, where a positive number indicates yellow, and a negative number indicates blue. All three values are required to completely describe an object's colour (Whetzel, 2016).

The colour of the microcapsules became browner, with more darkness (lower L* value), redness (higher a* value), and yellowness (higher b* value), on increasing the iron loading. Therefore, the higher the iron loading, the darker the premix (microcapsules). The darker colour is explained due to the formation of ferric hydroxides, which has a brown colour (Mellican et al., 2003). The premix with the lightest colour (closer to white) is Formulation A. As previously described; this premix contains the lowest iron loading (5%) among all prepared samples. Often, the colour of the iron premix has to be controlled depending on the purpose of iron fortification. Some formulations, such as those for the fortification of salt or rice, require a whiter premix, whereas formulations, such as those for tea or coffee fortification, might prefer a darker brown premix (Pratap-Singh et al., 2018). The optimized formulations have a white colour, yet, there is a possibility of using a

small amount of colourant to darken the colour of the premix. In such cases, the L*a*b* data in Table 2-7 could guide the amount of colourants needed for matching the desired colour of the product.

Sample	L*	a*	b*
Run 1	74.25 ± 2.50	2.67 ± 0.21	16.79 ± 0.93
Run 2	73.07 ± 0.17	2.81 ± 0.03	18.80 ± 0.09
Run 3	72.21 ± 0.36	3.17 ± 0.03	19.83 ± 0.11
Run 4	68.71 ± 0.41	3.73 ± 0.02	21.60 ± 0.05
Run 5	72.76 ± 0.23	2.54 ± 0.02	17.54 ± 0.11
Run 6	71.56 ± 0.09	3.42 ± 0.02	19.80 ± 0.04
Run 7	74.24 ± 0.18	2.65 ± 0.01	17.40 ± 0.02
Run 8	70.23 ± 0.25	3.87 ± 0.03	20.69 ± 0.06
Run 9	72.07 ± 0.28	3.16 ± 0.04	18.47 ± 0.10
Run 10	78.86 ± 0.25	1.14 ± 0.03	10.74 ± 0.05
Run 11	76.08 ± 0.11	1.62 ± 0.01	12.39 ± 0.05
Run 12	79.12 ± 0.20	1.84 ± 0.03	15.24 ± 0.05
Run 13	75.10 ± 0.27	1.69 ± 0.03	12.98 ± 0.03
Run 14	78.95 ± 0.17	1.42 ± 0.03	12.39 ± 0.05
Run 15	73.42 ± 0.20	2.80 ± 0.01	17.08 ± 0.04
Formulation A	83.66 ± 0.04	0.50 ± 0.02	7.77 ± 0.10
Formulation B	76.08 ± 0.11	1.62 ± 0.01	12.39 ± 0.05
Formulation C	78.31 ± 0.30	0.99 ± 0.04	10.19 ± 0.12

Table 2-7: Colour Measurements of the Experimental Runs and Optimized Formulations of Microencapsulated Iron and Zinc.

2.5 Conclusions

Whey protein isolate and Eudraguard® were investigated as potential encapsulating agents for the microencapsulation of iron and zinc. While the encapsulation efficiency of iron was 96.5%, the encapsulation of zinc in the same premix was 42%. The iron and zinc loading was found to affect the degree of encapsulation efficiency, where an increase in encapsulation efficiency is observed as the iron and zinc loading decreases. The lower iron and zinc loading could be beneficial depending on the context; for example, this study found that as the iron loading increases, the premix powder also becomes darker. Depending on the food vehicle, a lighter colour of premix can be advantageous. The encapsulation efficiency of zinc was low relative to that of iron, which could be attributed to electronegativity and lower atomic radius of iron, which facilitates its bonding with the carboxylic functional groups of the amino acids from the whey protein. Nevertheless, the Box-Behnken experimental design was able to optimize the encapsulation efficiency of iron and zinc, maximizing the encapsulation of iron to 100% and for zinc, to 52%. The spray drying was proven to be robust, given the strong correlation of the Box-Behnken design (R^2-adj of 87%) and experimental data used to corroborate the predictions of the model.

Furthermore, the yield of the premixes remained higher than 73% for the microencapsulated iron and zinc. This study highlights the use of two accessible GRAS materials as coating agents for the simultaneous microencapsulation of ferrous and zinc sulphate. Furthermore, this is the first study used to assess the microencapsulation of iron or zinc to avoid their interaction with tea polyphenols.

Chapter 3: Bioaccessibility and Release Modelling of Iron and Zinc

Microencapsulation for food fortification is among the best technologies to alleviate micronutrient deficiencies in developed countries. However, the bioaccessibility of the micronutrient premixes is a fundamental parameter to give insight into the overall effectiveness of the fortification strategy. In addition, the release kinetics of iron and zinc premixes to be mixed with food vehicles like salt, rice are of primary interest for many globally active fortification efforts. In this chapter, iron and zinc bioaccessibility and release kinetics were assessed through simulated digestion gastrointestinal (pH 2.0 and pH 6.6) on three optimized microencapsulated formulations containing ferrous and zinc sulphate ranging from 5-10% (w/w) using whey protein isolate (WPI) and Eudraguard® as coating materials. WPI and Eudraguard® ranged from 6-9% and 2% (w/v), respectively. A Caco-2 cell model was used to assess the uptake of iron and zinc from the optimized formulations. The microcapsules released close to 100% of the iron and zinc within 30 min at pH 2.0, and within 45 minutes of intestinal digestion at pH 6.6. Thus, the microcapsules showed higher resistance to intestinal conditions. The Higuchi mathematical model was found to best fit the experimental data for iron and zinc release, suggesting a transport phenomenon governed by the diffusion process through the coating material. The presence of whey protein from the microcapsules increased the uptake of both iron and zinc. Iron uptake increased by 73%, while zinc uptake increased by 81% compared to free zinc and iron. Although gastric emptying time is highly variable depending on the individual and foods being, the stomach emptying time can be as short as 10-15 min in an empty stomach. Thus, these microcapsules could prove more effective in fortified tea if taken with an empty stomach. The results from this study shall guide technology development using proteins that could increase the gastrointestinal conditions and cellular

absorption as well as understanding the complex release process into the release mechanisms of the specific material system used.

3.1 Introduction

Bioaccessibility is defined as the fraction of the compound that is released from its matrix in the gastrointestinal tract, and which thus becomes available for intestinal absorption (Bryszewska et al., 2019; Galanakis, 2017). On the other hand, bioavailability is defined as the fraction of the ingested compound that reaches blood circulation and ultimately is utilized for metabolic processes (Galanakis, 2017). Bioaccessibility can be evaluated by *in-vitro* digestion in simulated gastric and small intestine conditions, and bioavailability by Caco-2 cell uptake (Galanakis, 2017; Jovaní et al., 2001). Recently, this has been emphasized due to issues related to the inflammation of the intestinal tract when high doses of poorly absorbable iron forms are administered (Habeych et al., 2016). Despite iron and zinc being relatively stable at low pH, like in the stomach, the small intestine is a hostile environment because the presence of a more neutral pH can lead to the formation of hydroxide compounds such as ferric hydroxide. These compounds also reduce the absorption of iron and zinc in the small intestine. Thus, several experts agree that bioaccessibility is essential for enabling a successful fortification strategy.

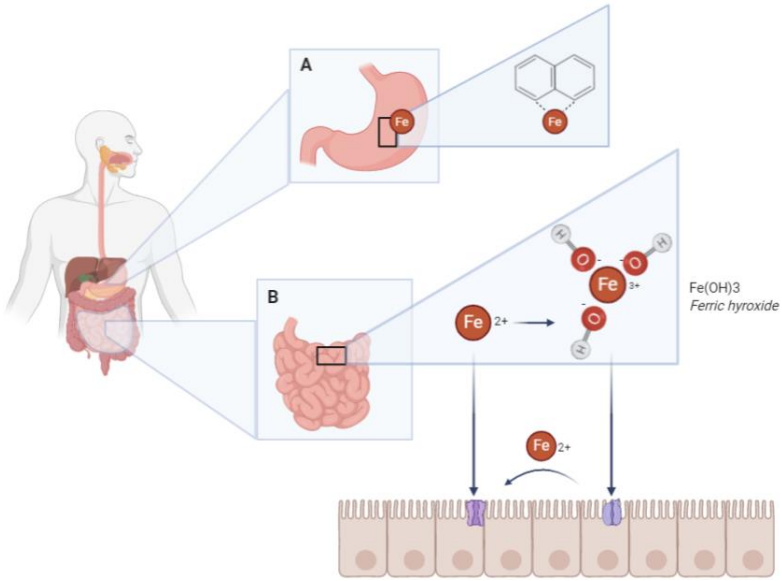

Figure 3-1: Iron Absorption Challenges in the Stomach and Small Intestine.

(A) Polyphenols in the stomach can chelate iron, making it unavailable for absorption. (B) Iron can also form ferric hydroxide ($Fe(OH)_3$), which is less soluble, therefore minimizing its absorption in the intestine. For iron ions, Fe^{3+} must be reduced to Fe^{2+} by reductases such as cytochrome *b* and then absorbed by the divalent metal transporter 1 (DMT1)

Iron chelation by polyphenols in the small intestine depends on the type of polyphenols present and their degree of protonation; thus, it is highly dependent on pH. As the pH increases, the formation of metal-polyphenol complexes increases. The pH effect on iron-polyphenol complex formation is particularly significant in the small intestine because the pH is close to neutral (Preedy, 2013).

Before a drug or compound of interest becomes bioaccessible, it first needs to be released from the microcapsule. In general, water-soluble drugs loaded into systems based on hydrophilic polymers are released from the matrix through water penetration into the matrix. Therefore, the

release of the drug from a polymeric matrix refers to the phenomenon of the migration of an active pharmaceutical ingredient from the interiors of a food matrix to its' surface and then diffusion from the surface to the medium. The release of a drug, or in this case, a micronutrient, is affected by many complex factors, such as the physical and chemical properties of the drug, polymer and surrounding medium, and the possible interactions with these (Freire et al., 2017).

Nevertheless, mathematical modelling can be used to simplify the complex release process and to gain insight into the release mechanisms of a specific material system. The zero-order, first-order, Weibull, Higuchi, and finally, Hixson and Crowell release models have mostly been used in the pharmaceutical industry in the area of drug delivery, but they can also be used in food systems.

The mathematical models allow us to measure critical kinetic parameters, such as the drug diffusion coefficient (Burschi, 2015). Elucidating the kinetics of release of a compound is of interest because it allows for the development of controlled release dosage forms to maintain a stable concentration or to obtain a desired drug release profile for a desired amount of time at the target site (Burschi, 2015; Dash et al., 2010).

The zero- and first-order models are the most common and studied models used in chemical engineering investigations (Pratap-Singh et al., 2018). Other models like the Higuchi model (Higuchi, 1963), Hixson-Crowell model (Hixson & Crowell, 1931), and Weibull model adapted by Lagenbucher (1972), are more sophisticated and can provide more information into the release kinetics. In the end, all of them address the rate of release of a solute from a matrix (Paul, 2011).

Given the importance of an adequate absorption of iron and zinc, the present chapter aims to evaluate the *in-vitro* bioaccessibility of these minerals using simulated gastrointestinal digestion. Furthermore, several studies have reported that whey proteins enhance the bioavailability of metal cations (Gandhi, Banjare, et al., 2019; Nakano et al., 2007; Shilpashree et al., 2018). Therefore, the effect of proteins on iron and zinc bioavailability in Caco-2 cells was also studied. Finally, the release behaviour was characterized by estimating the kinetics of release using the different mathematical models previously described. To achieve this, release behaviour under distinct pH simulating gastric or intestinal conditions were fitted using the mathematical models previously mentioned.

3.2 Materials

Ferrous sulphate and zinc sulphate heptahydrate were purchased from Fisher Scientific (U.S.A). For the gastrointestinal digestion, NaCl and $CaCl_2$ were purchased from Fisher Scientific (U.S.A). Pepsin was purchased from Ward's Science (Canada), while pancreatin was obtained from Sigma-Aldrich (U.S.A). The Caco-2 cells (HTB-37™) and the HepG2 (HB-8065™) cells were purchased from the American Type Culture Collection (ATCC®, U.S.A). The six-well Transwell® plate and the Transwell® membrane chain inserts (24 mm 0.4µm pore size) were purchased from Costar Corp (U.S.A). The reagents used for cell culture and maintenance, such as Dulbecco's Modified Eagle Medium (DMEM), fetal bovine serum, HEPES buffer Dulbecco's phosphate-buffered saline (DPBS) were all purchased from Sigma-Aldrich (U.S.A). The MTT reagent was also purchased from Sigma-Aldrich (U.S.A). Distilled and deionized water was used for all experiments.

3.3 Methods

3.3.1 Microcapsule preparation

The microencapsulated iron and zinc used in this study was prepared based on method 2.3.2 and 2.3.3 of Chapter 2. Briefly, 2% (w/v) of Eudraguard® (Evonik Industries, Switzerland) was dissolved in 200 ml of water. The mixture was heated to 90ºC for 10 minutes under agitation to allow Eudraguard® to dissolve completely. After heating, Eudraguard® was left to cool to 25ºC in ice. After, 6% and 9% (w/v) of WPI (Canadian Protein, Canada) was added and left for 5 minutes under agitation. Finally, 5%, 7% and 10% of iron and zinc (w/w) based on the WPI concentration were added. The mixed solution was then left to homogenize with agitation at 300 rpm for 5 minutes before spray drying using a B-290 Büchi Mini Spray Dryer (Buchi® Labortechnik AG, Switzerland). Aspiration was maintained at 100% (35m^3/h) to maximize the separation rate of the cyclone (Büchi, 2019), and spray gas flow rate or Q-flow was set to 40mm Hg or 473 L/h. The feed pump rate was set to 6 mL/min or 20% of the feed pump rate. The inlet temperature was set at 150˚C.

3.3.2 Determination of Iron and Zinc Content

The iron and zinc content of the microcapsules was measured using atomic absorption spectroscopy (AAS) using an Agilent 55B AA spectrometer (Agilent Technologies) available from the UBC Chemistry Department. Calibration curves for iron quantification were made by diluting a 1000 ppm iron standard in 2% HNO_3 (Ricca Chemical Company, U.S.A) to concentrations of 0.2 ppm, 0.5 ppm, 1 ppm, 5 ppm, and 10 ppm. Similarly, calibration curves for zinc were made by diluting a 1000 ppm zinc standard in 2% HNO_3 (Ricca Chemical Company, U.S.A) to

concentrations of 0.2 ppm, 0.5 ppm, 1 ppm, 1.5 ppm, 3 ppm, and 5 ppm for zinc. The calibration points were within the range of the maximum and minimum quantity of iron and zinc.

3.3.3 *In-vitro* Bioaccessibility by Simulated Gastrointestinal Digestion

In-vitro gastrointestinal assay was performed in a two-step approach by simulating the pH and enzymatic activity of the (1) stomach and (2) small intestine (duodenum and jejunum). This method, and the composition of the gastric and intestinal fluid is based on the work of Singh & Kitts (2019) with some modifications.

For the gastric digestion phase, 100 mg of microparticles were added into a plastic micromesh tea bag and then submerged in 100 ml of prepared gastric fluid for 1 hr at 37˚C and 80 rpm in a C25KC incubator shaker (New Brunswick Scientific, U.S.A). Before adding the microcapsules, the gastric fluid was left 2 hr at 37ºC. Samples of 1 ml were taken at 5, 10, 20, 30, 45 and 60 minutes. The plastic tea bag prevented from extracting the microcapsules that had not yet released the iron and zinc when taking the sample, thus minimizing error when quantifying the iron and zinc released. Samples were immediately centrifuged at 5000 rpm and 4ºC using a Sorvall Legend X1R Centrifuge (Thermo Scientific, U.S.A) and then kept in ice. This ensured that most of the enzyme is removed, and any remaining enzyme stops its hydrolytic activity at the time of sample collection. When collecting the samples, the pH was measured and readjusted to pH 2.0 with 0.1N HCl (Sigma-Aldrich, U.S.A) using an Accumet® AE 150 pH meter (Fisher Scientific, U.S.A). The gastric fluid was prepared by adding 2.0 g/L of NaCl (Fisher Scientific, U.S.A) and 1.0 g/L of pepsin (Ward's Science, Canada) in 1000 ml of double-distilled water. The gastric fluid was initially adjusted to pH 2.0 using 1N HCl and prepared before each experiment.

For the intestinal digestion phase, 100 mg of microparticles were also added into a plastic micromesh tea bag and then submerged in 100 ml of prepared intestinal fluid for 2 hr at 37˚C and 80 rpm in a C25KC incubator shaker (New Brunswick Scientific, U.S.A). Before adding the microcapsules, the intestinal fluid was left 2 hr at 37ºC. Samples were immediately centrifuged at 5000 rpm and 4ºC and then kept in ice. The pH was measured and readjusted to pH 6.6 with 0.1N NaOH (Anachemia, U.S.A) after taking each sample. The intestinal fluid was prepared before each experiment by adding 0.2 g/L of $CaCl_2$ (Fisher Scientific, U.S.A) and 3.0 g/L of pancreatin (Sigma-Aldrich, U.S.A) in 1000 ml of double-distilled water. The intestinal fluid was initially adjusted to pH 6.6 using 0.1N NaOH and was left 2 hr at 37ºC before adding the microcapsules.

The simulated gastric and intestinal digestion was performed in triplicates. The remaining intestinal digestion product was stored at -20ºC for use in the *in-vitro* bioaccessibility assay with the Caco-2 cells.

3.3.4 *In-vitro* Bioaccessibility by Caco-2 Cell Uptake

3.3.4.1 Cell Culture

The Caco-2 cells were purchased from the American Type Culture Collection (ATCC® HTB-37™). The cells were seeded at a density of 50,000 cells/cm^2 per filter in six well-plate polyester membrane chamber inserts (24 mm 0.4µm pore size; Transwell®, Costar Corp, U.S.A) in Dulbecco's Modified Eagle Medium (DMEM) (Sigma-Aldrich, U.S.A) with 10% v/v fetal bovine serum (Sigma-Aldrich, U.S.A), 25 mmol/L HEPES (Sigma-Aldrich, U.S.A) and 1% antibiotic antimycotic solution (Sigma-Aldrich, U.S.A). The cells were maintained at 37˚C, 5% CO_2 and

95% air atmosphere at constant humidity using an MCO-17AC CO_2 incubator (Sanyo Electric Biochemical, Japan)**.** The growing medium was changed every two days. The cells were used for experiments at 21 days post-seeding to ensure spontaneous differentiation of cells into a monolayer of enterocytes. This method was based on the work by García-Nebot et al. (2013) with some modifications.

3.3.4.2 Iron and Zinc Retention, Transport and Uptake in Caco-2 cells

This method and equations are based on the work of Jovaní et al. (2001). The iron and zinc cell retention, transport, and uptake (retention plus transport) were quantified using the product of the simulated intestinal digestion. The intestinal digestion product was treated for 10 minutes at 90ºC in a heated water bath and left to cool to 37ºC before adding it to the Caco-2 cells. This step was taken as a precaution to prevent the pancreatin present in the intestinal product from interfering with the cellular uptake.

Twenty-one days after initial seeding, spent culture medium was aspirated from the apical and basolateral chambers. The apical (cell monolayer) and basolateral surfaces were washed three times with Dulbecco's phosphate-buffered saline (DPBS, Sigma-Aldrich, U.S.A) at 37ºC. The basolateral chamber was filled with 2.5 ml of double-distilled water, and the apical compartment was filled with 1.5 ml of the intestinal digestion product. Retention and transport were measured after 2 hr of incubation at 37˚C, 5% CO_2 and 95% air atmosphere at constant humidity.

After incubation, 1 ml of sample from the basolateral and apical chamber was collected. Subsequently, the cell monolayer was washed three times with DPBS to remove any residual iron and zinc that was not taken by the cells and to remove any excess growth medium. After the cells

were lysed with 1.5 ml of 2% (w/v) SDS (Anachemia, U.S.A), 1 ml of sample was collected to determine mineral retention. The same procedure was followed with cells incubated with a blank solution in the basolateral and apical chambers. Differences between the iron and zinc content of the cell monolayer and the basolateral and apical chambers were used to calculate the iron and zinc uptake by the cells. The iron and zinc content of each sample was quantified using AAS, as described in method 3.3.2.

Retention percentages of iron and zinc were calculated according to the following equation:

$$Retention\ (\%) = \frac{C - C_{blank}}{T}\ x\ 100$$

Equation 3-1: Retention of Iron and Zinc

Where C = iron and zinc content in the cell monolayer, C_{blank} = iron and zinc content in the cell monolayer of the blank, and T = total iron and zinc present in the intestinal product added.

On the other hand, transport percentages of iron and zinc were calculated according to the following equation:

$$Transport\ (\%) = \frac{B - B_{blank}}{T}\ x\ 100$$

Equation 3-2: Retention of Iron and Zinc

Where B = iron and zinc content in the basolateral chamber, B_{blank} = iron and zinc content in the basolateral chamber of the blank, and T = total iron and zinc present in the intestinal product added.

The uptake is the addition of the iron or zinc present in the cells, plus the iron and zinc transferred from the cells to the basolateral chamber. Therefore, the uptake is defined with the following equation:

$$Uptake\ (\%) = Retention + Transport$$

Equation 3-3: Uptake of Iron and Zinc

3.3.4.3 MTT Cell Viability Assay

A methyl thiazolyl tetrazolium (MTT) cell viability was performed using HepG2 cells with the product of the intestinal digestion. The cells were incubated for 72 hrs at 37˚C, 5% CO_2 and 95% air atmosphere and constant humidity using an MCO-17AC CO_2 incubator (Sanyo Electric Biochemical, Japan). To investigate the impact of the microcapsules on cell viability, 1.5×10^4 cells per well were seeded in 96-well plates and incubated for 2 h. DMEM culture medium without the intestinal product of the microcapsule's digestion was used as a control. After 2 h of incubation, the cells were washed with 200 μL of DPBS (Sigma-Aldrich, U.S.A) at 37ºC. The medium containing MTT (200 μL, 5 mg mL−1 MTT in DMEM) was added to each well. After 4 h of incubation, the medium was removed, and 200 μL of 2% SDS (Anachemia, U.S.A) was added to dissolve the formed formazan crystals. Absorbance was measured at 570 nm using an infinite M200 Pro UV-Vis spectrophotometer (Tecan, U.S.A)**.** Cell viability (%) was calculated by dividing the absorbance of each cell well that was incubated with the microcapsules divided by the absorbance of the cell control. This method is based on the work of Shao et al. (2018).

3.3.5 Statistical Analysis

Each series of the assays described represent three replicates of the experimental protocol. All data in this chapter was analyzed in Microsoft Excel (version 1908, Microsoft). The retention, transport,

and uptake were analyzed with the student's t-test ($p < 0.05$) to determine if they were significantly different from each other. Microencapsulated iron and zinc release were fitted to the five most common mathematical models that assess the kinetics of the release of a compound of interest, as shown below.

The zero-order model (Equation 3-4) was used to describe the linear fitting between the release of iron/zinc and time:

$$Y = K_0 t + C_0$$

Equation 3-4: Zero-order Model.

Where *Y* is the percentage (w/w) of the iron and zinc at any specific time *t*, K_0 and C_0 are the slope of the intercept of the *y*-*t* curve, respectively.

The first-order model used describes the release by plotting the natural logarithm of the percentage of iron left in the microcapsule with time:

$$\ln(100 - Y) = K_1 t + C_1$$

Equation 3-5: First-order Model.

Where *Y* is the percentage (w/w) of the released iron and zinc at any specific time *t*, K_1 and C_1 are the slope of the intercept of the ln(100- *y*) vs. *t* curve, respectively.

The Weibull used was adapted from the original Weibull model (1951) to the release process by Lagenbucher (1972). The adapted Weibull model is described in the following equation:

$$log\left[-\ln\left(1 - \frac{Y}{100}\right)\right] = b\ logt - \log a$$

Equation 3-6. Adapted Weibull Model.

Where *Y* is the percentage (w/w) of the released iron and zinc at any specific time *t*, while *b*, and -log *a* are the slope and the intercept of the [-ln(1-*Y/100*)] vs. log *t* curve, respectively.

The Higuchi model describes a linear relationship between the release of iron and zinc and time:

$$Y = K_h t^{0.5}$$

Equation 3-7: Higuchi Model.

Where *Y* is the percentage (w/w) of the released iron and zinc at any specific time *t*, K_h is the slope of the log *Y* vs. $t^{0.5}$ curve, respectively.

Finally, the Hixson and Crowell model used describes the cubic root of the iron left in the matrix with respect to time:

$$(100 - Y)^{1/3} = K_s t + C_s$$

Equation 3-8: Hixson & Crowell Model.

Where *Y* is the percentage (w/w) of the released iron and zinc at any specific time *t*, K_s and C_s are the slope of the intercept of the $(100\text{-}Y)^{1/3}$ vs. *t* curve, respectively.

The R^2-adjusted was used to assess the goodness-of-fit of the kinetic release models. Student's t-test was conducted for comparing two sets of data to determine if they were significantly different from each other. All experimental results were expressed as mean ± standard deviation.

3.4 Results and Discussion

3.4.1 Bioaccessibility of Iron and Zinc in Simulated Gastric and Intestinal Conditions

The percentage of iron released from the microcapsules in pH 2.0 solution is shown in Figure 3-2A. As previously mentioned, this pH is used as an estimate of simulated gastric acid. Most of the microcapsules released close to 100% of the iron within 30 min at pH 2.0. All formulations

showed a sharp release of iron almost within the first 10 minutes of gastric digestion, releasing between 60 to 65% of the iron.

Figure 3-2B shows the percentage of zinc release from the microcapsules at pH 2.0. The zinc release also showed a sharp release within the first 10 minutes of gastric digestion. However, unlike the iron release, 65 to 75% of zinc was released in the first 10 minutes. This could be attributed to the low encapsulation efficiency of zinc; thus, at the initial time, more zinc is already released. The same behaviour is seen at pH 6.6 or intestinal conditions.

Formulation A and Formulation B have very similar release profiles for both iron and zinc, as shown in the sigmoidal shape of the release curve in gastric conditions. The similarities in their release profile could be attributed to the amount of WPI and Eudraguard®, which are present in similar quantities in both formulations (see Table 2-4 and Table 2-5). The only difference is that the iron loading is lower in Formulation A.

Formulation C at 20 minutes reached 100% iron and zinc release, while Formulation A and B obtained 85% iron release and 95% zinc release during the same time. The difference in release could be explained by the amount of Eudraguard® relative to its WPI composition. Eudraguard® is composed of a modified starch (exact composition not disclosed by manufacturer), which provides resistance to gastrointestinal conditions (Barbosa et al., 2017; Demetriades & Williams, 2016; Evonik, 2018). Formulation C has less Eudraguard® relative to its WPI composition compared to Formulation A and B, as shown in Table 2-4. The higher amount of WPI of the microcapsules could make the microcapsule formulation particularly favourable for proteolytic

hydrolysis by the pepsin enzyme present in the artificial gastric juice. Therefore, the faster release of iron and zinc in Formulation C is attributed to less coating material resistant to gastric conditions (Eudraguard®) and a higher presence of whey proteins present at the surface of the microcapsule.

Lambert et al. (2008) microencapsulated a bile salt hydrolase enzyme using whey proteins and gum arabic. The study found that these microcapsules remain stable in simulated intestinal conditions (pH 2.0, 15 min). It seems that the gelling of the gum arabic in acidic environments and the reported acid resistance of the whey protein protected the enzyme from gastric conditions. Even though these results appear encouraging, again, the use of appropriate simulated conditions is of great importance. The time in the simulated gastric fluid was significantly reduced to 15 min, compared to 2 h recommended by the USP (United States Pharmacopeia). However, literature on the use of WPI for enteric coatings is still scarce and is a possible avenue for further development.

A

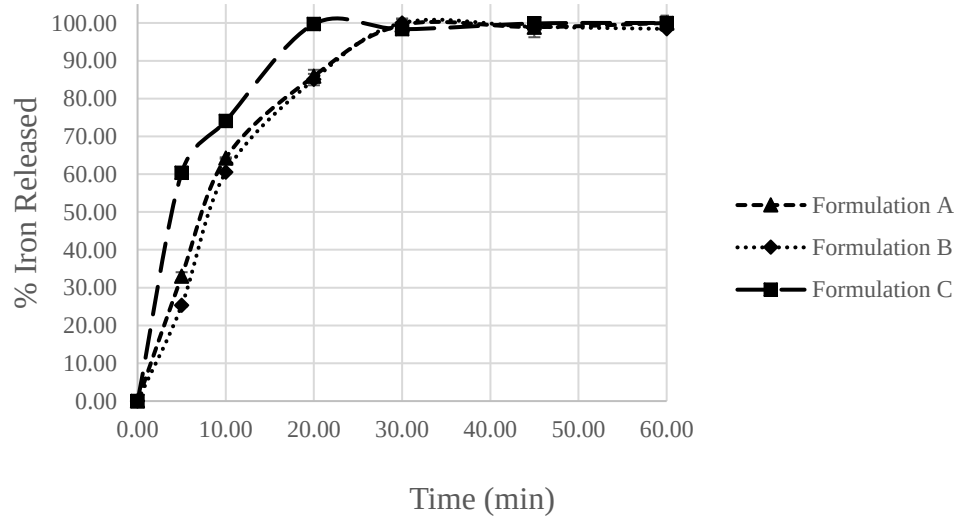

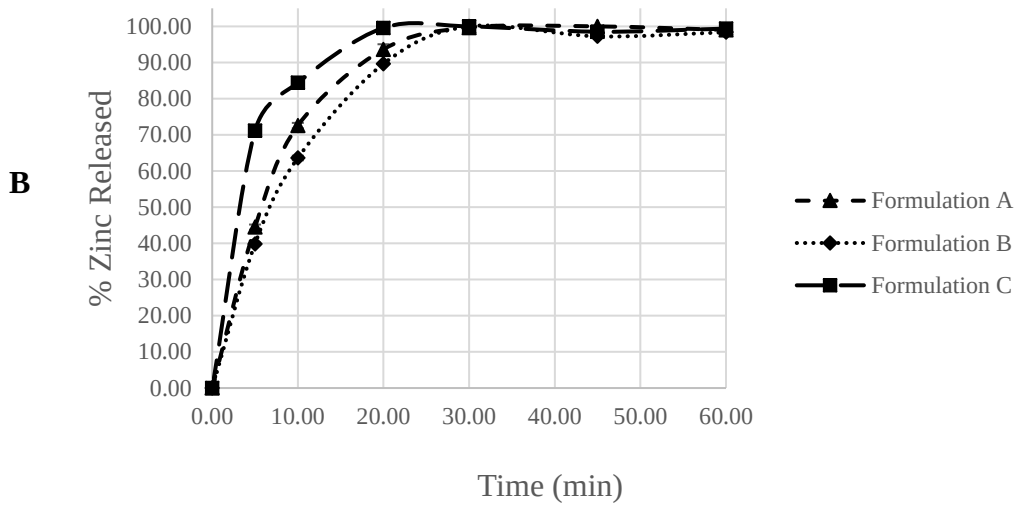

Figure 3-2: Iron(A) and Zinc (B) Released from Microcapsules at pH 2.0 or Gastric Conditions.

Figure 3-3A and B depict the iron and zinc release at pH 6.6, respectively. pH 6.6 is representative of the duodenum and jejunum, which are the segments of the small intestines where iron and zinc is absorbed. Additionally, this pH also represents the pH of water when cooking/processing and the pH of human saliva, which can vary from pH 5.9 to pH 7.9 (Pratap-Singh et al., 2018).

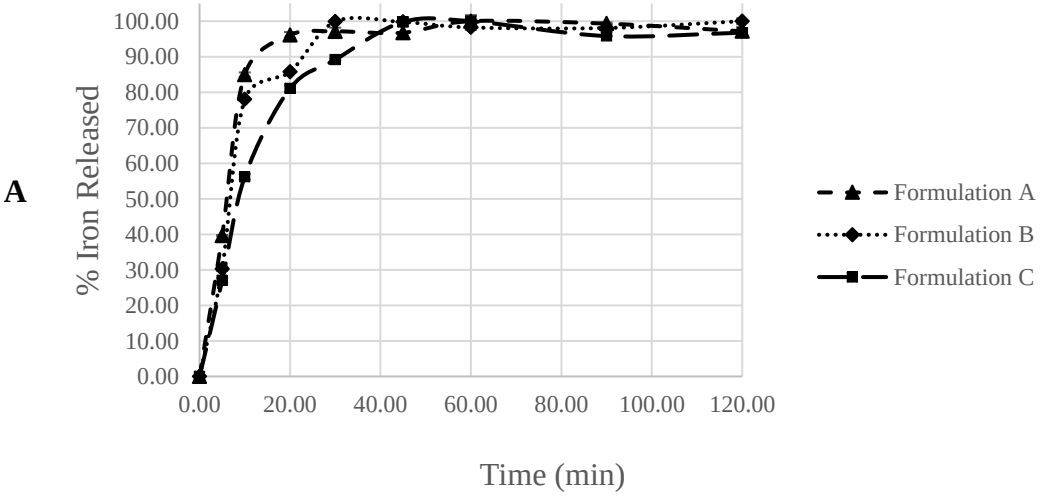

B

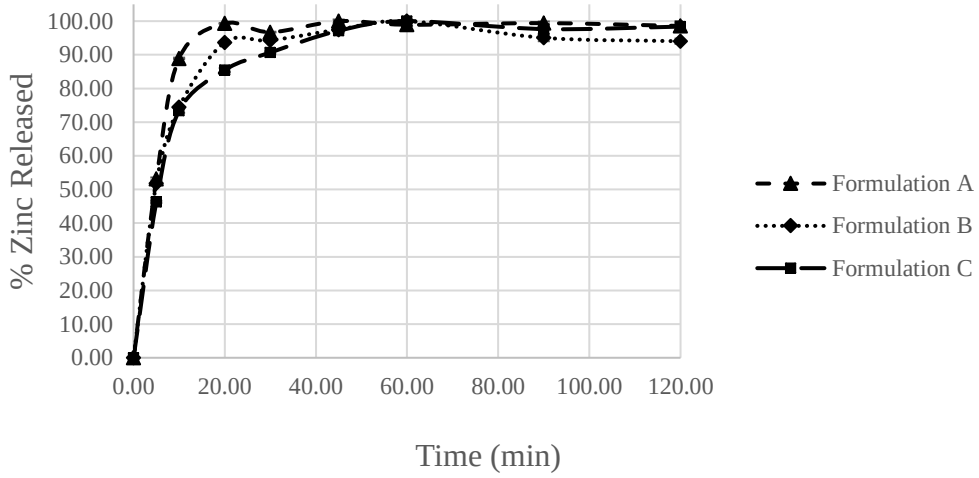

Figure 3-3: Iron(A) and Zinc (B) Released from Microcapsules at pH 6.6 or Intestinal Conditions

The iron and zinc release at intestinal conditions showed a similar sharp release profile compared to their release in gastric conditions. After 10 minutes of intestinal digestion, 25 to 40% of iron was released, while 45 to 60% of zinc was released. All formulations achieved 100% iron and zinc release after 45 minutes of intestinal digestion. At gastric conditions, 100% iron and zinc release was achieved after 30 minutes. Thus, the microcapsules showed higher resistance to intestinal conditions.

Unlike in gastric conditions, Formulation C showed a slower release at pH 6.6. This behaviour can be seen by the percentage release after 20 minutes, where 100% of the iron and zinc were released in gastric conditions, while 80 to 85% of iron and zinc were released in intestinal conditions. This behaviour was not observed in Formulation A and B in which after 20 minutes of intestinal and gastric digestion, 85 to 95% of iron and zinc is released.

In-vitro bioaccessibility was calculated as the percentage of iron or zinc released after 30 min, which is the approximate minimal time spent by food in the stomach (Pratap-Singh et al., 2018).

For all formulations, the bioaccessibility of iron and zinc is 100% in both gastric and intestinal conditions.

Ideally, once the iron or zinc is released in the stomach, it should remain available for absorption in the intestine. Regarding iron and zinc fortification with microencapsulation, the best approach is that the micronutrient is released from the microcapsule shortly after it moves to intestinal conditions. The approximate minimum time food spends in the stomach is 30 min and can last as much as 4 hr (Degen & Phillips, 1996; Hellmig et al., 2006). The absorption of iron and zinc occurs at intestinal conditions; therefore, a feasible approach involves using a coating material that remains stable during gastric conditions, but that releases its encapsulated compounds once the pH changes to intestinal conditions. Eudraguard® can provide such characteristics (Barbosa et al., 2017); however, this was not observed in the prepared microcapsules. If Eudraguard® was used in higher quantities, it could be expected that the microcapsules are more resistant to gastric conditions. According to a patent by Demetriades & Williams (2016); they formulated a microcapsule containing Eudraguard® as their coating material to target minimal release (less than 20%) at pH 1.2 for 2 hours, and the other is manufactured for complete release (at least 80%) at pH 6.5 over 3 hours. However, the exact composition of the microcapsules, the encapsulated compound and other details in the patent are not disclosed.

Based on the iron and zinc release observations for pH 2.0 and pH 6.6, all formulations resulted in an *in-vitro* bioaccessibility of 100% in 30 minutes. While iron and zinc sulphate used in this study remains highly stable under gastric conditions (Johnson et al., 2012), the microcapsules could provide some protection in that period. When the stomach is empty, the stomach emptying time

can be as short as 10-15 min (Barbosa et al., 2017; Ziessman et al., 2009). Thus, these microcapsules could be used for fortifying tea when taken in an empty stomach.

On the other hand, the intestinal residence time is also highly variable and dependent upon many factors (Barbosa et al., 2017). However, the high *in-vitro* bioaccessibility of iron and zinc for all formulations under intestinal conditions is desirable because iron and zinc are absorbed right after gastric emptying, in the duodenum and upper part of the jejunum.

3.4.2 Release Kinetics in Gastric and Intestinal Conditions

The fitted parameters for iron release are shown in Table 3-1 . The mean of the R^2-adjusted in gastric conditions of the zero-order model was 0.56 ± 0.09, respectively. The first-order model obtained a mean R^2-adjusted of 0.62 ± 0.35. On the other hand, at intestinal conditions, the R^2-adjusted of the zero-order model was 0.34 ± 0.07, while the first-order model was 0.28 ± 0.24. The low value of these coefficients suggest that the zero- and first-order models could not produce a good fit for the release behaviour in gastro-intestinal conditions because the acceptable range for R^2 is > 0.7 (Pratap-Singh et al., 2018). On the other hand, the fitted parameters for zinc release are shown in Table 3-2. The zero- and first-order models resulted in a bad fit for the release behaviour in gastrointestinal conditions, which is reflected in a mean R^2-adjusted below 0.62 at gastric conditions and mean R^2-adjusted below 0.33 at intestinal conditions in both models.

The Weibull model gave the best fit for iron release with a mean R^2-adjusted of 0.85 ± 0.10 at gastric conditions, while the mean R^2-adjusted at intestinal conditions was 0.66 ± 0.07. Unlike in the iron release kinetics, the zinc release did not fit the Weibull model best. The Weibull model

obtained a mean R^2-adjusted of 0.64 ± 0.14 at gastric conditions, while the mean R^2-adjusted at intestinal conditions was 0.53 ± 0.07.

The Hixson-Crowell obtained a low mean R^2-adjusted (< 0.7) in gastric and intestinal conditions for both iron and zinc release, suggesting it is a bad model fit for the release process of these minerals. The Hixson and Crowell model assumes that the release of the drug due to the diminishing surface of the matrix, while the Higuchi model assumes that the release is through a diffusion process. Both the Hixson-Crowell and Higuchi models are used for modelling the release behaviour of microencapsulated iron (Pratap-Singh et al., 2018). Nevertheless, they cannot be compared because the physical phenomena that govern their mathematical assumptions are different.

Although the Weibull model resulted in the best fit, and it is a mathematical model used to describe matrix systems, the Weibull model is not recommended to model a release process in a microencapsulated. Its limitation arises in *in-vitro/in-vivo* models because the model lacks the kinetic dissolution properties of the drug due to the absence of any single parameter related to the dissolution rate of the drug (Burschi, 2015; Papadopoulou et al., 2006; Pratap-Singh et al., 2018).

In terms of the absolute value of the R^2-adjusted means, the fitting order of the models in gastric and intestinal conditions for iron release is: Weibull > Higuchi > Hixson-Crowell > First-order > Zero-order. For the zinc release, The models fitted order of the gastric and intestinal release as follows: Higuchi > Weibull > Hixson-Crowell > First-order > Zero-order.

On one side, the iron release was best explained by the Weibull model, while the Higuchi model best explained the zinc release. The question that remains is which model best described the release kinetics of the system between the Higuchi and the Weibull models. While comparing the iron and release with the Weibull and Higuchi models, the Higuchi model produced similar mean R^2-adjusted coefficients. The mean R^2-adjusted of the Higuchi model was 0.81 ± 0.09 and 0.49 ± 0.14 at gastric and intestinal conditions. The mean R^2-adjusted of the Weibull model was 0.85 ± 0.10 at gastric conditions, while the mean R^2-adjusted at intestinal conditions was 0.66 ± 0.07.

Because the Higuchi model was developed to describe the drug release as a diffusion process based on Fick's law; it is commonly used in to study the release of water-soluble drugs incorporated into semi-solid and solid matrices (Paul, 2011; Pratap-Singh et al., 2018) of sphere morphology (Freire et al., 2017). In the pharmaceutical industry, the Higuchi model describes the release of a drug in transdermal systems and matrix tablets with water-soluble drugs (Pratap-Singh et al., 2018). The microencapsulated iron and zinc coated with WPI and Eudraguard® resembles the latter case. Given the limitations of the Weibull model despite its best fit based on the mean R^2-adjusted in both gastric and intestinal conditions, and because the Higuchi model best characterizes the drug release system, the Higuchi model was found to fit the iron and zinc release from the microcapsules best.

In the Higuchi model, the square of the Higuchi dissolution constant (K_h) is directly related to the diffusivity of the solute or drug from the matrix or coating material (Pratap-Singh et al., 2018); therefore, a higher value of K_h results in a higher diffusion of the drug from the matrix to the surrounding fluid. The relation between the dissolution constant and diffusivity depends on the

type of material and its surface properties such as morphology and size (Pratap-Singh et al., 2018). Based on the K_h values of the Higuchi model, at gastric conditions, the mean K_h = 15.77 ± 0.5 while at pH 6.6 or intestinal conditions, K_h = 12.24 ± 0.5. Therefore, at intestinal conditions, iron is released slower. This release behaviour is desired and is consistent with the results described in the previous section.

Amongst the optimized Formulations A, B and C (Table 3-1) in gastric conditions, Formulation A and B, which were composed of 6% WPI, 2% Eudraguard® and 5% Fe/Zn Loading, and 6% WPI, 2% Eudraguard® and 10% Fe/Zn Loading resulted in the largest diffusion constant (K_h = 15.31 and K_h = 15.55). They also did not provide the slowest release in intestinal conditions (K_h =12.37). In contrast, Formulation C, which was composed of the highest concentration of WPI (9%), and 2% Eudraguard® and 7% Fe/Zn Loading, resulted in the lowest diffusion constant (K_h = 11.85) for iron at intestinal conditions.

Based on the K_h values of the Higuchi model for zinc release, at gastric conditions, the mean K_h = 16.15 ± 0.48 while at pH 6.6 or intestinal conditions, mean K_h = 12.39 ± 0.5. Therefore, at intestinal conditions, zinc is released slower. This release behaviour is desired and is consistent with the result described in the previous section. Compared to the K_h of iron release, both are very similar. The similarity in results is not surprising as both iron and zinc are in high water solubility form and are protected with the same materials under the same conditions. The similarity among the K_h values for the iron and zinc release process suggests that this model fits well for both components.

Amongst the optimized Formulations A, B and C (Table 3-2) in gastric conditions for zinc release; Formulation C, which was composed of the highest concentration of WPI (9%), and 2% Eudraguard® and 7% Fe/Zn Loading, resulted in the highest diffusion constant (K_h = 16.76). However, this same formulation resulted in the lowest diffusion constant (K_h = 12.22) at intestinal conditions. These calculations confirm the results found in the previous sections.

Despite the limitations of the Weibull model and its low model fit compare to the Higuchi model, it can still also be used to describe other deductions in the release system. In the Weibull model, a value < 1 in the *b* parameter or constant suggests that the dissolution profile is parabolic, meaning that the drug release has a higher initial slope and after, the release adopts an exponential shape (Paolino et al., 2019; Papadopoulou et al., 2006). For both iron zinc release at intestinal conditions, these values are below one, indicating that the iron and zinc release increases exponentially with time. This is desirable because both iron and zinc are absorbed right after it passes gastric conditions in the duodenum and upper jejunum. If the iron is not released in this small segment of the small intestine before passing to the large intestine to be excreted, the absorption window can be lost.

Model		**Zero Order**				**First Order**				**Higuchi**			**Hixson-Crowell**				**Weibull**			
	pH	K_0	C_0	R^2	R^2 adj	K_1	C_1	R^2	R^2 adj	K_h	R^2	R^2 adj	K_0	C_0	R^2	R^2 adj	b	a	R^2	R^2 adj
Formulation A (6.2% WPI, 2% Eudraguard®, 5% Fe/Zn loading)	2.0	1.46	33.35	0.68	0.62	-0.17	5.27	0.88	0.86	15.55	0.89	0.87	-0.07	4.15	0.90	0.88	1.27	19.17	0.96	0.95
	6.6	0.50	57.71	0.35	0.25	-0.04	2.64	0.23	0.12	12.50	0.61	0.55	-0.02	2.98	0.44	0.36	0.65	3.07	0.64	0.58
Formulation B (6% WPI, 2% Eudraguard®, 10% Fe/Zn loading)	2.0	1.51	30.13	0.69	0.63	-0.10	3.61	0.28	0.14	15.31	0.88	0.86	-0.07	4.01	0.69	0.62	1.21	18.10	0.76	0.70
	6.6	0.57	52.51	0.41	0.33	-0.07	3.67	0.67	0.62	12.37	0.68	0.63	-0.03	3.24	0.58	0.52	0.88	6.80	0.79	0.75
Formulation C (9% WPI, 2.3% Eudraguard®, 7% Fe/Zn loading)	2.0	1.22	46.50	0.52	0.43	-0.17	4.51	0.90	0.88	16.46	0.79	0.75	-0.07	3.61	0.78	0.73	0.99	5.57	0.91	0.89
	6.6	0.63	45.33	0.50	0.43	-0.04	3.04	0.20	0.09	11.85	0.76	0.73	-0.03	3.45	0.48	0.41	0.87	8.66	0.71	0.66

Table 3-1: Parameters and Coefficients of the Fitted Models Tested of Microencapsulated Iron Release

Model		**Zero Order**				**First Order**				**Higuchi**			**Hixson-Crowell**				**Weibull**			
	pH	K_0	C_0	R^2	R^2 adj	K_1	C_1	R^2	R^2 adj	K_h	R^2	R^2 adj	K_0	C_0	R^2	R^2 adj	K_0	C_0	R^2	R^2 adj
Formulation A (6.2% WPI, 2% Eudraguard®, 5% Fe/Zn loading)	2.0	1.33	40.51	0.59	0.51	-0.14	4.10	0.56	0.47	16.07	0.84	0.81	-0.07	3.78	0.75	0.70	1.06	8.45	0.86	0.82
	6.6	0.46	62.23	0.31	0.21	-0.03	1.88	0.16	0.04	12.72	0.57	0.51	-0.02	2.69	0.37	0.28	0.53	1.70	0.55	0.47
Formulation B (6% WPI, 2% Eudraguard®, 10% Fe/Zn loading)	2.0	1.38	36.26	0.64	0.57	-0.09	3.42	0.24	0.08	15.61	0.87	0.85	-0.06	3.83	0.64	0.57	0.97	7.95	0.69	0.61
	6.6	0.47	58.05	0.34	0.25	-0.03	2.69	0.14	0.02	12.23	0.62	0.56	-0.02	3.02	0.35	0.26	0.53	2.26	0.53	0.45
Formulation C (9% WPI, 2.3% Eudraguard®, 7% Fe/Zn loading)	2.0	1.08	52.77	0.43	0.31	-0.09	2.57	0.27	0.12	16.76	0.70	0.64	-0.05	3.16	0.54	0.45	0.66	1.91	0.59	0.49
	6.6	0.54	53.84	0.44	0.36	-0.04	3.16	0.26	0.16	12.22	0.71	0.67	-0.03	3.32	0.57	0.51	0.67	3.83	0.72	0.67

Table 3-2: Parameters and Coefficients of the Fitted Models Tested of Microencapsulated Zinc Release

3.4.3 Bioaccessibility of Iron and Zinc in Caco-2 Cells

Iron and zinc uptake by the Caco-2 cells are shown in Table 3-3 and Table 3-4, respectively. Cell viability after 2 h of exposure to the intestinal product (uptake solutions) was assessed by performing an MTT assay as described in method 3.3.4.3. Cell viability was above 75% for all cell wells.

Two controls were assessed. Control I either contained iron *or* zinc, while Control II contained iron *and* zinc. It is well known that iron and zinc absorption is reduced in a dosage-dependent manner if both are present in the same solution (Cámara et al., 2007; Failla, 1995; Gropper et al., 2008; Jovaní et al., 2001). Therefore, the two controls provide a point of reference when investigating the effect of the whey proteins present in the microcapsule and its effect on iron and zinc cellular uptake.

On average, the uptake of iron is reduced by 51% in the presence of zinc. According to a study, zinc reduced iron uptake by 80% at a molar ratio of 2.5:1 (zinc:iron) and by 66% when it was present in solution in a molar ratio of 1:1 (zinc:iron) (Crofton et al., 1989). The latter resembles the molar ratio used in this study, providing very similar results. On the other hand, the overall uptake of zinc in the presence of iron is reduced by 32%. This is shown in the results in Table 3-4. Iron and zinc compete for the same protein carriers known as carrier-mediated transport proteins. Nevertheless, this antagonistic effect also depends on the affinity of these divalent cations by the carrier-mediated transport proteins. In general, the affinity of the transport proteins in the brush border to divalent cations are as follows: $Cu^{2+} > Zn^{2+} > Fe^{2+} > Mn^{2+} > Ca^{2+} > Mg^{2+}$ (Cámara & Amaro, 2003). Zinc has more affinity for the transport proteins involved, and this confirms the

results obtained previously, where zinc uptake is less affected than iron in the presence of each other in the same solution.

On the other hand, the presence of protein (whey protein) from the microcapsules increased the uptake of both iron and zinc. Given that the concentration of iron in the basolateral chamber was below the limit of detection, the uptake is the same as the retention, 58% ± 2.41. Iron retention from the prepared microcapsules (iron within the Caco-2 cells), on average, was 58% ± 2.41. This represents a 73% increase in iron retention compared to free iron and zinc present in the same solution without the presence of whey proteins from the microcapsules. Zinc retention also increased. Zinc retention in the cells from the prepared microcapsules was, on average, 71.20% ± 5.74. The zinc concentration in the basolateral chamber below the limit of detection; therefore, the uptake of zinc is 71.20% ± 5.74. Zinc uptake increased by 81% compared to free zinc and iron present in the same solution without the presence of whey proteins from the microcapsules.

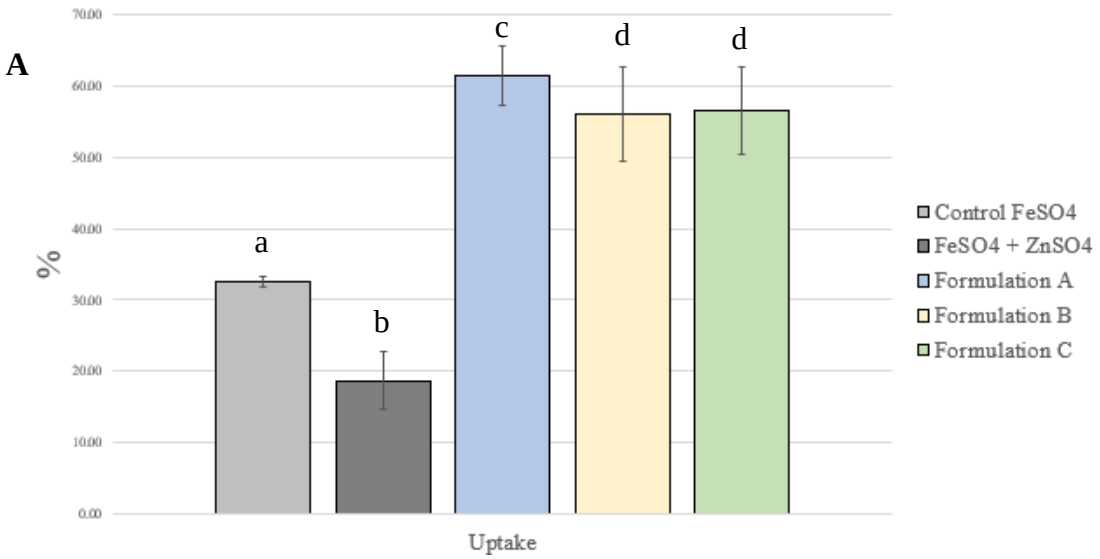

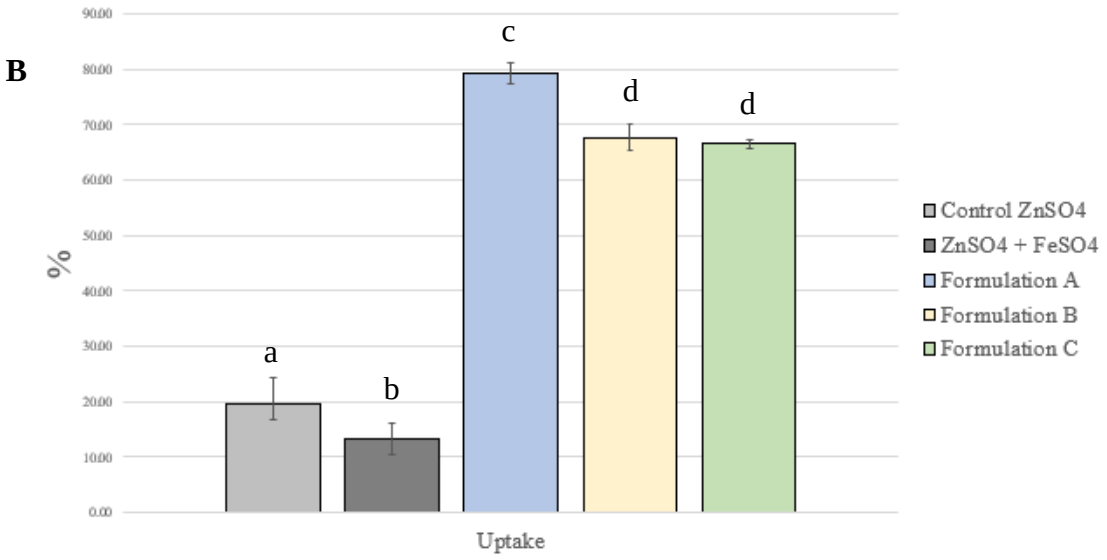

Figure 3-4: Iron (A) and Zinc (B) Uptake in Caco-2 cells. Different letters (a-d) indicate statistically significant differences ($p < 0.05$).

Caco-2 cells have been extensively used and are a well established *in-vitro* model to assess human intestinal iron and zinc absorption. On confluence, these cells spontaneously differentiate to exhibit many of the morphological and functional features of normal mature small intestinal enterocytes. As in the human intestine, Caco-2 cells display enhanced transepithelial transport of iron in iron-depleted cells and express divalent metal transporter-1 (DMT-1), duodenal ferrireductase, ferroportin-1 (FPN-1), hephaestin, transferrin receptor-1, and ferritin, which are involved in iron absorption (Kim et al., 2011). The DMT-1 protein transporter is mainly involved in iron and zinc absorption (Yamaji et al., 2001).

For several decades, nutrition researchers have suggested that dietary protein sources positively influence iron and zinc bioavailability. This effect is often referred to as the 'meat-factor.' Although the 'meat factor' remains unclear, it seems that peptides released during the digestion of

proteins bind iron to form complexes within the intestinal lumen, which increases its solubility (Berner & Miller, 1985). This is especially true for proteins with high contents of sulphur-containing amino acids, such as cysteine and methionine. Cysteine, histidine, lysine, and some amino acid mixtures increase iron absorption *in-vivo*. The suggested action of the amino acids is to either chelate the iron (thereby preventing its precipitation or polymerization) or to reduce the iron to the more soluble ferrous form (Kane & Miller, 1984). Cysteine and methionine have sulfhydryl groups of amino acids that reduce ferric iron to its soluble form, ferrous iron (Cámara et al., 2007). Glutathione, a tripeptide containing cysteine, is shown to enhance iron absorption from a vegetable meal (Layrisse et al., 1984). Given that these amino acids are present in the overall protein composition in whey, the enhancing effect of the whey proteins on iron and zinc Caco-2 cell uptake provides more evidence as to the so-called 'meat-factor. The enhancing effect of the whey proteins could be attributed to the chemical reduction of iron by the sulphur-containing amino acids that act in a very similar manner to ascorbate, which is a well-known iron absorption enhancer, and it has been found to stimulate iron uptake (Kim et al., 2011).

A study by Cámara et al. (2007) and Jovaní et al. (2001) reported that meals with increased protein content increased the uptake of iron and zinc. However, it is worth mentioning that these studies are based on meals in which there does not seem to be a consensus on the best experimental approach for assessing mineral availability when taken alongside meals. While single meal experiments may not be reflective of a real-life situation, long-term studies may be more realistic, but they are more challenging to control. Also, differences in the iron status of the subjects, variability in the phytate content of the meals or other metal uptake inhibitors and choice of food preparation needs to be considered.

Other authors have documented the potential enhancing effects of whey proteins on iron and zinc bioavailability (Gandhi, Devi, et al., 2019; Nakano et al., 2007). In a study by Gandhi et al. (2019), iron was 80% more bioavailable in rats fed with microencapsulated iron in whey proteins compared to the control group, in which only 37% of iron remained bioavailable. The iron content of the WPC-Fe complex was estimated as 11.04 ± 0.22 mg of the powder, although not confirmed experimentally. In comparison, the microencapsulated iron developed in this thesis project contains between 5.1 – 10 mg/g powder and iron was absorbed 73% more in the Caco-2 cells when present along with whey proteins. than the control sample. In a similar study by Nakano et al. (2007), they assessed the bioavailability of iron-fortified whey protein concentrate (Fe-WPC) in rats. The hemoglobin concentration in the fed rats with Fe-WPC was 88.5% compared to 66.5% of that in rats fed the control diet. Lastly, Remondetto et al. (2004) reported that the iron in whey protein hydrogels was superior in intracellular iron absorption in the Caco-2 system.

	Initial Fe added	Retention		Transport		Uptake	
	mg/l	mg/l	%	mg/l	%	mg/l	%
Control I ($FeSO_4$)	9.39 ± 0.06	2.06 ± 0.55	21.27 ± 5.71	1.09 ± 0.05	11.25 ± 0.70	3.15 ± 0.62	32.52 ± 0.70
Control II ($FeSO_4$ + $ZnSO_4$)	9.50 ± 0.11	0.82 ± 0.14	10.89 ± 1.97	0.41 ± 0.44	5.08 ± 5.09	1.23 ± 0.28	15.97 ± 4.00
Formulation A (6% WPI, 2% Eudraguard®, 5% Fe/Zn loading)	8.88 ± 0.00	3.53 ± 0.37	61.39 ± 4.19	n.d.	n.d.	3.53 ± 0.37	61.39 ± 4.19
Formulation B (6% WPI, 2% Eudraguard®, 10% Fe/Zn loading)	19.18 ± 0.37	8.84 ± 1.59	56.07 ± 6.61	n.d.	n.d.	8.84 ± 1.59	56.07 ± 6.61
Formulation C (9% WPI, 2% Eudraguard®, 7% Fe/Zn loading)	14.65 ± 0.56	4.36 ± 0.26	56.51 ± 6.19	n.d.	n.d.	4.36 ± 0.26	56.51 ± 6.19

Mean values ± standard deviation (n = 3)

Uptake = retention + transport

n.d., not detectable

Table 3-3: Iron Retention, Transport and Uptake by Caco-2 cells

	Initial Zn added	Retention		Transport		Uptake	
	mg/l	mg/l	%	mg/l	%	mg/L	%
Control I ($ZnSO_4$)	6.59 ± 0.02	1.27 ± 0.33	17 .28 ± 4.62	0.06 ± 0.08	11.25 ± 0.70	1.33 ± 0.67	19.60 ± 4.62
Control II ($ZnSO_4$ in $FeSO_4$)	6.57 ± 0.00	0.93 ± 0.22	13.18 ± 2.83	n.d.	n.d.	0.93 ± 0.22	13.18 ± 2.83
Formulation A (6% WPI, 2% Eudraguard®, 5% Fe/Zn loading)	5.24 ± 0.41	0.06 ± 0.00	79.29 ± 1.79	n.d.	n.d.	0.06 ± 0.00	79.29 ± 1.79
Formulation B (6% WPI, 2% Eudraguard®, 10% Fe/Zn loading)	9.94 ± 0.41	0.11 ± 0.01	67.72 ± 2.40	n.d.	n.d.	0.11 ± 0.01	67.72 ± 2.40
Formulation C (9% WPI, 2% Eudraguard®, 7% Fe/Zn loading)	7.82 ± 0.17	0.07 ± 0.01	66.60 ± 0.76	n.d.	n.d.	0.07 ± 0.01	66.60 ± 0.76

Mean values ± standard deviation (n = 3)

Uptake = retention + transport

n.d., not detectable

Table 3-4: Zinc Retention, Transport and Uptake by Caco-2 cells

3.5 Conclusions

Bioaccessibility is essential for enabling a successful fortification strategy. Recently, this has been emphasized due to issues related to the inflammation of the intestinal tract when high does of poorly bioavailable iron forms are administered. Furthermore, if a fortification strategy based on microencapsulation proves that microencapsulation technique is useful for protecting the compounds of interest against other food components, this might prove useless if the compound of interest is not taken by the intestinal cells so it can be used for normal metabolic functions and processes.

In this study, most of the microcapsules released close to 100% of the iron and zinc within 30 min at pH 2.0. On the other hand, 100% iron and zinc were released after 45 minutes of intestinal digestion (pH 6.6). Thus, the microcapsules showed higher resistance to intestinal conditions. In general, Eudraguard® is a functional coating that provides resistance to gastric and intestinal conditions. While the WPI coating did not provide much protection against gastric and intestinal digestion, the whey proteins present in the coating, once broken down by the proteolytic enzymes in our stomach and intestine, provided the functional characteristic of increasing cellular uptake as shown by the results from the Caco-2 cell model. The presence of whey protein from the microcapsules increased the uptake of both iron and zinc. Iron uptake increased by 73%, while zinc uptake increased by 81% compared to free zinc and iron sulphate.

Elucidating the kinetics of release of a compound is of interest because it allows for the development of controlled-release and to measure critical physical parameters, such as the drug diffusion coefficient. The Higuchi model was found to best fit the experimental data for iron and

zinc release, suggesting a transport phenomenon governed by the diffusion process through the coating material. The results from this study shall guide technology development using proteins that could increase the gastrointestinal conditions and cellular absorption as well as understanding the complex release process into the release mechanisms of a specific material system.

Chapter 4: Prevention of Metal-Polyphenol Complex in Fortified Tea

Tea is the second most consumed beverage in the world, thus providing an opportunity for iron fortification. Its fortification with iron presents technical challenges because iron forms a blue-purple complex with polyphenols present in the tea that makes both of them unavailable for absorption. This study aims to investigate the iron-polyphenol complex formation in a gallic acid and black tea solution from previously developed microencapsulated iron in whey proteins and Eudraguard® (Chapter 2) using a previously developed spectrophotometric method. Adjustment and control of the pH is important when quantifying this complex formation. Complex formation in MES (pH 5.5, pH 6.6) and PIPES (pH 6.6, pH 7.0) buffers were compared in buffered and unbuffered gallic acid in 0.3mM ferrous sulphate solution. Iron-fortified tea using three microencapsulated formulations containing 5.1, 7.7 and 10.0 mg free iron per gram of microcapsules were assessed for their ability to avoid complex formation in black tea. Gallic acid in MES at pH 5.5 and pH 6.6 and PIPES buffer at pH 6.6 was found to be more stable than unbuffered gallic acid. After 50 minutes, more than 80% of the total iron within the microcapsules was released. Considering that tea is drunk within the first 15 minutes, between 75 to 85% of iron has complexed with polyphenols in gallic acid. In tea, iron complexes with polyphenols between 37 to 85% after 30 minutes. The use of microencapsulated iron and chelated iron sources and reducing agents is an area worth investigating for the development of iron-fortified tea. Therefore, technology developed to avoid its interaction with polyphenols in tea has the potential to reduce iron deficiency caused by inadequate iron intake through traditional diets.

4.1 Introduction

Polyphenols that are protonated have a very low affinity for divalent cations such as ferrous iron; however, when polyphenols are deprotonated, the polyphenols have a strong affinity for the cation. Among the very diverse chemical structures of polyphenols, the number of phenol rings plays a role in its affinity for the metal cation. A polyphenol with multiple attached rings have less affinity for metal cations than a polyphenol with a single phenol ring. pH also affects the affinity of the polyphenol to bind to a divalent cation. Between pH 5.0 and pH 7.0, polyphenols complex with iron in a 1:2 iron:polyphenol ratio. Complexes at this pH are blue-purple (Perron & Brumaghim, 2009). At pH < 4.0, polyphenols bind iron in a 1:1 ratio, forming complexes that are blue-green. Between pH 5.0 to 7.2, a mixture of both 1:2 and 1:3 iron:polyphenol complexes form (Perron & Brumaghim, 2009). At pH > 8 and above, the 1:3 iron:polyphenol complexes dominate, which are red (Perron & Brumaghim, 2009; Templeton, 2002). From the information above, one can see that the iron-polyphenol complex formation is more prevalent as the pH increases.

Additionally, the colour formation indicates that the amount of complex can be quantified using a spectrophotometric method. The absorption wavelength of each iron:polyphenol ratio (1:1, 1:2, 1:3) is different. At a 1:1 iron:polyphenol ratio, the complex is blue-green and absorbs at about 670 nm; at a 1:2 ratio, the complex is blue-purple and absorbs between 542 to 561 nm for gallates, or 561 to 586 nm for catecholate.; and at a 1:3 ratio the complex is red and absorbs between 490 and 520 nm. Fe^{2+} complexes of polyphenol ligands are colourless in the absence of oxygen (Perron & Brumaghim, 2009). A previously developed spectrophotometric method described the quantification of the iron-polyphenol complex (McGee & Diosady, 2018b). However, the use of buffers to maintain the pH stable during the iron-polyphenol an unknown to be investigated.

pH adjustment and control are achieved with the use of buffering compounds. However, common buffering compounds such as Tris, citrate, acetate, and phosphate salts are known to sequester metal cations (Alimentarius, 2019; Ferreira et al., 2015). If a buffer sequesters metal-cations, it could significantly influence the rate of iron and zinc complexation to the polyphenols, making the results inaccurate.

Specialized biological buffer solutions have been developed to lessen the interaction with the buffering agent and the metal cations. Among them, zwitterionic N-substituted amino sulfonic acids, usually known as Good's buffers (Table 4-1), were developed. Although widely used, some can still bind metals; therefore, the selection of a buffer that does not interact or interacts minimally with iron and zinc must be carefully considered (Ferreira, Pinto, Soares, & Soares, 2015).

Buffering Agent	**Effective pH Range**	**pKa (25ºC)**	**pKa (37ºC)**
MES	5.5 – 6.7	6.10	5.97
PIPES	6.1 – 7.5	6.76	6.66
MOPSO	6.2-7.6	6.90	6.75
MOPS	6.5-7.9	7.20	7.02

Table 4-1: Useful pH Ranges and pKa Values of some of Good's Biological Buffers with Low Metal Affinity

Modified from (Aldrich, 2020)

According to various studies, MES buffer does not interact with iron or zinc. On the other hand, MOPS and MOPSO buffer have structural similarity with MES buffer, so a similar behaviour is expected (Ferreira et al., 2015). PIPES buffer, which has a different structure than MES because it contains a piperazine ring, also shows minimal complexation with iron and zinc (Ferreira et al.,

2015). According to the analysis by Ferreira, where he used the stability constants reported in the literature and analyzed relevant metal-buffer pair interactions using a chemical speciation simulation; 14 buffers are recommended to avoid metal-buffer interactions: MES, PIPES, MOPSO, MOPS, HEPES, MOBS, HEPPSO, POPSO, EPPS, HEPBS, CHES, CAPSO, CAPS, and CABS (Ferreira et al., 2015).

The research question driving the development of this chapter is focused on determining the efficacy of the microencapsulated iron to avoid the iron-polyphenol complex formation in black tea. To the best of our knowledge, there are no previous published studies on this subject with microencapsulated iron. Additionally, given the importance of maintaining the pH stable during this reaction, MES and PIPES at different pH were tested to elucidate interactions between a buffer solution and iron-polyphenol complex formation. A decision must be made on whether to use buffer solutions or resort to the use of strong acids and bases for pH adjustment during experimentation.

4.1 Materials

Black tea was purchased from Davidson's Organic Teas (U.S.A). Ferrous sulphate and zinc sulphate heptahydrate was purchased from Fisher Scientific (U.S.A). Quantification of polyphenols was done with gallic acid purchased from Alfa Aesar (U.S.A). Folin & Ciocalteu's reagent was purchased from Merck KGaA (Germany), while the sodium carbonate solution was purchased from Fisher Scientific (U.S.A). For the pH control, MES hydrate was purchased from Alfa Aesar (U.S.A). PIPES free acid buffer was purchased from VWR Chemicals (U.S.A). Distilled and deionized water was used for all experiments.

4.2 Methods

4.2.1 Microcapsule preparation

The microencapsulated iron and zinc used in this study was prepared based on method 2.3.2 and 2.3.3 of Chapter 2. Briefly, 2% (w/v) of Eudraguard® (Evonik Industries, Switzerland) was dissolved in 200 ml of water. The mixture was heated to 90ºC for 10 minutes under agitation to allow Eudraguard® to dissolve completely. After heating, Eudraguard® was left to cool to 25ºC in ice. After 6% and 9% (w/v) of WPI (Canadian Protein, Canada) was added and left for 5 minutes under agitation. Finally, 5%, 7% and 10% of iron and zinc (w/w) based on the WPI concentration were added. The mixed solution was then left to homogenize with agitation at 300 rpm for 5 minutes before spray drying using a B-290 Büchi Mini Spray Dryer (Buchi® Labortechnik AG, Switzerland). Aspiration was maintained at 100% (35m^3/h) to maximize the separation rate of the cyclone (Büchi, 2019), and spray gas flow rate or Q-flow was set to 40mm Hg or 473 L/h. The feed pump rate was set to 6 mL/min or 20% of the feed pump rate. The inlet temperature was set at 150˚C.

4.2.2 Tea Preparation

Double distilled water was heated to boiling point (~ 100ºC) using a heated plate. The hot water was added to the tea leaves (Davidson's Organic Teas, U.S.A) in an Erlenmeyer flask. The tea leaves added were in a 1% (w/v). The mixture of tea leaves and water was gently stirred with the help of a magnetic stirrer. After 5 minutes, it was allowed to steep. Finally, the tea was poured through a strainer to separate the liquid (tea) from the tea leaves. There was ~ 1-2 g of water loss due to evaporation and some water retained in the strainer during this step. The tea was then filtered using a Whatman® No.4 filter (GE Healthcare Life Sciences, U.S.A). This method of tea

preparation is based on recommendations from distinct loose-leaf black tea manufacturers on the work of McGee and Diosady (2017).

4.2.3 Quantification of Phenolic Compounds in Black Tea

The method used for the quantification of polyphenols in brewed tea was based on the method by Chen et al. (2018). A calibration curve was prepared using gallic acid (Alfa Aesar, U.S.A) diluted to 0.1 – 1 g/L. The gallic acid was then mixed with Folin & Ciocalteu's reagent (Merck KGaA, Germany) and allowed to react for 5 minutes. After, a 7.5% sodium carbonate solution (Fisher Scientific, U.S.A) was added and then agitated. Finally, double deionized water was added to the solutions to dilute to the proper concentrations. A blank was also prepared that did not contain gallic acid. The solutions were allowed to rest for 30 minutes, and the absorbance was measured at 765 nm using an infinite M200 Pro UV-Vis spectrophotometer (Tecan, U.S.A). The concentration of phenolic compounds was reported in terms of gallic acid equivalents (GAE).

4.2.4 pH Control and Buffer Solutions

Five different pH were investigated for iron-polyphenol complex formation; pH 1.0, pH 2.0 and pH 3.0 (stomach pH), pH 5.0 (representative of the pH of tea) and pH 6.6 and pH 7 (approximation of small intestine pH). The pH was maintained using buffer solutions for pH > 5.0. Buffer solutions were prepared at a concentration of 0.4 M and then diluted to 0.2 M using a 2.2 g/L of gallic acid solution. The buffer solutions were prepared as outlined in Table 4-2.

Buffer	Effective pH buffering range	Target pH	Molarity (M)
MES hydrate	5.5 – 6.7	5.5	0.4
		6.6	0.4
PIPES free acid	6.1 – 7.5	6.6	0.4
		7.0	0.4

Table 4-2: Buffers Used to Maintain the Target pH

Once the ferrous sulphate at known concentrations (0.1-1.0 mM) was added to the buffered gallic acid (1.1 g/L), the solution was lightly shaken and left covered with aluminum foil for 30 minutes to prevent photo-degradation of the gallic acid. The solutions were then scanned from 400 to 800 nm using a spectrophotometer. Scans of polyphenol solutions that did not contain added iron were subtracted from scans of samples with added iron to account for the absorbance caused solely by the polyphenols. The same procedure was followed for another solution of gallic acid (1.1g/L) but adjusted to pH 6.6 using NaOH.

4.2.5 Iron-Polyphenol Complex Quantification in Gallic Acid and Black Tea

The method used for iron-polyphenol quantification was based on the new method developed by McGee and Diosady. In short, a calibration curve was made between 0.1 and 1.0 mM ferrous sulphate in 1.1g/L buffered (MES) gallic acid (pH 5.5). Absorbance was measured at 555nm using an infinite M200 Pro UV-Vis spectrophotometer (Tecan, U.S.A)**.** The net absorbance was calculated by subtracting the absorbance of the blank from the sample absorbance (2018b). The quantities of iron-polyphenol complex were reported as “ferrous sulphate in gallic acid equivalents” (FeS/GAE).

200 mg of microparticles were added into a plastic micromesh tea bag and then submerged in 100 ml of prepared buffered gallic acid or brewed black tea. Samples of 1 ml were taken at 5, 10, 15, 20, 25, 30, 40, 45, 50, 55 and 60 minutes. The plastic tea bag prevented from extracting the microcapsules that had not yet released the iron when obtaining the sample, thus minimizing error when quantifying the iron-polyphenol complex. Samples were immediately centrifuged at 5000 rpm and 15ºC using a Sorvall Legend X1R Centrifuge (Thermo Scientific, U.S.A). Absorbance was measured at 555nm using an infinite M200 Pro UV-Vis spectrophotometer (Tecan, U.S.A). The net absorbance was calculated by subtracting the absorbance of the blank from the sample absorbance.

4.3 Statistical Analysis

Each series of methods described represent three replicates of the experimental protocol. All data in this chapter was analyzed in Microsoft Excel (version 1908, Microsoft). Student's t-test was conducted for comparing two sets of data to determine if they were significantly different from each other. All experimental results were expressed as mean ± standard deviation.

4.4 Results and Discussion

4.4.1 Black Tea Polyphenol Concentration and pH

Polyphenol concentration and pH are expected to affect the degree of metal-polyphenol complex; therefore, it is imperative to gain a deeper understanding. Environmental factors and cultivating and processing practices also affect the polyphenol concentration present in tea products (Heimler et al., 2017; Manach et al., 2004). For example, a decrease in polyphenols content is correlated to a higher nitrogen supply in the soil, which is dependent on both the inherent properties of the soil

(geography) and either conventional, sustainable or organic practices, as well as processing methods (Heimler et al., 2017). Because of the wide variety of polyphenols present and the high number of factors that can modify their concentration in foods, no reference food-composition tables have been established, unlike for micronutrients and vitamins (Manach et al., 2004). Therefore, characterizing these two parameters can also give us insight into their variability.

Although a 3-5 minute steeping time is typical and is recommended by different tea manufacturers and is also performed in different scientific studies (*Caraway Tea*, 2020; Komes et al., 2010; Lang, 2012), tea can be brewed (steeped) for more extended periods, depending on cultural or personal preferences.

Black tea polyphenol extractions were performed at different steeping times using 1% (w/w) (Table 4-3). The amount of total polyphenols in tea leaves was found to be 1.07 ± 5.20 gGAE/L or 107.72 ± 52 mg GAE/g tea leaves after five minutes of steeping. A Canadian study found that the polyphenol concentration of black tea leaves sourced from India is 212 ± 7 mg GAE/g tea leaves (1% w/w); however, this concentration corresponds to an extraction done during one hour and using 50% N,N-dimethylformamide (DMF) aqueous solution as the extraction solvent and done four-times consecutively with the same sample (McGee, 2017). Thus, this polyphenol concentration would represent the maximum total polyphenol concentration found in the black tea leaves. A similar study using 50% N,N-dimethylformamide (DMF) aqueous solution as the extraction solvent found a total polyphenol content in black tea of 131.9 mg GAE/g tea leaves (Turkmen et al., 2006).

A study by Rechner et al. (2002) in which the polyphenol content of seven brands of UK market black tea, once brewed, were measured for total polyphenol content contained 1.14 g GAE/L after brewing for 1 minute in deionized water. Another study found the total polyphenol content of the U.K market black tea to be 0.76 g GAE/L (Lakenbrink et al., 2000). The study by Rechner et al. was performed using the same extraction solvent (deionized water) and is in close agreement with the results of this study. However, the difference in total polyphenol concentration among all these studies highlight the variability of total polyphenol concentration in tea products; thus, it is essential to characterize the tea used in this study for further testing the metal-polyphenol complex.

Table 4-3 also shows the different pH measured dependent on brewing time. A slight decrease in pH can be observed as the brewing time increases. The average pH at all brewing times (1, 5, 10, and 15 minutes) was 5.12 ± 0.11.

Brewing Time (mins)	**% (w/w)**	**mg GAE/g leaves**	**pH**
1	1	68.09 ± 2.41	5.30 ± 0.02
5	1	107.72 ± 5.20	5.12 ± 0.06
10	1	117.34 ± 0.99	5.00 ± 0.04
15	1	123.22 ± 2.34	5.09 ± 0.01

Table 4-3: Effect of Brewing Time on polyphenol content and pH

4.4.2 pH Control and Stability

Metal-polyphenol complex is known to be affected by pH (Mcdonald et al., 1996). Therefore, the pH must remain stable throughout this interaction. Control of pH can be achieved with the use of a buffer solution. Gallic acid and tea polyphenols are potent chelating agents (McGee, 2017) when present at a high concentration, as in the case of tea, the interactions between buffering agents and iron were expected to be minimal. However, it is known that some buffers such as phosphate buffer can interfere with metal chelation (Ferreira et al., 2015), therefore affecting the iron-polyphenol complex (McGee, 2017). No literature report was found on the use of MES and PIPES buffer solutions in the presence of metal cations and polyphenols. However, there is scientific evidence suggesting that these two buffers have negligent interactions with cations like iron and zinc (Ferreira et al., 2015). Therefore, this was an unknown to be investigated in gallic acid.

Buffering agents have an effective pH range to maintain the pH stable. MES and PIPES buffers were chosen to maintain the pH stable because their buffering range is within range of the pH of tea and the small intestine (Table 4-2). pH 5.5, pH 6.6, and pH 7.0 were selected for the buffer solutions. pH 5.0 is representative of the pH of the brewed tea. However, MES buffer is only useful in maintaining pH at pH 5.5, so this was selected as a representation of the pH of tea. pH 6.6 and 7.0 were chosen as the pH representative of the site of absorption of iron and zinc, the small intestine. The difference is that some authors use pH 6.6 as a pH representative of the small intestine, because the duodenum has a pH of 6.0 while the jejunum has a pH of 7.4 (average pH 6.6). For both MES and PIPES buffers, their buffering capacity is adequate at pH 6.6, so at this pH, the iron-polyphenol complex was compared. PIPES buffer is only useful in maintaining the pH at 7.0, so only this buffering agent was used at pH 7.0. Furthermore, to gain a better

understanding of how the buffer could affect the complex formation, the buffer solutions were compared to using NaOH and HCl for pH adjustment.

4.4.2.1 MES and PIPES Buffer at pH 6.6

In preliminary testing, to maintain adequate pH with the addition of ferrous sulphate and gallic acid, MES and PIPES buffer solutions both at pH 6.6 needed to be at a concentration of 0.2 M.

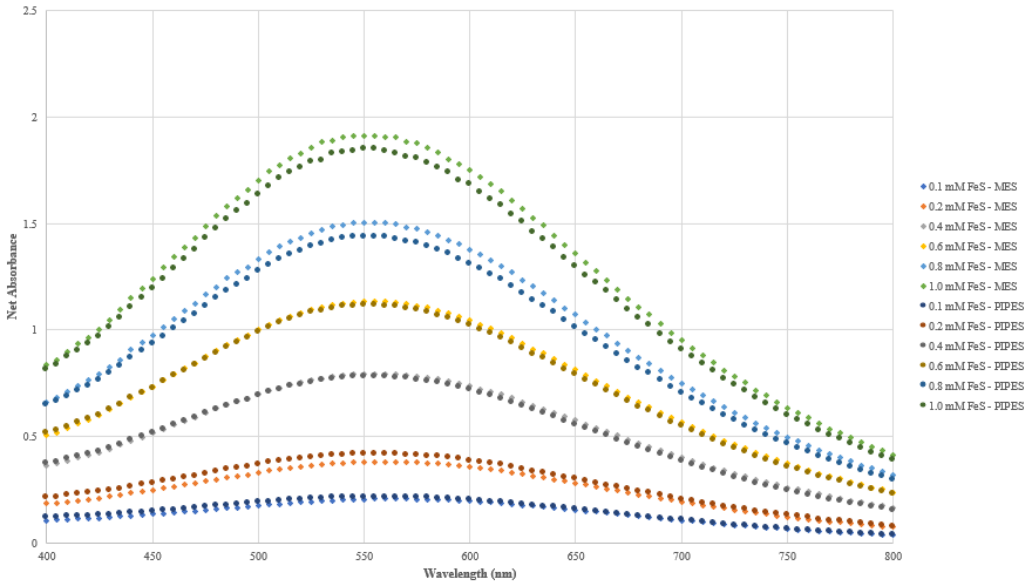

Figure 4-1: Spectrophotometric Scans of Iron Complex Formation in Gallic Acid at pH 6.6 using MES and PIPES Buffers

The wavelength of maximum absorbance for both MES and PIPES buffer at pH 6.6 is 560 nm. Table 4-4 shows the net absorbance values of MES and PIPES buffer at 560 nm. At pH 6.6. MES buffer has a slightly higher absorbance as opposed to the PIPES buffer; however, the differences in net absorbance values among the two are not significant ($p > 0.05$). Therefore, it can be assumed that MES and PIPES buffers behave similarly during the iron-polyphenol complex.

Ferrous Sulphate mM	MES pH 6.6	PIPES pH 6.6
0.1	0.2060	0.2154
0.2	0.3813	0.4179
0.4	0.7943	0.7813
0.6	1.1339	1.1147
0.8	1.5016	1.4354
1	1.9082	1.8404

Table 4-4: Absorbance Values of the Iron Complex at pH 6.6 using MES and PIPES Buffer

The absorbance of the iron polyphenol complex in gallic acid buffered with MES buffer was also compared to the absorbance of the complex formation with gallic acid adjusted to the same pH using only NaOH. At this pH, the wavelength of peak absorbance is also 560 nm; however, the amount of polyphenol complex formation was lower when the buffering agent was not used. This behaviour can be seen by the height of their respective absorbance peaks in Figure 4-2. The difference in absorption is higher as the concentration of iron increases (Table 4-5) and are significantly different ($p < 0.05$).

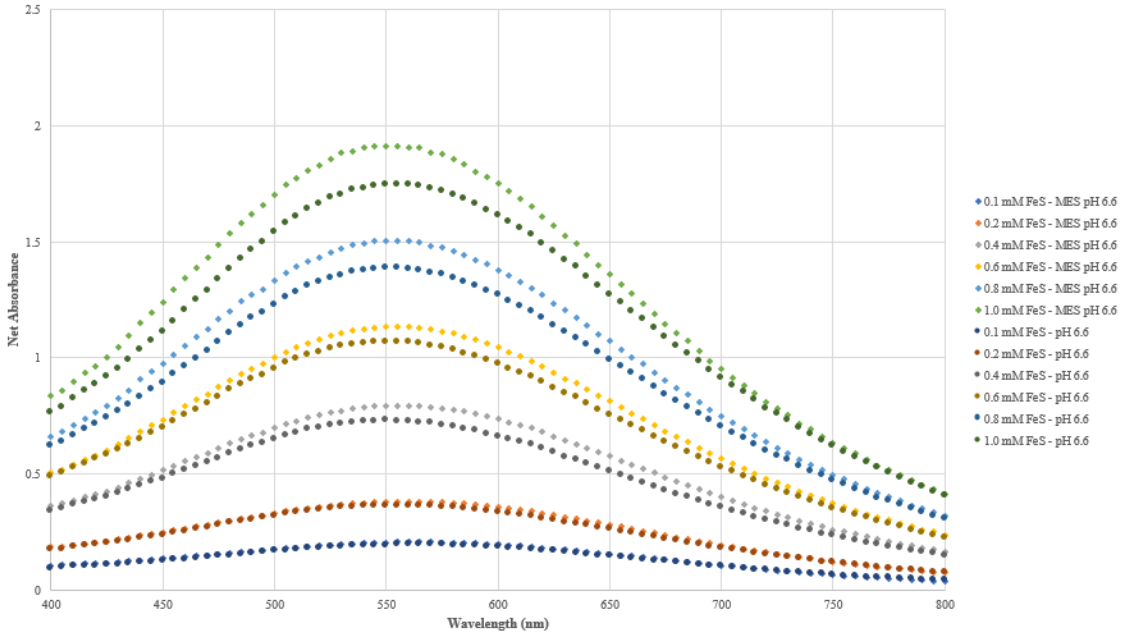

Figure 4-2: Spectrophotometric Scans of Iron Complex Formation at pH 6.6 with Buffered and Unbuffered (NaOH) Gallic Acid

Ferrous Sulphate mM	MES pH 6.6	pH 6.6
0.1	0.2060	0.1955
0.2	0.3813	0.3641
0.4	0.7943	0.7277
0.6	1.1339	1.0674
0.8	1.5016	1.3848
1	1.9082	1.7490

Table 4-5: Absorbance Values of Iron Complex Formation at pH 6.6 with Buffered and Unbuffered Gallic Acid.

4.4.2.2 MES Buffer at pH 5.5

As previously mentioned, pH 5.0 is representative of the pH of the brewed tea. Because a buffering agent that is capable of buffering around this pH is not available, MES buffer at pH 5.5 provided the closest approximation. To maintain the pH stable after the addition of ferrous sulphate and

gallic acid, the buffer solution required to have a 0.2 M concentration. Results of the absorbance scan at pH 5.5 in both buffered and unbuffered gallic acid are shown in

Figure **4-3** and Table 4-6. At this pH, in both buffered and unbuffered gallic acid, the wavelength of peak absorbance occurs at 555 nm. However, the amount of iron-polyphenol complex formation was significantly ($p < 0.05$) lower when the buffering agent was not used. The same phenomenon occurs in buffered and unbuffered gallic acid at pH 6.6 using MES and PIPES buffer.

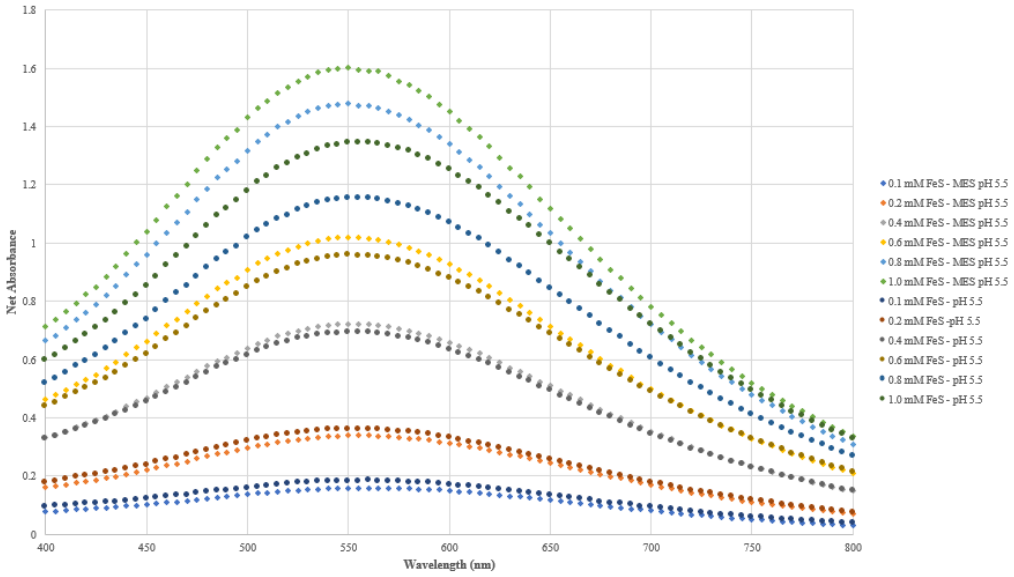

Figure 4-3: Spectrophotometric Scans of Iron Complex Formation at pH 5.5 with Buffered and Unbuffered Gallic Acid

Ferrous Sulphate mM	MES pH 5.5	pH 5.5 (NaOH)
0.1	0.1588	0.1833
0.2	0.3385	0.3614
0.4	0.7215	0.6939
0.6	1.0194	0.9578
0.8	1.4785	1.1545
1	1.6027	1.3439

Table 4-6: Absorbance Values of Iron Complex Formation at pH 5.5 with Buffered and Unbuffered Gallic Acid

4.4.2.3 PIPES Buffer at pH 7.0

The iron-polyphenol complex was also observed at pH 7.0 using buffered gallic acid in PIPES buffer and compared to the iron-gallate complex formation with unbuffered gallic acid (NaOH) at the same pH. To effectively maintain the pH stable, the PIPES buffer also had to be at a concentration of 0.2 M. Absorbance scans were also performed from 400 to 800 nm using a spectrophotometer. Results of the absorbance scan at pH 7.0 in both buffered and unbuffered gallic acid are shown in Figure 4-4 and Table 4-7. At this pH, the wavelength of maximum absorbance in buffered and unbuffered gallic acid are different. In buffered gallic acid, the wavelength of maximum absorbance is 545 nm while in unbuffered gallic acid at the same pH. The wavelength of maximum absorbance is 565 nm, which is consistent with what has been reported previously (McGee & Diosady, 2018b). The change in peak absorbance can be seen in Figure 4-4 as a shift of the absorbance curve to the left. The shift in peak absorbances could suggest a possible interaction with either iron or the gallic acid. The amount of iron-polyphenol complex formation was lower when the buffering agent was not used and is significantly different ($p < 0.05$). The same phenomenon occurs in buffered and unbuffered gallic acid at pH 5.5 and pH 6.6.

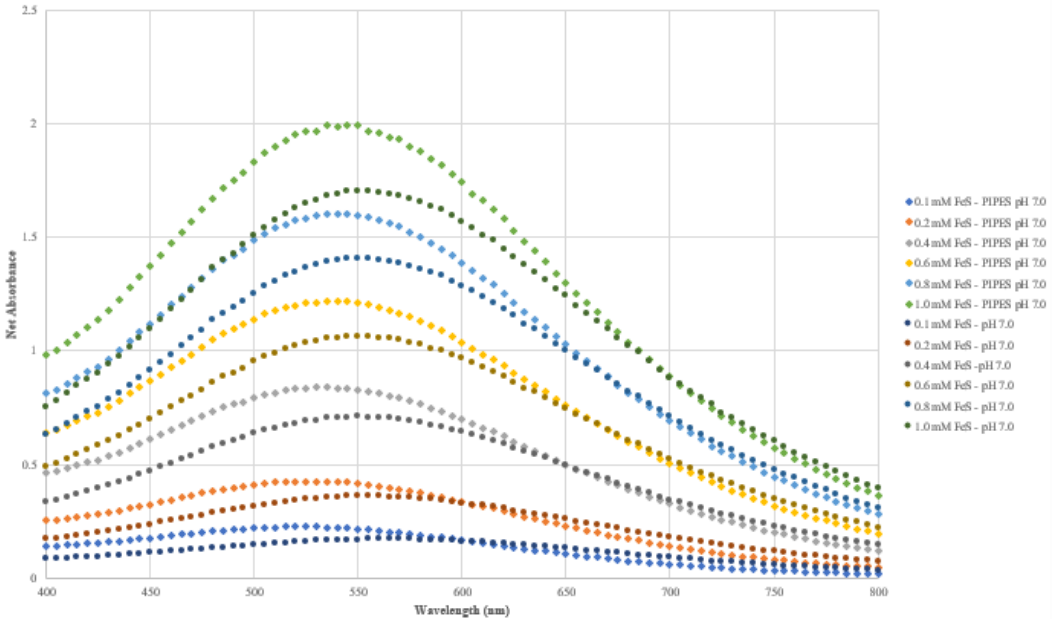

Figure 4-4: Spectrophotometric Scans of Iron Complex Formation at pH 7.0 with Buffered and Unbuffered Gallic Acid

Ferrous Sulphate mM	PIPES pH 7.0	pH 7.0
0.1	0.2077	0.1711
0.2	0.4035	0.3594
0.4	0.8127	0.7072
0.6	1.1924	1.0595
0.8	1.5772	1.4027
1	1.9627	1.6991

Table 4-7: Absorbance Values of Iron Complex Formation at pH 7.0 with Buffered and Unbuffered Gallic Acid.

4.4.2.4 pH 1, pH 2 and pH 3

Ferrous sulphate has a pH of ~ 3.85 – 4.0 at 25ºC; on the other hand, gallic acid has a pH of ~ 3.5. pH 1.0, pH 2.0 and pH 3.0 were selected as the pH representative of gastric conditions. At this low pH levels, the use of a buffering agent was not needed because no iron-polyphenol complex formation occurred in 1 g/L gallic acid with 0.1-1.0 mM ferrous sulphate. This finding agrees with

other similar published results (Dueik et al., 2017; Mcdonald et al., 1996; McGee & Diosady, 2018a)

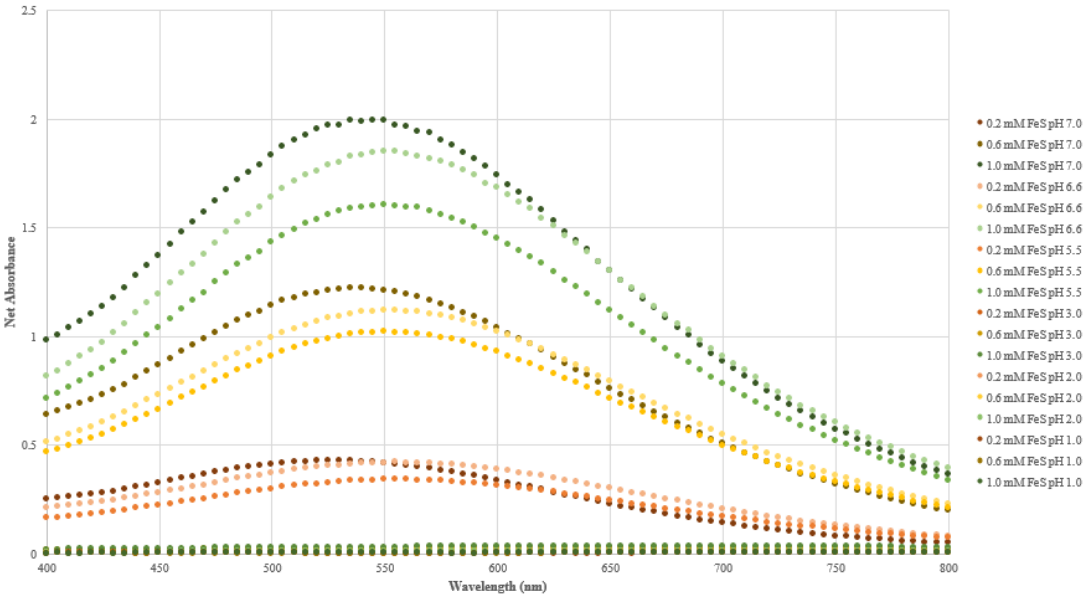

Figure 4-5 : Spectrophotometric Scans of Iron-Polyphenol Complex Formation in Gallic Acid at pH 1.0, pH 2.0, pH 3.0, pH 5.5, pH 6.6 and pH 7.0 from 0.1-1.0 mM of $FeSO_4$

4.4.3 Defining the Target Concentration for Iron and Zinc Fortified Tea

According to the research of McGee and Diosady (2018a), iron-fortified tea is set to have an iron fortification level of 0.3mM. This estimate is based on the RDA of iron and on the mean tea consumption, which is set to two cups of tea per day or 500ml of tea. The average consumption of tea per day is estimated to be 2-3 cups of tea (Scalbert & Williamson, 2000). In the UK, it is estimated that consumers have an average daily tea consumption per capita of 2.8 cups of tea (1 cup = 230 to 250 ml) containing 1% (w/w) of tea leaves (Lakenbrink et al., 2000; Rechner et al., 2009). The total tea consumption of tea can vary depending on personal habits and cultural

difference; however, according to the work of Huma et al. (2007), fortification levels of iron and zinc should be set to 20 to 40% of the RDA, to avoid overconsumption; thus, potential side effects.

The results to prove that 0.3mM of iron is an appropriate target fortification level are shown in Table 4-8 and Table 4-9 for vegetarians, according to the Health Canada guidelines. Since pregnant women are the most vulnerable group for iron deficiency, iron-fortified tea that contains 30% of the iron RDA is reasonable, which corresponds to 8.3 mg of free iron per 500 mL (2 cups) of tea consumption per day. At this proposed iron fortification level, the adult population would not receive more than 100% of the iron RDA, and the most vulnerable group (pregnant women) is way below the upper intake level of iron.

On the other hand, a zinc fortification level for tea has not been proposed. Our study proposes that zinc fortification levels in tea could be 0.12mM, which would be equivalent to 4 mg of zinc per day. This fortification level is also reasonable because it is 2.5 times the proposed fortification level of iron. The RDA of iron vs. zinc in women, which is between 18 to 20 mg of iron and 9 mg of zinc; this is 2 to 2.2 times iron vs. zinc. Table 4-10 shows the percentage of RDA based on the consumption of two cups of tea per day using a 0.12mM fortification level. At this proposed fortification level, pregnant women would receive 33% of their daily intake.

	Age (years)	mg/day	% RDA (2 cups or 500 ml of tea)
Male	14-18	11	73%
	>19	8	100%
Female	14-18	15	53%
	19-49	18	44%
	>50	8	100%
	Pregnancy	27	30%

Table 4-8: Percentage RDA Expected for Adults Drinking Two Cups of Iron Fortified Tea

	Age (years)	mg/day	% RDA (2 cups or 500 ml of tea)
Male	14-18	20	40%
	>19	14	57%
Female	14-18	27	30%
	19-49	33	24%
	>50	14	57%
	Pregnancy	49	16%

Table 4-9: Percentage RDA Expected for Vegetarian Adults Drinking Two Cups of Iron Fortified Tea

	Age (years)	mg/day	% RDA (2 cups or 500 ml of tea)
Male	14-18	11	36%
	>19	11	36%
Female	14-18	9	44%
	19-49	8	49%
	>50	8	49%
	Pregnancy	12	33%

Table 4-10: Percentage RDA Expected for Vegetarian Adults Drinking Two Cups of Zinc Fortified Tea

4.4.4 Effect of Gallic Acid Concentration on Iron Complex Formation

According to the literature, it is expected that the metal-polyphenol complex follows a first-order reaction rate (McGee, 2017; Perron et al., 2010; Perron & Brumaghim, 2009; Ryan & Hynes, 2007); therefore, polyphenol and Fe^{2+} initial concentration affect the degree of the metal-polyphenol complex formation. In other words, the reaction rate increases in proportion to increases in polyphenol concentration or Fe^{2+} concentration.

According to the results of the polyphenol concentration of black tea used in this study, black tea contains around 1.0 g GAE/L of polyphenols, which is equivalent to 6.0 mM GAE. Moreover, the defined target concentration for iron-fortified black tea is set to 0.3mM. Therefore, polyphenol is present at a molar concentration 20 times greater than iron. Taking into account these two parameters, it is expected that there is a large amount of polyphenols in black tea compared to the target amount of iron.

In this experiment, solutions of gallic acid (0.25 to 2 g/L) and ferrous sulphate (0.3 mM) were adjusted to pH 5.5 using MES buffer and scanned spectrophotometrically from 400 to 800 nm. According to the data, there is no substantial change in the maximum absorbance of the solutions (555nm) at the different concentrations of gallic acid, indicating that the amount of iron-polyphenol complex formation at all concentrations remains constant. Therefore, it can be safe to assume that results taken at 1.0 gGAE/L is representative of all practical tea polyphenol concentrations and that the iron-polyphenol complex formation measured in tea is also representative.

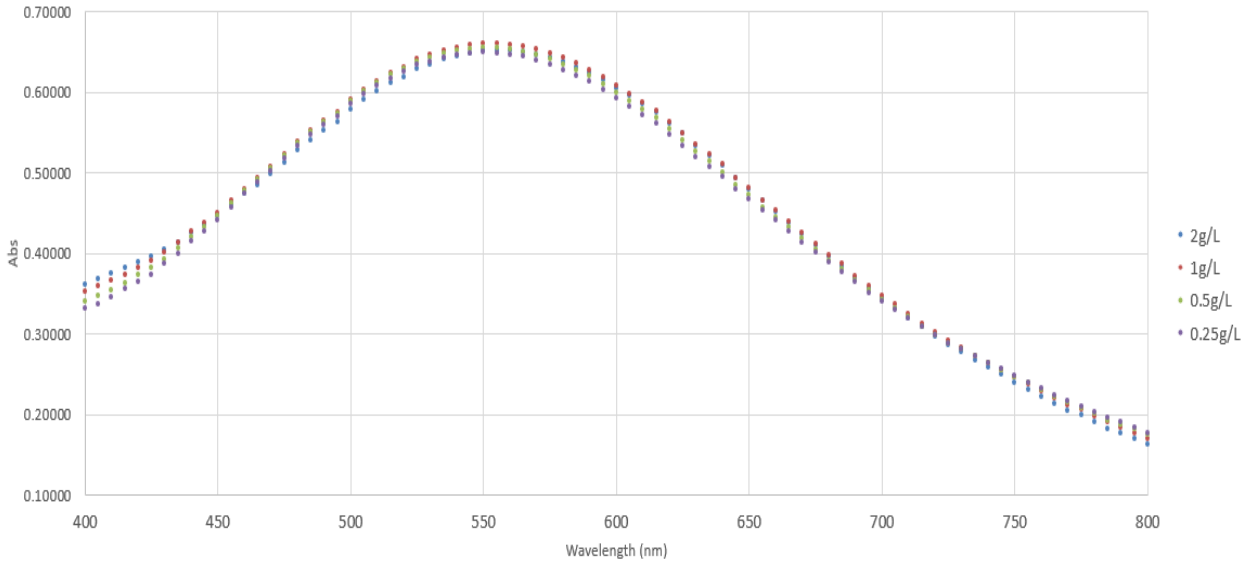

Figure 4-6: Effect of Gallic Acid Concentration on Iron Complex Formation

4.4.5 Iron-Polyphenol Complex Calibration Curves

The first iron-polyphenol complex quantification using a spectrophotometric method was developed by Brune et al. (1991). In method, tannic acid instead of gallic acid as the polyphenol standard was used. Also, ferric chloride was the iron source chose to quantify this because it has been traditionally used in a colorimetric assay to test for the presence of phenolic compounds, also known as the "ferric chloride test" (Pavia, 2005). Another study found that using tannic acid at 1g/L GAE results in precipitate formation when the iron is added, making it unsuitable for spectrophotometry quantification of the metal-polyphenol (McGee, 2017). Additionally, using gallic acid provides other advantages such as it is a simple well studied phenolic acid known to form coloured complexes with iron similar to tea polyphenols (McGee, 2017). Gallic acid is also the preferred polyphenol standard used in the Folin and Ciocalteu's phenol assay. Therefore, gallic acid was used for the iron-polyphenol complex calibration curve.

According to a previous study, spectrophotometric scans of black tea polyphenols with iron showed only a single absorbance peak. This peak corresponds to gallol complexes because the peak absorption occurs at ~578 nm as opposed to catechol complexes, which absorb at ~680 nm (BRUNE et al., 1991). Because of this, the quantification of iron-polyphenol complex in black tea or gallic acid can be done using a single wavelength (McGee & Diosady, 2018b). Evidence to support this can be found in the previous sections of this chapter, where there is a single absorbance peak at different pH. At pH 5.5, the absorbance is 555 nm, at pH 6.6 is 560 nm, and at pH 7.0, the absorbance is at 565 nm. These peak absorbance wavelengths correspond to gallic acid in MES or PIPES buffer.

4.4.6 Iron-Polyphenol Complex in Gallic Acid and Tea

Formulation A, Formulation B, and Formulation C were tested and compared on the amount of coloured iron complex formation in gallic acid and black tea at pH 5.5. When the black tea was tested at its polyphenol concentration (1.07gGAE/L) in the three optimized formulations, precipitation of the polyphenols with iron occurred (Figure 4-7). Therefore, the samples cannot be measured spectrophotometrically. Polyphenolic compounds can form more than two coordinate covalent bonds with a metal cation and thus are capable of oligomerization and polymerization (Hider et al., 2001). Precipitation likely occurred due to the polymerization of the polyphenols with iron because the polyphenols present in black tea have multiple iron-binding groups (Habeych et al., 2016). Because of this, the black tea extract was tested at a reduced polyphenol concentration of 0.107 gGAE/L, which successfully avoided polyphenol precipitation. Polyphenol precipitation did not occur at the suggested polyphenol concentration of 1.0 gGAE/L in buffered gallic acid (MES buffer).

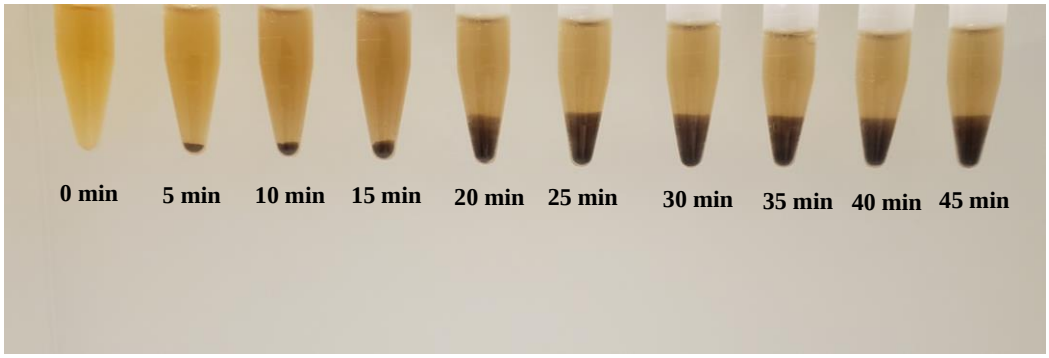

Figure 4-7: Precipitation of Polyphenols with Iron in Black Tea (1.07gGAE/L pH 5.20)

Absorbances in buffered gallic acid and black tea were recorded at 555nm every 5 minutes for 1.5 hrs at 25ºC. From the experimental data, the absorbances peaked and stayed stable after 60 minutes. Also, the microcapsules were dissolved entirely or disintegrated in the solution. Therefore, 60 minutes is the time it took for all iron to be released within the microcapsules in all formulations. A control was prepared to contain the same amount of iron and zinc present in each formulation, which was previously determined experimentally based on the methods in Chapter 2. Per 1.0 g of microcapsules, Formulation A has 5.10 mg of free iron, while Formulation B and C have 10.0 and 7.7 mg of free iron, respectively. In terms of free zinc content, Formulation A has 2.3 mg, Formulation B 4.5 mg, and Formulation C has 3.5 mg. After 60 minutes, net absorbances were very proximal to the net absorbance of the control.

After 20 minutes, more than 50% of the iron contained in all formulations was released in the gallic acid. After 50 minutes, more than 80% of the total iron within the microcapsules was released for all formulations. After 5 minutes in a buffered gallic acid solution, which is the recommended steeping time in tea beverages, 23% of iron was released from the microcapsules in

Formulation A while 20% and 17% was released from the microcapsules in Formulation B and C, respectively. On the other hand, after 5 minutes in a 0.107g/L black tea solution, 31.58% of iron was released from the microcapsules in Formulation A. 13.29%, and 13.91% of the total iron was released from Formulations A and B in black tea, respectively. After 50 minutes, more than 80% of the total iron within the microcapsules was released from all formulations. There are no significant differences ($p > 0.05$) in iron-polyphenol complex formation; therefore, the formulations show the same degree of resistance against the iron-polyphenol complex formation, regardless of composition. Graphs showing the percentage release of iron and net absorbances through time can be found in Appendix B.

Considering that tea is drunk within the first 30 minutes, between 75 to 85% of iron has complexed with polyphenols in gallic acid. In tea, iron complexes with polyphenols between 37 to 85% after 30 minutes. Thus, the results indicate that microencapsulated iron using whey proteins and Eudraguard® slows down the iron-polyphenol complex formation in the fortification of iron-fortified tea compared to free iron as ferrous sulphate.

Table 4-11 shows the amount of iron-polyphenol complex expressed in mM FeS/GAE (millimolar ferrous sulphate / gallic acid equivalents) after 30 minutes.

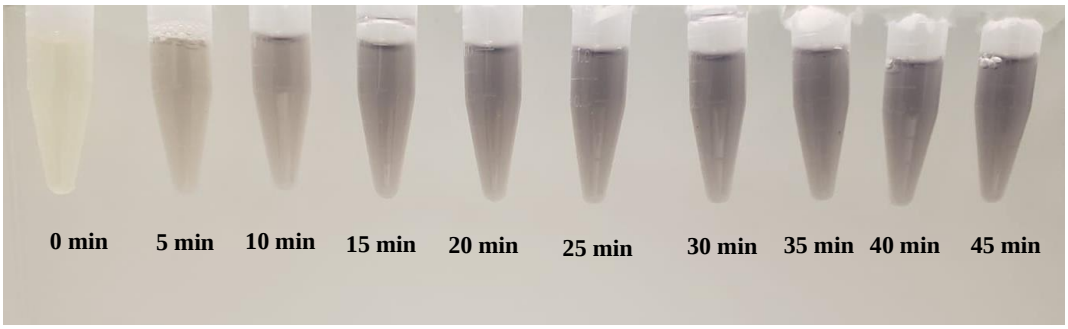

Figure 4-8: Iron-Polyphenol Complex Formation in Formulation A in Black Tea. 0.1g GAE/L, pH 5.2

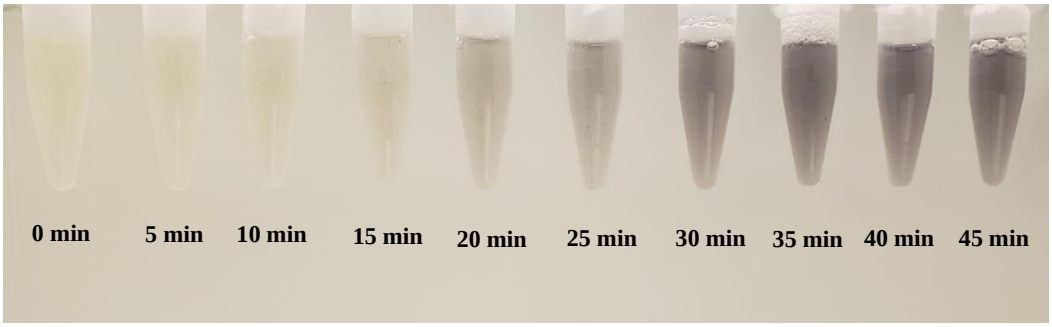

Figure 4-9: Iron-Polyphenol Complex Formation in Formulation B in Black Tea. 0.1g GAE/L pH 5.2

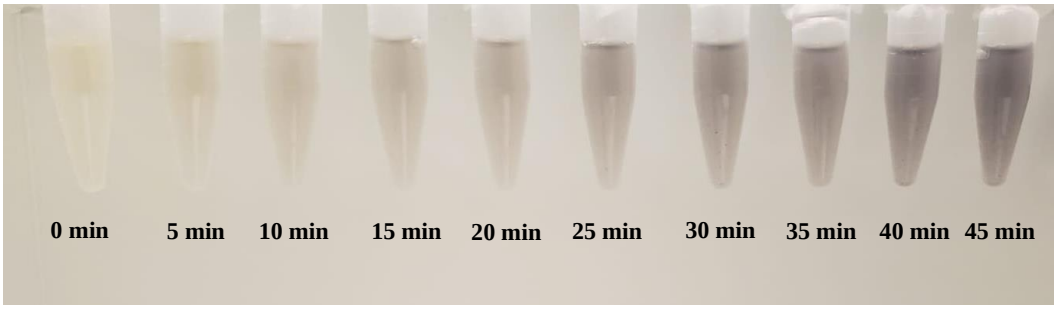

Figure 4-10: Iron-Polyphenol Complex Formation in Formulation C in Black Tea. 0.1g GAE/L pH 5.2

Microencapsulated Formulation	Phenolic Solution	pH	Iron Complex (mM FeS/GAE)
A	Gallic Acid (1 g/L)	5.5 ± 0.001	0.1662 ± 0.004
	Tea (0.107 g/L)	5.2 ± 0.012	0.1335 ± 0.009
B	Gallic Acid (1 g/L)	5.5 ± 0.001	0.3221 ± 0.002
	Tea (0.107 g/L)	5.2 ± 0.012	0.1547 ± 0.016
C	Gallic Acid (1 g/L)	5.5 ± 0.001	0.2568 ± 0.005
	Tea (0.107 g/L)	5.2 ± 0.012	0.2706 ± 0.001

Table 4-11: Comparison of Optimized Formulations on Iron-Polyphenol Complex Formation in Gallic Acid and Black Tea.

This previously developed analytical method allows for comparison of iron-polyphenol complex formation between simple polyphenolic compounds such as gallic acid and tea polyphenols (a complex system of polyphenols) at pH levels relevant to iron-fortified tea and its passage throughout the gastrointestinal tract. This method is also advantageous because it can allow comparing different iron sources for the prediction of the efficacy of different iron sources to prevent off-colour and allow for iron absorption into the body and to compare different complex prevention strategies and technologies.

The reaction of ferrous iron with a phenolic binding group such as gallol (the polyphenol group present in gallic acid (GA)) consists of (a) the deprotonation of polyphenols, (b) polyphenol binding of the first iron, (c) oxidation of the 1:1 iron-polyphenol complex, and finally (d) binding of another polyphenol to create a 1:2 iron-polyphenol complex which is purple. This reaction

requires oxygen for the autoxidation of iron. Since the gallic acid and tea solutions are exposed to air, oxygen is assumed not to be a limiting factor in this reaction; therefore, the reaction can be summarized as follows: (McGee, 2017)

$$Fe^{2+} \rightarrow [Fe(II)GA]$$

$$[Fe(II)GA] \rightarrow [Fe(III)GA]^{+}$$

Equation 4-1: Iron Autoxidation and Complexation with Gallic Acid

As this study is the first of its kind to use a microencapsulation technology to attempt to fortify tea, results can only be relatively compared to only two similar studies. In the first study, they tested ferric sodium EDTA in a 1.0 g/L gallic acid and 0.1g/ L black tea solution adjusted to pH 5.0 using NaOH. Ferric sodium EDTA formed only 5-6% of the iron-polyphenol complex that ferrous sulphate formed at the same pH. In the tea solution, 3% of the iron-polyphenol complex formed compared to ferrous sulphate at the same pH as well. (McGee & Diosady, 2018b). However, in this same study, they found that in tea extract at the expected polyphenol concentration of tea (1 gGAE/L), at pH 7, 70% of the complex formed. This observation highlights the necessity of quantifying iron-polyphenol complex formation in solutions of tea polyphenols at pH values representative of brewed tea and the site of absorption into the body as well as the importance of pH control. As previously mentioned, the reaction of polyphenols and iron is pH dependant as polyphenol groups need to be deprotonated for metal binding. As deprotonation occurs, the concentration of H^{+} increases in the system. Deprotonation of polyphenols causes the system to lower its pH. Thus, the importance of using a buffered system; otherwise, the precision of the iron-polyphenol complex might be compromised.

This study also did not provide the degree of iron-polyphenol formation overtime nor specified the time of the iron-polyphenol complex measurement. Thus, the stability of ferric sodium EDTA in gallic acid or black tea was not addressed as polyphenols are potent chelating agents. Nevertheless, chelated iron sources such as ferric sodium EDTA can prove useful to prevent iron-polyphenol complex formation by avoiding the polyphenols to attach to the iron atom; therefore, the iron remains in soluble form, enabling its proper absorption in the small intestine.

A strategy often used to prevent complex formation in iron-fortified wet foods such as tea is with the use of a competing metal that can compete for iron in the complex formation with a polyphenol (Habeych et al., 2016). Metal ions competing with the complexation of iron with polyphenols include divalent cations such as Zn^{2+}, Ca^{2+} and Mg^{2+}. The divalent cation must have a higher binding capacity than iron by increasing the concentration of the competing metal compared to iron, or the competing metal has higher binding capacity due to the innate characteristics of the metal. The binding capacity can be measured using a constant of affinity (K). Thus, if K_{MPP} is higher than K_{FePP} (Equation 4-2), where MPP is the competing metal polyphenol complex and FePP is the iron-polyphenol complex, the addition of the competing metal should be sufficient to inhibit the formation of the iron-polyphenol complex.

$$K_{MPP}[M] \gg K_{FePP}[Fe]$$

Equation 4-2

A study from Habeych et al. assessed the ability of Ca^{2+} and Mg^{2+} to prevent the iron complexation and, thus, colour changes. However, the colour formation was only observed for calcium and magnesium when concentrations were about 20 times higher. Calcium and magnesium have higher

RDAs than iron, yet for zinc, this is 2.5 times less (2016). A question arising from this study is if the zinc present with iron in the microcapsules plays a role in slowing down the complex formation. The zinc content in the microcapsules is 2.5 times less than that of iron (see section 4.4.3) because they were formulated within the established RDA requirements; therefore, it is expected that zinc does not compete for iron in the complex formation because it is present at a lower concentration. A study by Habeych et al. found that the zinc-binding constant to polyphenols is $K_{ZnPP} = 10^{12}$, while for iron-binding to polyphenols is $K_{ZnPP} = 10^{43}$. The polyphenol binding constant for iron is several magnitudes higher; therefore, the addition of zinc did not inhibit the complex formation (2016).

Another strategy to prevent complex formation is to use competing ligands to inhibit the complexation of iron with polyphenols. Similarly to Equation 4-2, the ligand competes with the polyphenols for binding. The higher the binding constant of the ligand, the less iron is complexed with polyphenols. The addition of chelating agents such as sodium gluconate, sodium citrate, tartaric acid, and disodium EDTA can also prevent the iron polyphenol complex because they can compete with polyphenol for iron. In a study by Dueik et al., the addition of disodium EDTA prevented iron-polyphenol complex formation by more than 80% in a 1:2 molar ratio (Fe:EDTA), allowing the black tea to retain an acceptable visual appearance Further increase in Fe:EDTA molar ratio did not provide a significant further reduction in complex formation. However, at a 1:1 molar ratio, only 29% of the iron-polyphenol complex was prevented. Therefore, increasing the Fe:EDTA ratio decreased the amount of iron forming the complex at the pH representative of tea (pH 5.0) (2017). The polyphenol concentration of tea used in this study was 1.87g/L.

There is a linear relationship between complex formation and bioaccessibility of iron from fortified tea. As the complex formation increases, bioaccessibility decreases. Bioavailability of iron-fortified tea in a Caco-2 cell model using 1:2 Fe:EDTA molar ratio was 62% and was significantly more bioavailable than when added with no protection (ratio 1 : 0) or at 1:1 ratio (Dueik et al., 2017).

Chelated iron sources such as ferric sodium EDTA form less iron-polyphenol complex in tea than simple and unprotected iron salts. However, ferric sodium EDTA may not be enough to prevent malabsorption because a significant amount of iron-polyphenol complex forms at pH 7 when tea extract is at a polyphenol concentration of 1 gGAE/L and ferric sodium EDTA is at a 0.3mM (McGee, 2017). On the other hand, when disodium EDTA is present at a 1:2 Fe:EDTA molar ratio, it significantly reduces complex formation, as per the results of the Caco-2 cell bioaccessibility tests with pre-simulated gastro-intestinal digestion at pH 6.5.

4.5 Conclusions

Polyphenol compounds need to be deprotonated for them to bind to iron and form a blue-purple iron-polyphenol complex that significantly decreases iron bioaccessibility. As the pH increases, the complex increases. Avoiding the formation of this complex is essential to maintain iron bioaccessible for use in the human body. MES and PIPES buffer are among the few buffering agents to be shown to have minimal interactions with iron. Gallic acid and tea polyphenols are potent chelating agents when present at a high concentration, as in the case of tea, the interactions between these buffering agents and iron are minimal. Gallic acid in MES and PIPES buffer show no change in maximum absorbance wavelength compared to gallic acid adjusted with NaOH when

tested within the effective buffering ranges of pH 5.5 and 6.6. However, the amount of polyphenol complex formation was lower when the buffering agent was not used. Therefore, MES and PIPES provide a more robust system for quantifying the iron-polyphenol complex. Iron-polyphenol complex formation does not occur below pH 3.0. The average pH of black tea at different brewing times was 5.12 ± 0.11. The newly developed method by the University of Toronto allows for iron-polyphenol complex quantification using only one wavelength that is dependent on the pH of the system. In the case of tea and gallic acid, the wavelength of absorption is 555 nM at pH 5.5. Additionally, this method allows for gallic acid to be used in the calibration curves, which allows for comparison in the literature on the iron-binding to polyphenols and future studies on iron fortification in polyphenol-rich foods.

The amount of total polyphenols in tea leaves was found to be 1.07 ± 5.20 gGAE/L or 107.72 ± 52 mg GAE/g tea leaves after five minutes of steeping. The tea source used in this study is comparatively high in polyphenol content. A suitable pH and polyphenol concentration for the representation of brewed tea was found to be pH 5.5 to allow the use of MES buffer and 1.0 gGAE/L. Per 1.0 g of microcapsules, Formulation A has 5.10 mg of free iron, while Formulation B and C have 10.0 and 7.7 mg of free iron, which is close to the proposed iron fortification level. This approach was seen to slow down the iron-polyphenol complex formation, but the addition of chelating or reducing agents might prove more useful when used along with a microencapsulation technology.

Chapter 5: Conclusion

This research is part of an integral contribution to the development of iron-fortified tea. The main objective of this thesis was an attempt to fortify black tea using microencapsulated iron and zinc and to investigate how this technology behaves in a gastrointestinal system, an *in-vitro* cell model, and a high polyphenolic beverage or solution. The main conclusions and contributions of this research are summarized as follows:

1. The development of an optimized microencapsulation containing iron and zinc using whey proteins and Eudraguard®, which are easily accessible and have GRAS status. The research question driving the development of this chapter is focused on determining the capability of these coating materials on encapsulating iron and zinc together.

1.1. The use of spray-drying technology for microencapsulation provides a robust process for microencapsulating iron and zinc. This is demonstrated by the encapsulation efficiencies corroborated experimentally using atomic absorption spectroscopy and the constant yield output of the spray-dryer.

1.2. A Box-Behnken response surface design was used to optimize encapsulation efficiency and yield of the microencapsulated iron. Response surface regression analysis determined that the amount of iron and zinc loading significantly affects encapsulation efficiency. The higher the iron and zinc loading, the lower the encapsulation efficiency. Yield is not affected because this is mainly affected by spray-drying process parameters, which were not varied in the experimental design.

1.3. Microencapsulation efficiency was optimized to above 97% encapsulation efficiency, while for zinc, this could be optimized up to 52%. The maximum yield is 73%.

1.4. The encapsulation efficiency is dependent on the inherent properties of the materials to bind iron and zinc. Iron is preferably bound to whey proteins, and this was seen experimentally. The encapsulation efficiency for iron was 50% greater than for zinc in the microcapsules. The electronegativity and atomic radius of iron and zinc could play a role in the preference of whey proteins to bind preferably to iron.

1.5. The free iron content per gram of microcapsules contained between 5.10 and 10.0 mg of iron, while free zinc ranged between 2.3 and 4.5 mg per gram.

1.6. Based on the results done using scanning electron microscopy, the size of the microcapsules varied between 1 - 20 μm. The shape of the microcapsules was spherical, with varied concavities on their surface. As the coating material increases, the microcapsules are more uniform and present fewer concavities.

1.7. Colour measurement using the HunterLab colorimeter determined that the colour of the microcapsules became browner, with more darkness (lower L* value), redness (higher a* value), and yellowness (higher b* value) as the iron loading increases. The predominant white colour of the developed microcapsules makes it very suitable for its application in salt and rice fortification.

2. The bioaccessibility in a gastrointestinal and Caco-2 cell model was assessed. The research question driving the development of chapter 3 is focused on determining the resistance of the microcapsules to gastric and small intestine conditions and in assessing the ability of whey proteins to increase bioaccessibility in an in-vitro model.

2.1. The gastrointestinal model followed a two-step approach by simulating the pH and enzymatic activity of the (1) stomach and (2) small intestine (duodenum and jejunum).

2.2. Eudraguard® showed some resistance to gastric and intestinal conditions. However, the whey proteins acting as containing material in the microcapsule made it susceptible to pancreatic and pepsin enzymatic degradation.

2.3. The microcapsules released close to 100% of iron and zinc at the stomach pH (pH 2.0) after 30 minutes. On the other hand, close to 100% of iron and zinc at the small intestine pH (pH 6.6) after 45 minutes. Thus, the microcapsules showed higher resistance to intestinal conditions.

2.5. Whey proteins have natural properties that make them capable of binding to iron and zinc. Amino acids present in the whey protein that contain carboxylic and sulphur groups are mainly involved in the mineral binding mechanism. The chelation of iron and zinc by the proteins maintains them soluble, therefore, increasing cellular uptake.

2.6. The presence of protein (whey protein) from the microcapsules increased the uptake of both iron and zinc. Iron and zinc uptake from the microcapsules were, on average, 58% ± 2.41 and 71.20% ± 5.74, respectively. The uptake of iron and zinc without the presence of whey proteins is, on average, 15.97± 4.00 and 13.18 ± 2.83, respectively. This is significantly lower than if the iron is protected and in the presence of whey proteins.

2.7. The Higuchi model was found best to fit the iron and zinc release from the microcapsules. A diffusion process governs the Higuchi model through the matrix. Therefore, increasing the amount of coating material will slow the rate of diffusion of the iron and zinc and make the microparticles more resistant to gastric and intestinal conditions. However, this may not be economically feasible.

3. The ability of the microencapsulated iron to avoid the formation of the iron-polyphenol complex was assessed in black tea. The research question driving the development of chapter 3 is focused on quantifying the iron -polyphenol complex formation in gallic acid and black tea using a newly developed spectrophotometric method developed by other authors.

3.1. Black tea polyphenol extractions were performed at different steeping times using 1% (w/w). The amount of total polyphenols in tea leaves was found to be 1.07 ± 5.20 gGAE/L or 107.72 ± 52 mg GAE/g tea leaves after five minutes of steeping. The average pH at all brewing times (1, 5, 10, and 15 minutes) was 5.12 ± 0.11.

3.2. MES and PIPES proved to be adequate buffers to use for the quantification of the iron-polyphenol complex. The formation of the iron-polyphenol complex is highly pH dependant; therefore, the use of a buffer with minimal interactions with metals is essential. The absorbance at pH 5.5 is 555nm, at pH 6.6 is 560nm, and at pH 7.0 is 565 nm. Iron-polyphenol complex formation does not occur at pH below 3.0.

3.3. The use of MES and PIPES buffers can be used and provide a more robust calibration curve for quantifying the iron-polyphenol complex. This is demonstrated by the high correlation between absorbance and iron concentration. However, careful attention needs to be assessed when the pH is higher than 6.6 because there is a shift in band peak absorption. This occurred with PIPES buffer pH 7.0.

3.4. A proposed iron fortification level for iron-fortified has been previously proposed at 0.3mM, which corresponds to 8.3 mg of free iron per 500 mL (2 cups) of tea consumption per day. Our study proposes a zinc fortification level of 0.12mM, which would be equivalent to 4 mg of zinc per day. This is 2.5 times less than iron. This fortification level seems reasonable because the

RDA of iron vs. zinc in women, which is between 18 to 20 mg of iron and 9 mg of zinc, is 2 to 2.2 times iron vs. zinc.

3.5. The microcapsules showed a slow-down in iron-polyphenol complex formation. Considering that tea is drunk within the first 30 minutes, between 75 to 85% of iron has complexed with polyphenols in gallic acid. In tea, iron complexes with polyphenols between 37 to 85% after 30 minutes.

5.1 Recommendations and Future Research Directions

This work was mainly focused on the attempt to develop iron and zinc fortified tea using spray-drying microencapsulation technology. My recommendations are focused on two perspectives. The first is focused on suggestions solely for the advancement of scientific knowledge related to iron- and zinc polyphenol chemistry for the development of better technologies for tea fortification. The second is focused on different technology applications to further the development of iron-fortified tea

Based on extensive scientific studies, some buffers can chelate metal cations like iron. When quantifying the iron-polyphenol complex, a buffering agent could disrupt the system, making the results unprecise. A more comprehensive study of the effect of different buffer solutions, including MES and PIPES buffers on iron-polyphenol complex formation, would be beneficial. Kinetic studies on buffer binding constants to metal cations are recommended. Kinetic studies could allow for the development of equilibrium models at different pH, iron sources, and iron concentrations. This could allow for prediction in high polyphenol containing foods and provide a deeper understanding of the extent of iron-polyphenol complex formation in foods.

Further bioaccessibility studies of iron and zinc fortified tea in a Caco-2 cell permeability testing and *in-vivo* testing should be conducted for a more thorough understanding of how whey proteins can increase iron and zinc absorption. Metal-binding to food components such as amino acids, peptides, and proteins can be monitored by isothermal titration calorimetry through direct measurement of heat changes during the binding reaction. Furthermore, a standard method and gastrointestinal fluid composition for assessing gastrointestinal bioaccessibility would be beneficial. The non-standardized protocols on how to perform gastric and intestinal modelling cause results not to be directly comparable with what has been reported in the literature.

Other fortification approaches for fortifying tea should be explored. Research into other coating materials that remain soluble and resist gastrointestinal conditions is worth considering. Chelated iron sources could prove beneficial for fortifying tea because it impedes the polyphenols from binding to iron and zinc, making them unavailable for absorption. Reducing agents such as ascorbate act in a similar manner. Ascorbate has been seen in literature to increase significantly iron absorption in highly chelating foods. Ascorbate is a vitamin, so it would add additional health benefits, and is GRAS. I suggest that further research is focused on determining the amount of sodium ascorbate that would be necessary to improve bioavailability. Furthermore, there can be synergistic effects among reducing and chelating agents. The investigation into potential synergistic effects of ascorbate and EDTA in preventing iron-polyphenol complex formation may lower production cost, stability of metal cations in tea, and acceptance by consumers.

Food fortification is only useful if the affected population accepts the fortified food. Tea is a complex system with great potential for consumer acceptance and distribution throughout the world. If a successful fortification technology is developed and more knowledge is discovered regarding the interaction of polyphenols with metal cations, the technique developed for the prevention of iron-polyphenol complex formation is expected to be easily adaptable to other high polyphenol beverages. The results of this thesis have the potential to guide the path to achieve an ultimate goal; reduce deaths and the prevalence of medical conditions caused by iron and zinc deficiencies through food fortification.

References

Abbasi, S., & Azari, S. (2011). Efficiency of novel iron microencapsulation techniques: Fortification of milk. *International Journal of Food Science and Technology*, *46*(9), 1927–1933. https://doi.org/10.1111/j.1365-2621.2011.02703.x

Acosta, E. (2009). Bioavailability of nanoparticles in nutrient and nutraceutical delivery. In *Current Opinion in Colloid and Interface Science* (Vol. 14, Issue 1, pp. 3–15). Elsevier. https://doi.org/10.1016/j.cocis.2008.01.002

Akhtar, S., Anjum, F. M., & Anjum, M. A. (2011). Micronutrient fortification of wheat flour: Recent development and strategies. *Food Research International*, *44*(3), 652–659. https://doi.org/10.1016/J.FOODRES.2010.12.033

Aldrich, S. (2020). *Buffer Reference Center | Sigma-Aldrich*. https://www.sigmaaldrich.com/life-science/core-bioreagents/biological-buffers/learning-center/buffer-reference-center.html

Alimentarius, C. (2019). *Food Additive Functional Classes*. http://www.fao.org/gsfaonline/reference/techfuncs.html

Allen, L., Benoist, B. De, Dary, O., & Hurrell, R. (2006). Guidelines on food fortification with micronutrients. *World Health Organization and Food and Agriculture Organization of the United Nations*. http://www.unscn.org/layout/modules/resources/files/fortification_eng.pdf

Ba, D., & Boyaci, I. H. (2007). Modeling and optimization i: Usability of response surface methodology. *Journal of Food Engineering*, *78*(3), 836–845. https://doi.org/10.1016/j.jfoodeng.2005.11.024

Barbosa, J., Conway, B., & Merchant, H. (2017). Going Natural: Using polymers from nature for gastroresistant applications. *British Journal of Pharmacy*, *2*(1), 14–30. https://doi.org/10.5920/bjpharm.2017.01

Benz, E., Berliner, N., & Schiffman, F. (Eds.). (2018). *Anemia*. https://books.google.ca/books?hl=en&lr=&id=HzdgDwAAQBAJ&oi=fnd&pg=PA39&dq=iron+in+the+human+body&ots=1r3Mk97d8I&sig=Ld8uKeixinG9jMtnMhL1KdfRBm0#v=onepage&q=iron in the human body&f=false

Blanco-Rojo, R., & Vaquero, M. P. (2019). Iron bioavailability from food fortification to precision nutrition. A review. *Innovative Food Science & Emerging Technologies*, *51*, 126–138. https://doi.org/10.1016/J.IFSET.2018.04.015

Branca, F., Mahy, L., & Mustafa, T. S. (2014). The lack of progress in reducing anaemia among women: the inconvenient truth. *Bulletin of the World Health Organization*, *92*(4), 231–231. https://doi.org/10.2471/blt.14.137810

Brown, K. H., Hambidge, K. M., & Ranum, P. (2010). Zinc Fortification of Cereal Flours: Current Recommendations and Research Needs. *Food and Nutrition Bulletin*, *31*(1_suppl1), S62–S74. https://doi.org/10.1177/15648265100311S106

BRUNE, M., HALLBERG, L., & SKÅNBERG, A.-B. (1991). Determination of Iron-Binding Phenolic Groups in Foods. *Journal of Food Science*, *56*(1), 128–131. https://doi.org/10.1111/j.1365-2621.1991.tb07992.x

Bryszewska, M. A., Tomás-Cobos, L., Gallego, E., Villalba, M. P., Rivera, D., Taneyo Saa, D. L., & Gianotti, A. (2019). In vitro bioaccessibility and bioavailability of iron from breads fortified with microencapsulated iron. *LWT*, *99*, 431–437. https://doi.org/10.1016/j.lwt.2018.09.071

Büchi. (2019). *B-290 Mini Spray Dryer Operation Manual 093001N en*. https://static1.buchi.com/sites/default/files/downloads/B-290_OM_en_I_0.pdf?cf595fc09d939d0eb8f2bee907c35bca8feeee47

Bürki, K., Jeon, I., Arpagaus, C., & Betz, G. (2011). New insights into respirable protein powder preparation using a nano spray dryer. *International Journal of Pharmaceutics*, *408*(1–2), 248–256. https://doi.org/10.1016/j.ijpharm.2011.02.012

Burschi, M. (2015). Mathematical models of drug release. In *Strategies to Modify the Drug Release from Pharmaceutical Systems* (pp. 63–86). Elsevier. https://doi.org/10.1016/b978-0-08-100092-2.00005-9

Butt, M. S., Imran, A., Sharif, M. K., Ahmad, R. S., Xiao, H., Imran, M., & Rsool, H. A. (2014). Black Tea Polyphenols: A Mechanistic Treatise. *Critical Reviews in Food Science and Nutrition*, *54*(8), 1002–1011. https://doi.org/10.1080/10408398.2011.623198

Cámara, F., & Amaro, M. (2003). Nutrional aspect of zinc availability. *International Journal of Food Sciences and Nutrition*, *54*(2), 143–151. https://doi.org/10.1080/0963748031000084098

Cámara, F., Barberá, R., Amaro, M. A., & Farré, R. (2007). Calcium, iron, zinc and copper transport and uptake by Caco-2 cells in school meals: Influence of protein and mineral interactions. *Food Chemistry*, *100*(3), 1085–1092. https://doi.org/10.1016/j.foodchem.2005.11.010

Caraway Tea. (2020). https://carawaytea.com/

Chen, Liang, Apostolides, Z., & Chen, Z.-M. (2013). "Global Tea Breeding." In *"Global Tea Breeding."* https://doi.org/10.1007/978-3-642-31878-8

Chen, Lingyun, Remondetto, G. E., & Subirade, M. (2006). Food protein-based materials as nutraceutical delivery systems. In *Trends in Food Science and Technology* (Vol. 17, Issue 5, pp. 272–283). Elsevier. https://doi.org/10.1016/j.tifs.2005.12.011

Chen, X. M., Ma, Z., & Kitts, D. D. (2018). Effects of processing method and age of leaves on

phytochemical profiles and bioactivity of coffee leaves. *Food Chemistry*, *249*, 143–153. https://doi.org/10.1016/j.foodchem.2017.12.073

Clegg, M. S., Keen, C. L., Lönnerdal, B., & Hurley, L. S. (1981). Influence of ashing techniques on the analysis of trace elements in animal tissue - I. Wet ashing. *Biological Trace Element Research*, *3*(2), 107–115. https://doi.org/10.1007/BF02990451

Clydesdale, F. (2016). Iron Fortification of Foods. In *Iron Fortification of Foods*. Elsevier Science. https://doi.org/10.1016/b978-0-121-77060-0.x5001-4

Crichton, R. (2016). Metal Chelation in Medicine. In *Metal Chelation in Medicine*. Royal Society of Chemistry. https://doi.org/10.1039/9781782623892

Crofton, R. W., Gvozdanovic, D., Gvozdanovic, S., Khin, C. C., Brunt, P. W., Mowat, N. A. G., & Aggett, P. J. (1989). Inorganic zinc and the intestinal absorption of ferrous iron. *American Journal of Clinical Nutrition*, *50*(1), 141–144. https://doi.org/10.1093/ajcn/50.1.141

Dary, O. (2002). Staple Food Fortification with Iron: a Multifactorial Decision. *Nutrition Reviews*, *60*(suppl_7), S34–S41. https://doi.org/10.1301/002966402320285083

Dash, S., Murthy, P., Nath, L., & Chowdury, P. (2010). *KINETIC MODELING ON DRUG RELEASE FROM CONTROLLED DRUG DELIVERY SYSTEMS*.

de Vos, P., Faas, M. M., Spasojevic, M., & Sikkema, J. (2010). Encapsulation for preservation of functionality and targeted delivery of bioactive food components. In *International Dairy Journal* (Vol. 20, Issue 4, pp. 292–302). https://doi.org/10.1016/j.idairyj.2009.11.008

Degen, L. P., & Phillips, S. F. (1996). Variability of gastrointestinal transit in healthy women and men. *Gut*, *39*, 299–305. https://doi.org/10.1136/gut.39.2.299

Demetriades, E., & Williams, T. (2016). *Compositions and methods for modified nutrient*

delivery.

Diarrassouba, F., Remondetto, G., Liang, L., Garrait, G., Beyssac, E., & Subirade, M. (2013). Effects of gastrointestinal pH conditions on the stability of the β-lactoglobulin/vitamin D3 complex and on the solubility of vitamin D3. *Food Research International*, *52*(2), 515–521. https://doi.org/10.1016/J.FOODRES.2013.02.026

Diosady, L. L., Alberti, J. O., Ramcharan, K., & Mannar, M. G. V. (2002). Iodine stability in salt double-fortified with iron and iodine. *Food and Nutrition Bulletin*, *23*(2), 196–207. https://doi.org/10.1177/156482650202300209

Disler, P. B., Lynch, S. R., Torrance, J. D., Sayers, M. H., Bothwell, T. H., & Charlton, R. W. (1975). *The mechanism of the inhibition of iron absorption by tea*. The South African Journal of Medical Sciences. https://europepmc.org/article/med/1862

Đorđević, V., Balanč, B., Belščak-Cvitanović, A., Lević, S., Trifković, K., Kalušević, A., Kostić, I., Komes, D., Bugarski, B., & Nedović, V. (2014). Trends in Encapsulation Technologies for Delivery of Food Bioactive Compounds. In *Food Engineering Reviews* (Vol. 7, Issue 4, pp. 452–490). https://doi.org/10.1007/s12393-014-9106-7

Dueik, V., Chen, B. K., & Diosady, L. L. (2017). Iron-Polyphenol Interaction Reduces Iron Bioavailability in Fortified Tea: Competing Complexation to Ensure Iron Bioavailability. *Journal of Food Quality*, *2017*, 1–7. https://doi.org/10.1155/2017/1805047

Dwyer, J. T., & Bailey, R. L. (2017). The role of fortification and dietary supplements in affluent countries: Challenges and opportunities. In *Sustainable Nutrition in a Changing World* (pp. 389–406). Springer International Publishing. https://doi.org/10.1007/978-3-319-55942-1_30

Evonik. (2018). *Nutraceutical coatings*. https://healthcare.evonik.com/product/health-care/en/products/nutritional-coatings/

Failla, M. L. (1995). Reduction of Fe(III) Is Required for Uptake of Nonheme Iron by Caco-2 Cells. *Article in Journal of Nutrition*. https://doi.org/10.1093/jn/125.5.1291

FAO. (2014). *Current Market Situation and Medium Term Outlook," in Committee on Commodity Problems Intergovernmental Group on Tea 21st Session,*. http://www.fao.org/3/a-i4480e.pdf.

FAO. (2018). *Global tea consumption and production driven by robust demand in China and India*. http://www.fao.org/news/story/en/item/1136255/icode/

Fernando, C. D., & Soysa, P. (2015). Extraction Kinetics of phytochemicals and antioxidant activity during black tea (Camellia sinensis L.) brewing. *Nutrition Journal*, *14*(1), 1–7. https://doi.org/10.1186/s12937-015-0060-x

Ferreira, C. M. H., Pinto, I. S. S., Soares, E. V., & Soares, H. M. V. M. (2015). (Un)suitability of the use of pH buffers in biological, biochemical and environmental studies and their interaction with metal ions-a review. In *RSC Advances* (Vol. 5, Issue 39, pp. 30989–31003). Royal Society of Chemistry. https://doi.org/10.1039/c4ra15453c

Foegeding, E. A., Davis, J. P., Doucet, D., & McGuffey, M. K. (2002). Advances in modifying and understanding whey protein functionality. *Trends in Food Science and Technology*, *13*(5), 151–159. https://doi.org/10.1016/S0924-2244(02)00111-5

Freire, M. C., Alexandrino, F., Marcelino, H. R., Picciani, P. H. de S., Silva, K. G. de H. e, Genre, J., Oliveira, A. G. de, & Egito, E. S. T. do. (2017). Understanding Drug Release Data through Thermodynamic Analysis. *Materials*, *10*(6), 651. https://doi.org/10.3390/ma10060651

Galanakis, C. (2017). *What is the Difference Between Bioavailability Bioaccessibility and Bioactivity of Food Components? | SciTech Connect*. Elsevier SciTech Connect.

http://scitechconnect.elsevier.com/bioavailability-bioaccessibility-bioactivity-food-components/

Galloway, G. (2017). *Ottawa still failing to provide adequate health care on reserves: report - The Globe and Mail*. The Globe and Mail. https://www.theglobeandmail.com/news/politics/ottawa-still-failing-to-provide-adequate-health-care-on-reserves-report/article33746065/

Gandhi, K., Banjare, I. S., Sao, K., Arora, S., & Pandey, V. (2019). Physicochemical Properties and Oxidative Stability of Milk Fortified with Spray Dried Whey Protein Concentrate–Iron Complex and in vitro Bioaccessibility of the Added Iron. *Food Technology and Biotechnology*, *57*(1), 0–3. https://doi.org/10.17113/ftb.57.01.19.5945

Gandhi, K., Devi, S., Gautam, P. B., Sharma, R., Mann, B., Ranvir, S., Sao, K., & Pandey, V. (2019). Enhanced bioavailability of iron from spray dried whey protein concentrate-iron (WPC-Fe)complex in anaemic and weaning conditions. *Journal of Functional Foods*, *58*, 275–281. https://doi.org/10.1016/j.jff.2019.05.008

García-Nebot, M. J., Barberá, R., & Alegría, A. (2013). Iron and zinc bioavailability in Caco-2 cells: Influence of caseinophosphopeptides. *Food Chemistry*, *138*(2–3), 1298–1303. https://doi.org/10.1016/j.foodchem.2012.10.113

Gharsallaoui, A., Roudaut, G., Chambin, O., Voilley, A., Eau, R. S., Actives, M., & Macromolécules, A. (2007). Applications of spray-drying in microencapsulation of food ingredients: An overview. *Food Research International*, *40*(9), 1107–1121. https://doi.org/10.1016/j.foodres.2007.07.004

Gibson, R. S. (2012a). A Historical Review of Progress in the Assessment of Dietary Zinc Intake as an Indicator of Population Zinc Status. *Advances in Nutrition*, *3*(6), 772–782.

https://doi.org/10.3945/an.112.002287

Gibson, R. S. (2012b). Zinc deficiency and human health: Etiology, health consequences, and future solutions. In *Plant and Soil* (Vol. 361, Issues 1–2, pp. 291–299). Springer. https://doi.org/10.1007/s11104-012-1209-4

Goud, K., Desai, H., & Park, H. J. (2005). Recent Developments in Microencapsulation of Food Ingredients. *Drying Technology*, *23*(7), 1361–1394. https://doi.org/10.1081/DRT-200063478

Gropper, S. A. S., Smith, J. L. (Professor of nutrition), & Carr, T. P. (2008). *Advanced nutrition and human metabolism*.

Habeych, E., van Kogelenberg, V., Sagalowicz, L., Michel, M., & Galaffu, N. (2016). Strategies to limit colour changes when fortifying food products with iron. *Food Research International*, *88*, 122–128. https://doi.org/10.1016/J.FOODRES.2016.05.017

Health Canada. (2006). *Dietary Reference Intakes - Canada.ca*. https://www.canada.ca/en/health-canada/services/food-nutrition/healthy-eating/dietary-reference-intakes/tables/reference-values-elements-dietary-reference-intakes-tables-2005.html

Health Canada. (2018). *Iron and Your Health | HealthLinkBC File 68c*. https://www.healthlinkbc.ca/healthlinkbc-files/iron-health

Heimler, D., Romani, A., & Ieri, F. (2017). Plant polyphenol content, soil fertilization and agricultural management: a review. In *European Food Research and Technology* (Vol. 243, Issue 7, pp. 1107–1115). Springer Verlag. https://doi.org/10.1007/s00217-016-2826-6

Hellmig, S., Von Schöning, F., Gadow, C., Katsoulis, S., Hedderich, J., Fölsch, U. R., & Stüber, E. (2006). Gastric emptying time of fluids and solids in healthy subjects determined by 13C

breath tests: influence of age, sex and body mass index. *Journal of Gastroenterology and Hepatology*, *21*(12), 1832–1838. https://doi.org/10.1111/j.1440-1746.2006.04449.x

Hider, R. C., Liu, Z. D., & Khodr, H. H. (2001). Metal chelation of polyphenols. *Methods in Enzymology*, *335*, 190–203. https://doi.org/10.1016/S0076-6879(01)35243-6

Higuchi, T. (1963). Mechanism of sustained-action medication. Theoretical analysis of rate of release of solid drugs dispersed in solid matrices. *Journal of Pharmaceutical Sciences*, *52*(12), 1145–1149. https://doi.org/10.1002/jps.2600521210

Hixson, A. W., & Crowell, J. H. (1931). Dependence of Reaction Velocity upon surface and Agitation: I—Theoretical Consideration. *Industrial and Engineering Chemistry*, *23*(8), 923–931. https://doi.org/10.1021/ie50260a018

Hooda, J., Shah, A., & Zhang, L. (2014). Heme, an essential nutrient from dietary proteins, critically impacts diverse physiological and pathological processes. In *Nutrients* (Vol. 6, Issue 3, pp. 1080–1102). MDPI AG. https://doi.org/10.3390/nu6031080

Horton, S. (2006). The Economics of Food Fortification. *The Journal of Nutrition*, *136*(4), 1068–1071. https://doi.org/10.1093/jn/136.4.1068

Huma, N., Salim-Ur-Rehman, Anjum, F. M., Murtaza, M. A., & Sheikh, M. A. (2007). Food fortification strategy - Preventing iron deficiency anemia: A review. *Critical Reviews in Food Science and Nutrition*, *47*(3), 259–265. https://doi.org/10.1080/10408390600698262

Hurrell, R. F., Reddy, M. B., Juillerat, M., & Cook, J. D. (2006). Meat Protein Fractions Enhance Nonheme Iron Absorption in Humans. *J. Nutr*, *136*, 2808–2812. https://academic.oup.com/jn/article-abstract/136/11/2808/4664211

Johnson, D. B., Kanao, T., & Hedrich, S. (2012). Redox Transformations of Iron at Extremely Low pH: Fundamental and Applied Aspects. *Frontiers in Microbiology*, *3*(MAR), 96.

https://doi.org/10.3389/fmicb.2012.00096

Jovaní, M., Barberá, R., Farré, R., & Martín De Aguilera, E. (2001). *Calcium, Iron, and Zinc Uptake from Digests of Infant Formulas by Caco-2 Cells*. https://doi.org/10.1021/jf010106t

Kim, E., Ham, S., Bradke, D., Ma, Q., & Han, O. (2011). Bioactive Dietary Polyphenolic Compounds Reduce Nonheme Iron Transport across Human Intestinal Cell Monolayers. In *J. Nutr* (Vol. 141). https://doi.org/10.3945/jn.110.134031

King, J. C., Shames, D. M., & Woodhouse, L. R. (2000). Zinc Homeostasis in Humans. *The Journal of Nutrition*, *130*(5), 1360S-1366S. https://doi.org/10.1093/jn/130.5.1360S

Komes, D., Horžić, D., Belščak, A., Ganić, K. K., & Vulić, I. (2010). Green tea preparation and its influence on the content of bioactive compounds. *Food Research International*, *43*(1), 167–176. https://doi.org/10.1016/j.foodres.2009.09.022

Krężel, A., & Maret, W. (2016). The biological inorganic chemistry of zinc ions. *Archives of Biochemistry and Biophysics*, *611*, 3–19. https://doi.org/10.1016/j.abb.2016.04.010

Krokida, M. (2018). *Thermal and Nonthermal Encapsulation Methods - Magdalini Krokida - Google Books*. CRC Press. https://books.google.ca/books?hl=en&lr=&id=YnE3DwAAQBAJ&oi=fnd&pg=PT15&dq=Common+Coating+Materials+for+Microencapsulation+in+the+Food+Industry&ots=BR9D3ugYEz&sig=jANFYtltkFgcrwAw6M8nfCIXmbs#v=onepage&q= The most commonly used wall materials &f=false

Lakenbrink, C., Lapczynski, S., Maiwald, B., & Engelhardt, U. H. (2000). Flavonoids and other polyphenols in consumer brews of tea and other caffeinated beverages. *Journal of Agricultural and Food Chemistry*, *48*(7), 2848–2852. https://doi.org/10.1021/jf9908042

Lambert, J. M., Weinbreck, F., & Kleerebezem, M. (2008). In vitro analysis of protection of the

enzyme bile salt hydrolase against enteric conditions by whey protein-gum arabic microencapsulation. *Journal of Agricultural and Food Chemistry*, *56*(18), 8360–8364. https://doi.org/10.1021/jf801068u

Lang, K. (2012). What goes into brewing an exceptional pot of tea? *CTVNews*. https://www.ctvnews.ca/what-goes-into-a-perfect-cup-of-tea-1.756946

Langenbucher, F. (1972). Letters to the Editor: Linearization of dissolution rate curves by the Weibull distribution. *Journal of Pharmacy and Pharmacology*, *24*(12), 979–981. https://doi.org/10.1111/j.2042-7158.1972.tb08930.x

Layrisse, M., Martínez-Torres, C., Leets, I., Taylor, P., & Ramírez, J. (1984). Effect of Histidine, Cysteine, Glutathione or Beef on Iron Absorption in Humans | The Journal of Nutrition | Oxford Academic. *The Journal of Nutrition*, *114*(1), 217–223. https://academic.oup.com/jn/article-abstract/114/1/217/4755529

Lei, J., Zhang, M. qiu, Huang, C. yu, Bai, L., & He, Z. hu. (2008). Effects of ascorbic acid and citric acid on iron bioavailability in an in vitro digestion/ Caco-2 cell culture model. *Journal of Southern Medical University*, *28*(10), 1743–1747.

Livney, Y. D. (2015). Nanostructured delivery systems in food: latest developments and potential future directions. *Current Opinion in Food Science*, *3*, 125–135. https://doi.org/10.1016/j.cofs.2015.06.010

Lopez, A., Cacoub, P., Macdougall, I. C., & Peyrin-Biroulet, L. (2016). Iron deficiency anaemia. *The Lancet*, *387*(10021), 907–916. https://doi.org/10.1016/S0140-6736(15)60865-0

Manach, C., Scalbert, A., Morand, C., Rémésy, C., & Jiménez, L. (2004). Polyphenols: food sources and bioavailability. In *Am J Clin Nutr* (Vol. 79). https://academic.oup.com/ajcn/article-abstract/79/5/727/4690182

Massounga Bora, A. F., Ma, S., Li, X., & Liu, L. (2018). Application of microencapsulation for the safe delivery of green tea polyphenols in food systems: Review and recent advances. In *Food Research International* (Vol. 105, pp. 241–249). Elsevier Ltd. https://doi.org/10.1016/j.foodres.2017.11.047

Maxfield, L., & Crane, J. (2019). *Zinc Deficiency*. Sampson Regional Health Center. https://www.ncbi.nlm.nih.gov/books/NBK493231/

Mayo-Wilson, E., Junior, J. A., Imdad, A., Dean, S., Chan, X. H. S., Chan, E. S., Jaswal, A., & Bhutta, Z. A. (2014). Zinc supplementation for preventing mortality, morbidity, and growth failure in children aged 6 months to 12 years of age. *Cochrane Database of Systematic Reviews*, *5*. https://doi.org/10.1002/14651858.CD009384.pub2

McClements, D. J., Decker, E. A., & Weiss, J. (2007). Emulsion-based delivery systems for lipophilic bioactive components. *Journal of Food Science*, *72*(8), R109–R124. https://doi.org/10.1111/j.1750-3841.2007.00507.x

Mcdonald, M., Mila, I., & Scalbert, A. (1996). *Precipitation of Metal Ions by Plant Polyphenols: Optimal Conditions and Origin of Precipitation*. https://pubs.acs.org/sharingguidelines

McGee, E. (2017). *Prevention of Iron-Polyphenol Complex Formation in Iron Fortified Tea*. https://search.proquest.com/docview/2011031169?pq-origsite=summon

McGee, E., & Diosady, L. L. (2018a). Prevention of iron-polyphenol complex formation by chelation in black tea. *LWT*, *89*, 756–762. https://doi.org/10.1016/j.lwt.2017.11.041

McGee, E., & Diosady, L. L. (2018b). Development of Spectrophotometric Quantification Method of Iron-Polyphenol Complex in Iron-Fortified Black Tea at Relevant pH Levels. *Food Analytical Methods*, *11*(6), 1645–1655. https://doi.org/10.1007/s12161-018-1147-8

Mehansho, H. (2006). Iron Fortification Technology Development: New Approaches. *The*

Journal of Nutrition, *136*(4), 1059–1063. https://doi.org/10.1093/jn/136.4.1059

Mellican, R. E., Mehansho, H., & Suzanne Nielsen, S. (2003). *The Role of Iron and the Factors Affecting Off-Color Development of Polyphenols*. https://doi.org/10.1021/jf020681c

Minitab. (2020). *What are individual desirability and composite desirability? - Minitab*. https://support.minitab.com/en-us/minitab/18/help-and-how-to/modeling-statistics/using-fitted-models/supporting-topics/response-optimization/what-are-individual-desirability-and-composite-desirability/

Moll, R., & Davis, B. (2017). Iron, vitamin B 12 and folate. *Medicine*, *45*(4), 198–203. https://doi.org/10.1016/j.mpmed.2017.01.007

Murugesan, R., & Orsat, V. (2012). Spray Drying for the Production of Nutraceutical Ingredients-A Review. In *Food and Bioprocess Technology* (Vol. 5, Issue 1, pp. 3–14). Springer-Verlag. https://doi.org/10.1007/s11947-011-0638-z

Nakano, T., Goto, T., Nakaji, T., & Aoki, T. (2007). Bioavailability of iron-fortified whey protein concentrate in iron-deficient rats. *Asian-Australasian Journal of Animal Sciences*, *20*(7), 1120–1126. https://doi.org/10.5713/ajas.2007.1120

Nedović, V., Kalušević, A., Manojlović, V., Petrović, T., & Bugarski, B. (2013). Encapsulation Systems in the Food Industry. In Stavros YanniotisPetros TaoukisNikolaos G. StoforosVaios T. Karathanos (Ed.), *Food Engineering Series* (pp. 229–253). Springer. https://doi.org/10.1007/978-1-4614-7906-2_13

Neufeld, L. M., Baker, S., Garrett, G. S., & Haddad, L. (2017). Coverage and Utilization in Food Fortification Programs: Critical and Neglected Areas of Evaluation. *The Journal of Nutrition*. https://doi.org/10.3945/jn.116.246157

NHS. (2020). *Zinc - Health Professional Fact Sheet*. https://ods.od.nih.gov/factsheets/Zinc-

HealthProfessional/#en2

O'Brien, K. O., & Ru, Y. (2017). Iron status of North American pregnant women: an update on longitudinal data and gaps in knowledge from the United States and Canada. *The American Journal of Clinical Nutrition*, *106*(Supplement 6), 1647S-1654S. https://doi.org/10.3945/ajcn.117.155986

Obón, J. M., Castellar, M. R., Alacid, M., & Fernández-López, J. A. (2009). Production of a red-purple food colorant from Opuntia stricta fruits by spray drying and its application in food model systems. *Journal of Food Engineering*, *90*(4), 471–479. https://doi.org/10.1016/j.jfoodeng.2008.07.013

Onsekizoglu Bagci, P., & Gunasekaran, S. (2017). Iron-encapsulated cold-set whey protein isolate gel powder – Part 1: Optimisation of preparation conditions and in vitro evaluation. *International Journal of Dairy Technology*, *70*(1), 127–136. https://doi.org/10.1111/1471-0307.12317

Paolino, D., Tudose, A., Celia, C., Di Marzio, L., Cilurzo, F., & Mircioiu, C. (2019). Mathematical models as tools to predict the release kinetic of fluorescein from lyotropic colloidal liquid crystals. *Materials*, *12*(5). https://doi.org/10.3390/ma12050693

Papadopoulou, V., Kosmidis, K., Vlachou, M., & Macheras, P. (2006). On the use of the Weibull function for the discernment of drug release mechanisms. *International Journal of Pharmaceutics*, *309*(1–2), 44–50. https://doi.org/10.1016/j.ijpharm.2005.10.044

Paul, D. R. (2011). Elaborations on the Higuchi model for drug delivery. In *International Journal of Pharmaceutics* (Vol. 418, Issue 1, pp. 13–17). Elsevier. https://doi.org/10.1016/j.ijpharm.2010.10.037

Pavia, D. L. (2005). *Introduction to Organic Laboratory Techniques: A Small Scale Approach*.

https://books.google.com/books?id=ega5c11VHvkC&pgis=1

Peña-Rosas, J. P., De-Regil, L. M., Garcia-Casal, M. N., & Dowswell, T. (2015). Daily oral iron supplementation during pregnancy. In *Cochrane Database of Systematic Reviews* (Vol. 2015, Issue 7, pp. 1–527). Europe PMC Funders. https://doi.org/10.1002/14651858.CD004736.pub5

Perron, N. R., & Brumaghim, J. L. (2009). A review of the antioxidant mechanisms of polyphenol compounds related to iron binding. *Cell Biochemistry and Biophysics*, *53*(2), 75–100. https://doi.org/10.1007/s12013-009-9043-x

Perron, N. R., Wang, H. C., Deguire, S. N., Jenkins, M., Lawson, M., & Brumaghim, J. L. (2010). *Kinetics of iron oxidation upon polyphenol binding † †*. https://doi.org/10.1039/c0dt00752h

Petry, N., Olofin, I., Hurrell, R., Boy, E., Wirth, J., Moursi, M., Donahue Angel, M., Rohner, F., Petry, N., Olofin, I., Hurrell, R. F., Boy, E., Wirth, J. P., Moursi, M., Donahue Angel, M., & Rohner, F. (2016). The Proportion of Anemia Associated with Iron Deficiency in Low, Medium, and High Human Development Index Countries: A Systematic Analysis of National Surveys. *Nutrients*, *8*(11), 693. https://doi.org/10.3390/nu8110693

Plietker, B. (2008). *Iron catalysis in organic chemistry : reactions and applications*. http://webcat2.library.ubc.ca/vwebv/holdingsInfo?bibId=3994531

Pratap-Singh, A., Siddiqui, J., & Diosady, L. L. (2018). Characterizing the pH-Dependent Release Kinetics of Food-Grade Spray Drying Encapsulated Iron Microcapsules for Food Fortification. *Food and Bioprocess Technology*, *11*(2), 435–446. https://doi.org/10.1007/s11947-017-2022-0

Preedy, V. (2013). Tea in Health and Disease Prevention. In *Tea in Health and Disease*

Prevention. Elsevier Inc. https://doi.org/10.1016/C2010-0-64948-0

Public Health Agency of Canada. (2017). *Evaluation of Health Canada's First Nations Health Facilities Program 2010-2011 to 2014-2015 - Canada.ca*. https://www.canada.ca/en/health-canada/corporate/transparency/corporate-management-reporting/evaluation/first-nations-health-facilities-program-2010-2011-2014-2015.html

Ramanathan, G. (2016). *Colorimeter vs. Spectrophotometer: What's the Difference?* Hunterlab. https://blog.hunterlab.com/blog/color-measurement-2/colorimeter-vs-spectrophotometer-knowing-the-differences-among-color-measurement-technologies/

Ramos, Ó. L., Fernandes, J. C., Silva, S. I., Pintado, M. E., & Malcata, F. X. (2012). Edible Films and Coatings from Whey Proteins: A Review on Formulation, and on Mechanical and Bioactive Properties. In *Critical Reviews in Food Science and Nutrition* (Vol. 52, Issue 6, pp. 533–552). https://doi.org/10.1080/10408398.2010.500528

Rechner, A. R., Wagner, E., Van Buren, L., Van De Put, F., Wiseman, S., & Rice-Evans, C. A. (2009). *Black Tea Represents a Major Source of Dietary Phenolics Among Regular Tea Drinkers*. https://doi.org/10.1080/1071576021000006707

Reddy, M. B., Hurrell, R. F., & Cook, J. D. (2006). Meat Consumption in a Varied Diet Marginally Influences Nonheme Iron Absorption in Normal Individuals. *Nutrient Physiology , Metabolism , and Nutrient-Nutrient Interactions, December 2005*, 576–581.

Remondetto, G. E., Beyssac, E., & Subirade, M. (2004). Iron availability from whey protein hydrogels: An in vitro study. *Journal of Agricultural and Food Chemistry*, *52*(26), 8137–8143. https://doi.org/10.1021/jf040286h

Rigon, R. T., & Zapata Noreña, C. P. (2016). Microencapsulation by spray-drying of bioactive compounds extracted from blackberry (rubus fruticosus). *Journal of Food Science and*

Technology, *53*(3), 1515–1524. https://doi.org/10.1007/s13197-015-2111-x

Ryan, P., & Hynes, M. J. (2007). The kinetics and mechanisms of the complex formation and antioxidant behaviour of the polyphenols EGCg and ECG with iron(III). *Journal of Inorganic Biochemistry*, *101*(4), 585–593. https://doi.org/10.1016/j.jinorgbio.2006.12.001

Scalbert, A., & Williamson, G. (2000). Dietary Intake and Bioavailability of Polyphenols. *J. Nutr*, *130*, 2073–2085. https://academic.oup.com/jn/article-abstract/130/8/2073S/4686322

Shilpashree, B. G., Arora, S., Kapila, S., & Sharma, V. (2018). Physicochemical characterization of mineral (iron/zinc) bound caseinate and their mineral uptake in Caco-2 cells. *Food Chemistry*, *257*, 101–111. https://doi.org/10.1016/j.foodchem.2018.02.157

Shilpashree, B. G., Arora, S., & Sharma, V. (2016). Preparation of iron/zinc bound whey protein concentrate complexes and their stability. *LWT - Food Science and Technology*, *66*, 514–522. https://doi.org/10.1016/j.lwt.2015.11.005

Shishir, M. R. I., & Chen, W. (2017). Trends of spray drying: A critical review on drying of fruit and vegetable juices. *Trends in Food Science & Technology*, *65*, 49–67. https://doi.org/10.1016/J.TIFS.2017.05.006

Singh, A., & Kitts, D. D. (2019). *In Vitro* Bioaccessibility of Tart Cherry Anthocyanins in a Health Supplement Mix Containing Mineral Clay. *Journal of Food Science*, *84*(3), 475–480. https://doi.org/10.1111/1750-3841.14455

Stoltzfus, R. J., Mullany, L., & Black, R. E. (2018). *Iron deficiency anaemia*.

Sugiarto, M., Ye, A., & Singh, H. (2009). Characterisation of binding of iron to sodium caseinate and whey protein isolate. *Food Chemistry*, *114*(3), 1007–1013. https://doi.org/10.1016/j.foodchem.2008.10.062

Tang, N., & Skibsted, L. H. (2016). Zinc bioavailability from whey. Enthalpy-entropy

compensation in protein binding. *Food Research International*, *89*, 749–755. https://doi.org/10.1016/j.foodres.2016.10.002

Taulier, N., & Chalikian, T. V. (2001). Characterization of pH-induced transitions of β-lactoglobulin: Ultrasonic, densimetric, and spectroscopic studies. *Journal of Molecular Biology*, *314*(4), 873–889. https://doi.org/10.1006/jmbi.2001.5188

Templeton, D. (2002). *Molecular and Cellular Iron Transport*. https://doi.org/10.1201/9780367800536

Turkmen, N., Sari, F., & Velioglu, Y. S. (2006). Effects of extraction solvents on concentration and antioxidant activity of black and black mate tea polyphenols determined by ferrous tartrate and Folin-Ciocalteu methods. *Food Chemistry*, *99*(4), 835–841. https://doi.org/10.1016/j.foodchem.2005.08.034

Van Der Burg-Koorevaar, M. C. D., Miret, S., & Duchateau, G. S. M. J. E. (2011). Effect of milk and brewing method on black tea catechin bioaccessibility. *Journal of Agricultural and Food Chemistry*, *59*(14), 7752–7758. https://doi.org/10.1021/jf2015232

Venkatesh Mannar, M. G., & Hurrell, R. (2018). Food Fortification in a Globalized World. In *Food Fortification in a Globalized World*. https://doi.org/10.1016/c2014-0-03835-x

Wallace, D. F. (2016). The Regulation of Iron Absorption and Homeostasis. *The Clinical Biochemist. Reviews*, *37*(2), 51–62. http://www.ncbi.nlm.nih.gov/pubmed/28303071

Whetzel, N. (2016). *Measuring Color using Hunter L, a, b versus CIE 1976 L*a*b* - AN-1005b – Hunterlab*. https://support.hunterlab.com/hc/en-us/articles/204137825-Measuring-Color-using-Hunter-L-a-b-versus-CIE-1976-L-a-b-AN-1005b

WHO. (2011). *The global prevalence of anaemia in 2011*. 1–48. www.who.int

WHO. (2018). *Childhood and maternal undernutrition*. The World Health Report.

https://www.who.int/whr/2002/chapter4/en/index3.html

WHO. (2020). *WHO guidance helps detect iron deficiency and protect brain development*. https://www.who.int/news-room/detail/20-04-2020-who-guidance-helps-detect-iron-deficiency-and-protect-brain-development

Widlansky, M. E., Duffy, S. J., Hamburg, N. M., Gokce, N., Warden, B. A., Wiseman, S., Keaney, J. F., Frei, B., & Vita, J. A. (2005). Effects of black tea consumption on plasma catechins and markers of oxidative stress and inflammation in patients with coronary artery disease. *Free Radical Biology and Medicine*, *38*(4), 499–506. https://doi.org/10.1016/J.FREERADBIOMED.2004.11.013

Xin Huang, L., Filková, I., & Mujumdar, A. (2010). Industrial Spray Drying Systems. *Handbook of Industrial Drying, Third Edition*, 191–226. https://doi.org/10.1201/9781420017618.ch10

Xiong, C., Liu, C., Pan, W., Ma, F., Xiong, C., Qi, L., Chen, F., Lu, X., Yang, J., & Zheng, L. (2015). Non-destructive determination of total polyphenols content and classification of storage periods of Iron Buddha tea using multispectral imaging system. *Food Chemistry*, *176*, 130–136. https://doi.org/10.1016/J.FOODCHEM.2014.12.057

Yamaji, S., Tennant, J., Tandy, S., Williams, M., Singh Srai, S. K., & Sharp, P. (2001). Zinc regulates the function and expression of the iron transporters DMT1 and IREG1 in human intestinal Caco-2 cells. *FEBS Letters*, *507*(2), 137–141. https://doi.org/10.1016/S0014-5793(01)02953-2

Zhang, S. Q., Yu, X. F., Zhang, H. B., Peng, N., Chen, Z. X., Cheng, Q., Zhang, X. L., Cheng, S. H., & Zhang, Y. (2018). Comparison of the Oral Absorption, Distribution, Excretion, and Bioavailability of Zinc Sulfate, Zinc Gluconate, and Zinc-Enriched Yeast in Rats. *Molecular Nutrition and Food Research*, *62*(7), 1700981.

https://doi.org/10.1002/mnfr.201700981

Zheng, Y. (2002). *Tea: Bioactivity and Therapeutic Potential* (Y. Zhen (Ed.)). Taylor & Francis.

Ziessman, H. A., Chander, A., Clarke, J. O., Ramos, A., & Wahl, R. L. (2009). The added diagnostic value of liquid gastric emptying compared with solid emptying alone. *Journal of Nuclear Medicine*, *50*(5), 726–731. https://doi.org/10.2967/jnumed.108.059790

Zijp, I. M., Korver, O., M Tijburg, L. B., & Seshadri, S. (2000). Effect of Tea and Other Dietary Factors on Iron Absorption. *Critical Reviews in Food Science and Nutrition*, *40*(5), 371–398. https://doi.org/10.1080/10408690091189194

Zijp, I. M., Korver, O., & Tijburg, L. B. M. (2000). Effect of tea and other dietary factors on iron absorption. *Critical Reviews in Food Science and Nutrition*, *40*(5), 371–398. https://doi.org/10.1080/10408690091189194

Appendices

Appendix A Development of Microencapsulated Iron and Zinc

	Coded Levels			Uncoded Levels				
RunOrder	**WPI**	**Eudraguard**	**Fe/Zn Loading**	**WPI (g)**	**Eudragard (g)**	**Fe+Zn (g)**	**Fe (g)**	**Zn (g)**
1	-1	0	1	6	8	2.4	1.71	0.69
2	0	1	1	12	12	4.8	3.43	1.37
3	0	-1	1	12	4	4.8	3.43	1.37
4	1	0	1	18	8	7.2	5.14	2.06
5	0	0	0	12	8	3	2.14	0.86
6	1	1	0	18	12	4.5	3.21	1.29
7	0	0	0	12	8	3	2.14	0.86
8	1	-1	0	18	4	4.5	3.21	1.29
9	0	0	0	12	8	3	2.14	0.86
10	-1	0	-1	6	8	0.6	0.43	0.17
11	0	-1	-1	12	4	1.2	0.86	0.34
12	-1	1	0	6	12	1.5	1.07	0.43
13	1	0	-1	18	8	1.8	1.29	0.51
14	0	1	-1	12	12	1.2	0.86	0.34
15	-1	-1	0	6	4	1.5	1.07	0.43
16	0	1	-1	12	12	1.2	0.86	0.34
17	1	-1	0	18	4	4.5	3.21	1.29
18	0	0	0	12	8	3	2.14	0.86
19	0	1	1	12	12	4.8	3.43	1.37
20	-1	0	-1	6	8	0.6	0.43	0.17
21	0	0	0	12	8	3	2.14	0.86
22	-1	1	0	6	12	1.5	1.07	0.43
23	1	0	-1	18	8	1.8	1.29	0.51
24	-1	0	1	6	8	2.4	1.71	0.69
25	0	-1	1	12	4	4.8	3.43	1.37
26	1	1	0	18	12	4.5	3.21	1.29
27	-1	-1	0	6	4	1.5	1.07	0.43
28	0	-1	-1	12	4	1.2	0.86	0.34
29	1	0	1	18	8	7.2	5.14	2.06
30	0	0	0	12	8	3	2.14	0.86

Table A-5-1: Box-Behnken Design Used to Optimize the Microencapsulation of Iron and Zinc

Appendix B Iron-Polyphenol Complex Formation of Microencapsulated Iron

B.1 Iron-Polyphenol Complex in Buffered Gallic Acid

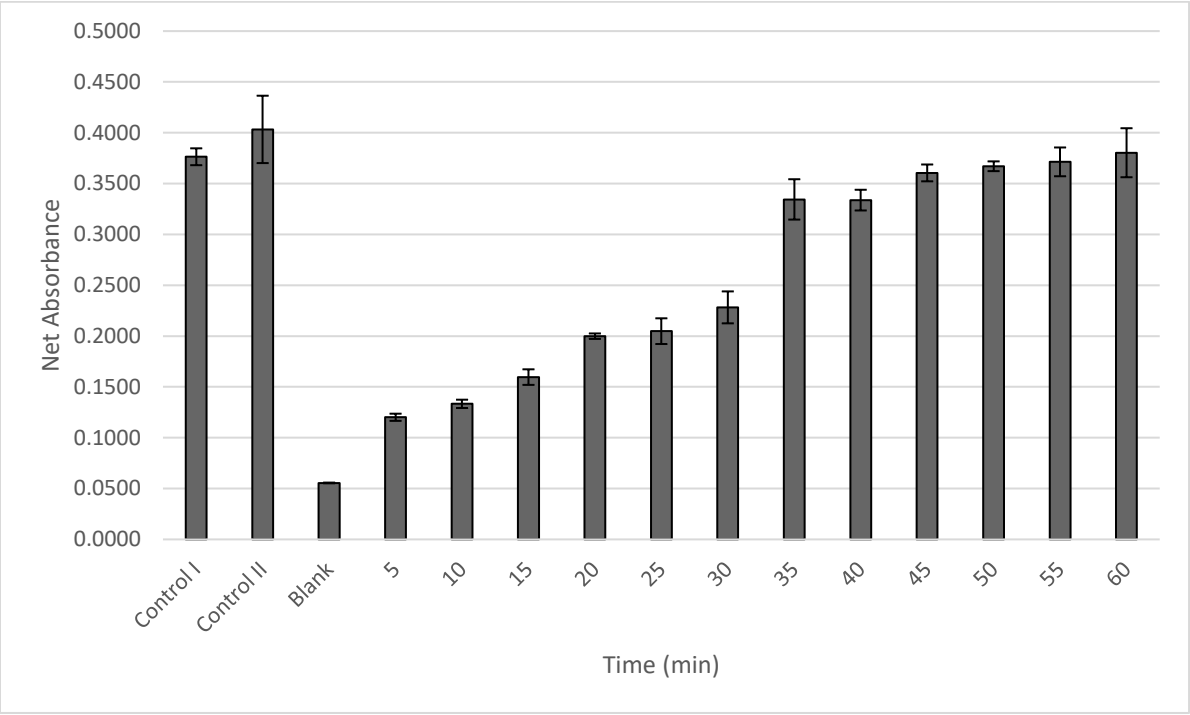

Figure B-5-1: Net Absorbances of the Iron-Polyphenol Complex Formation in Formulation A (6.2% WPI, 2% Eudraguard®, 5% Fe/Zn loading) in Buffered Gallic Acid. 555nm pH 5.5

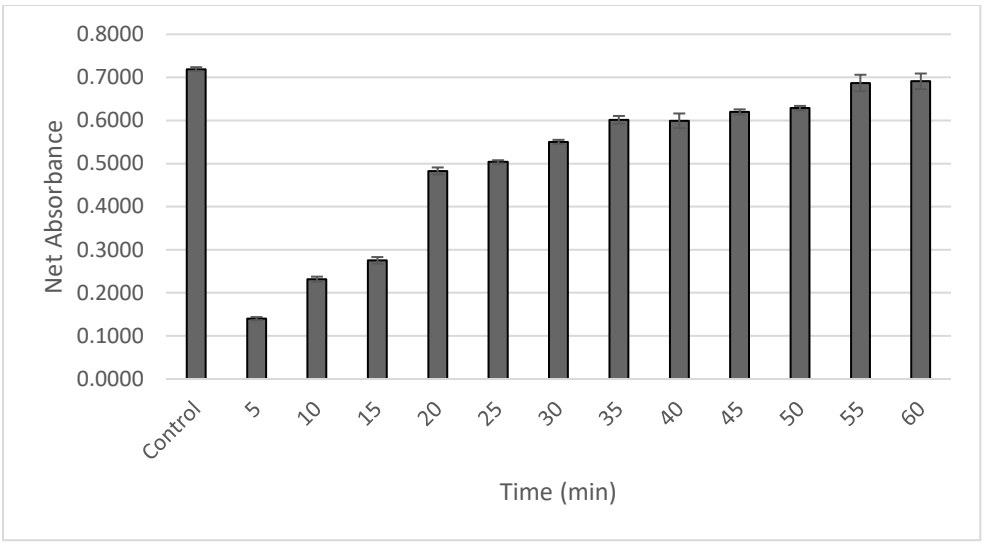

Figure B-5-2: Net Absorbances of the Iron-Polyphenol Complex Formation in Formulation B (6% WPI, 2% Eudraguard®, 10% Fe/Zn loading) in Buffered Gallic Acid. 555nm pH 5.5

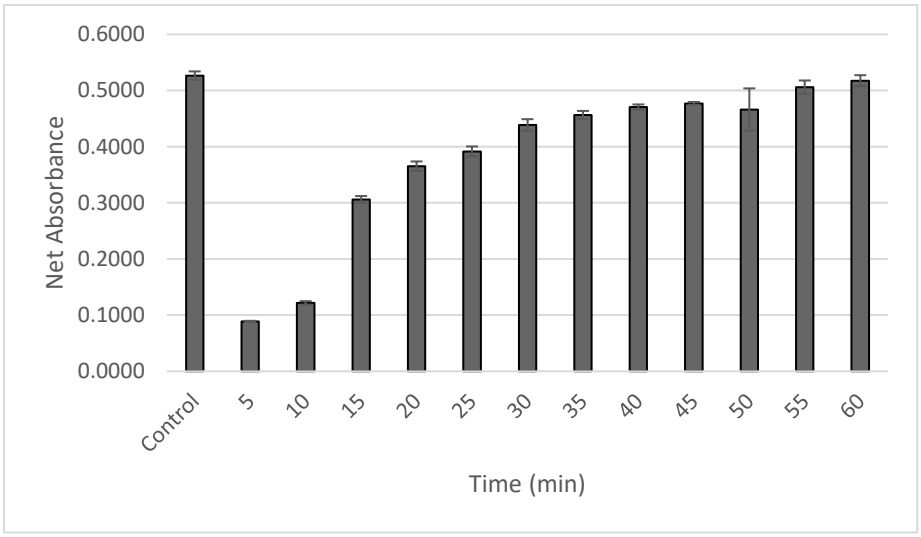

Figure B-5-3: Net Absorbances of the Iron-Polyphenol Complex Formation in Formulation C (9% WPI, 2.3% Eudraguard®, 7% Fe/Zn loading) in Buffered Gallic Acid. 555nm pH 5.5

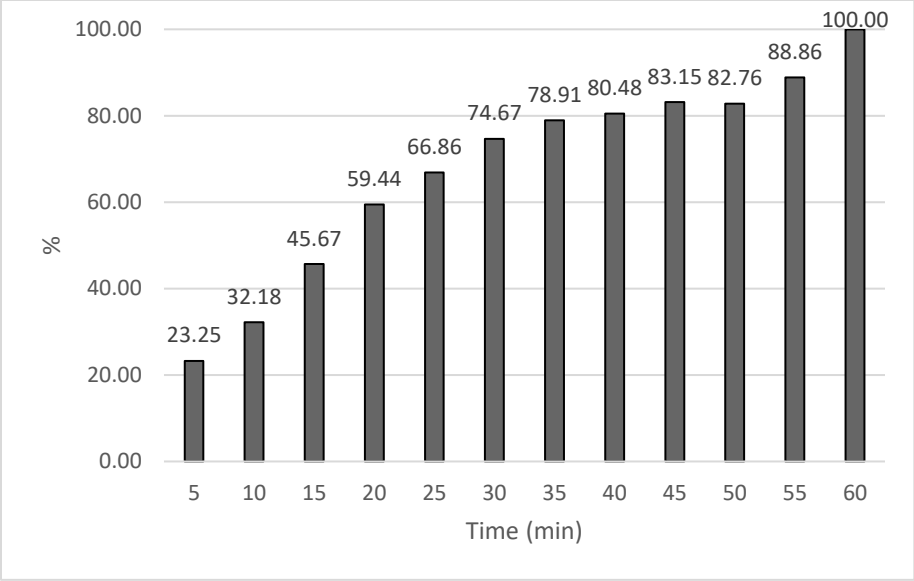

Figure B-5-4: Percentage Iron-Polyphenol Complex Formation in Formulation A (9% WPI, 2.3% Eudraguard®, 7% Fe/Zn loading) in Buffered Gallic Acid. 555nm pH 5.5

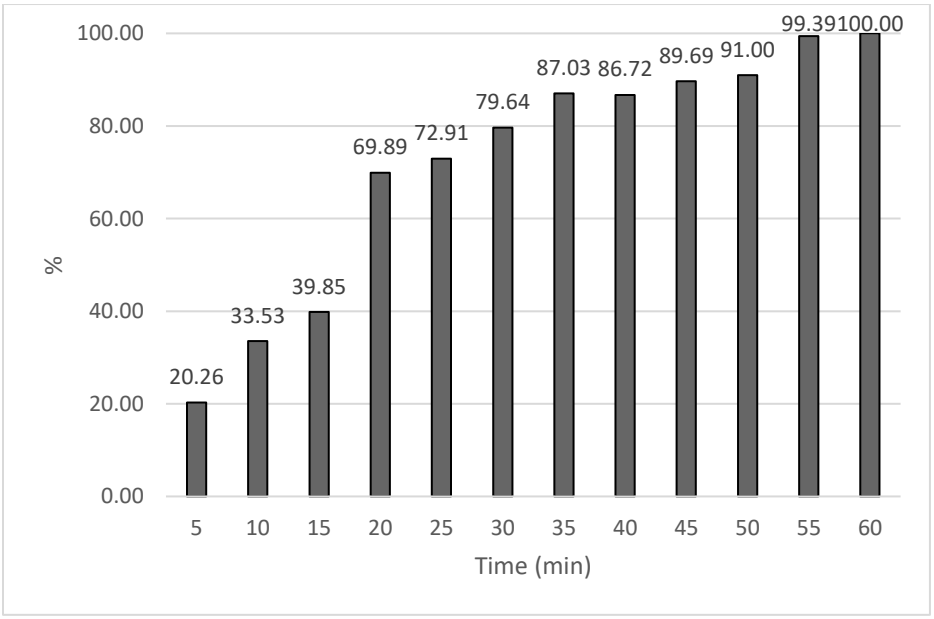

Figure B-5-5: Percentage Iron-Polyphenol Complex Formation in Formulation B (9% WPI, 2.3% Eudraguard®, 7% Fe/Zn loading) in Buffered Gallic Acid. 555nm pH 5.5

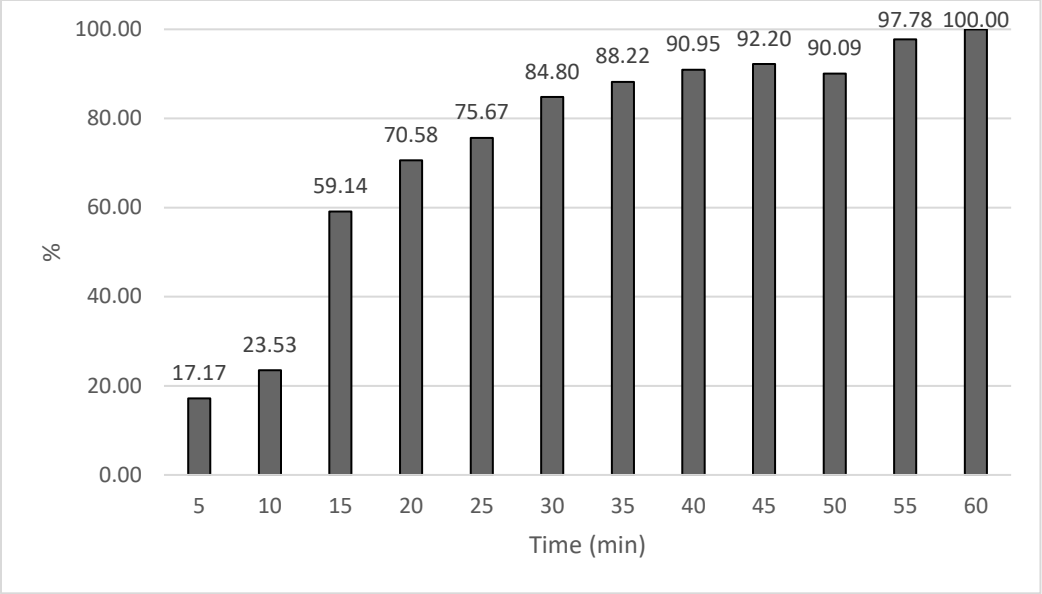

Figure B-5-6: Percentage Iron-Polyphenol Complex Formation in Formulation C (9% WPI, 2.3% Eudraguard®, 7% Fe/Zn loading) in Buffered Gallic Acid. 555nm pH 5.5

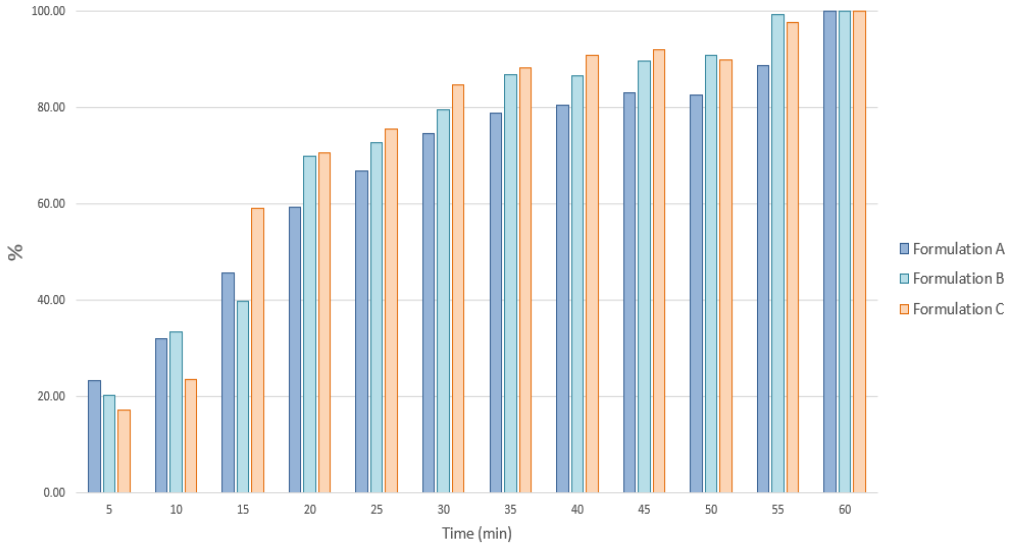

Figure B-5-7: Percentage Iron-Polyphenol Complex Formation in Formulation A, B, and C in Buffered Gallic Acid. 555nm pH 5.5

B.2 Iron-Polyphenol Complex in Black Tea

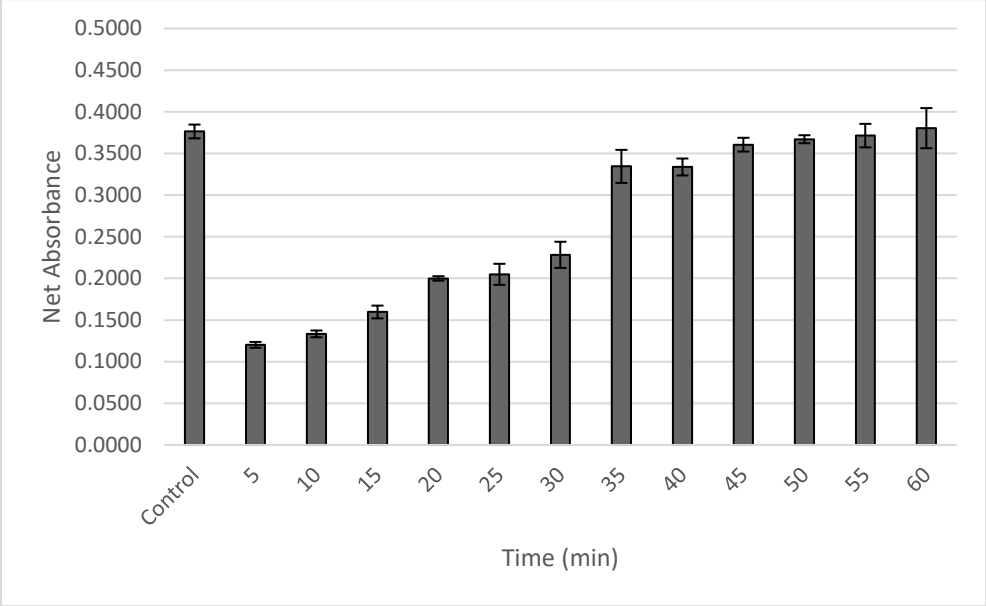

Figure B-5-8: Net Absorbances of the Iron-Polyphenol Complex Formation in Formulation A (6.2% WPI, 2% Eudraguard®, 5% Fe/Zn loading) in Black Tea. 555nm pH 5.2

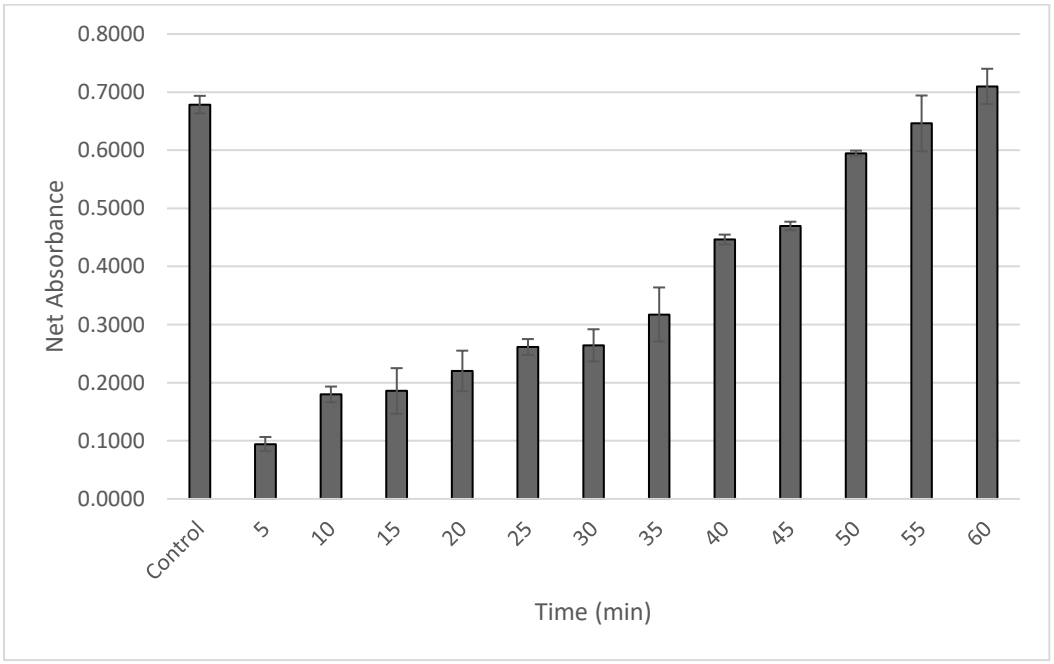

Figure B-5-9: Net Absorbances of the Iron-Polyphenol Complex Formation in Formulation B (6.2% WPI, 2% Eudraguard®, 5% Fe/Zn loading) in Black Tea. 555nm pH 5.2

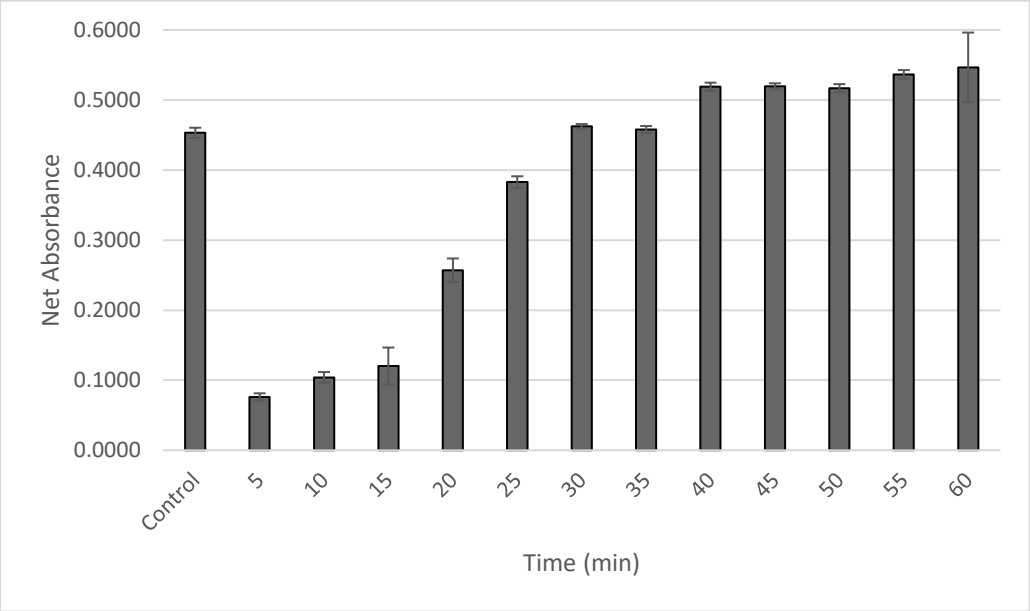

Figure B-5-10: Net Absorbances of the Iron-Polyphenol Complex Formation in Formulation C (6.2% WPI, 2% Eudraguard®, 5% Fe/Zn loading) in Black Tea. 555nm pH 5.2

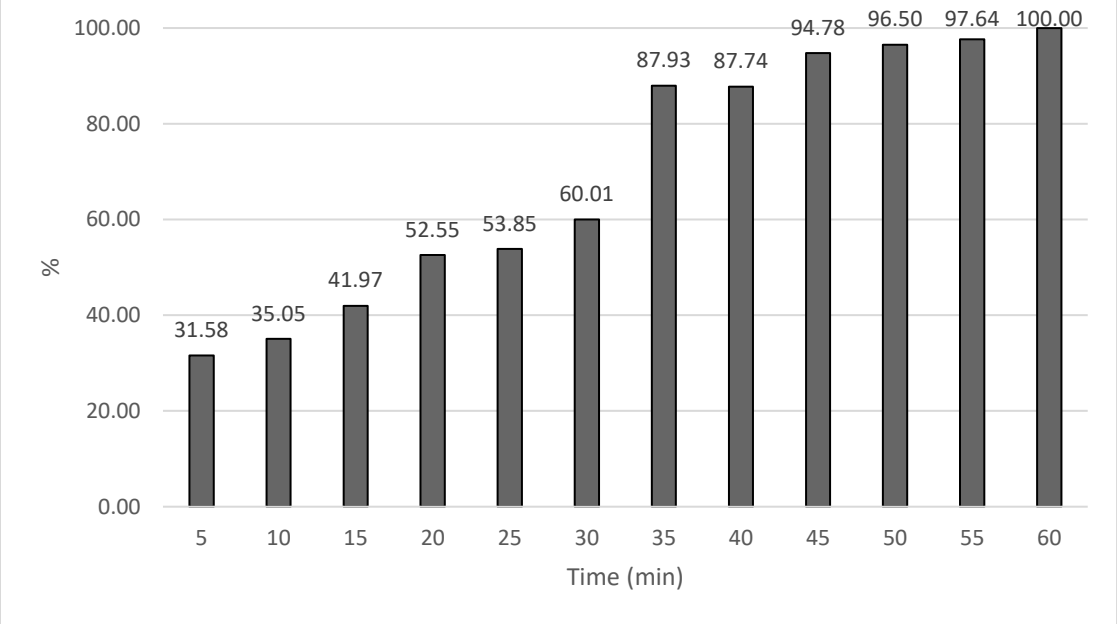

Figure B-5-11: Percentage Iron-Polyphenol Complex Formation in Formulation A (9% WPI, 2.3% Eudraguard®, 7% Fe/Zn loading) in Black Tea. 555nm pH 5.2

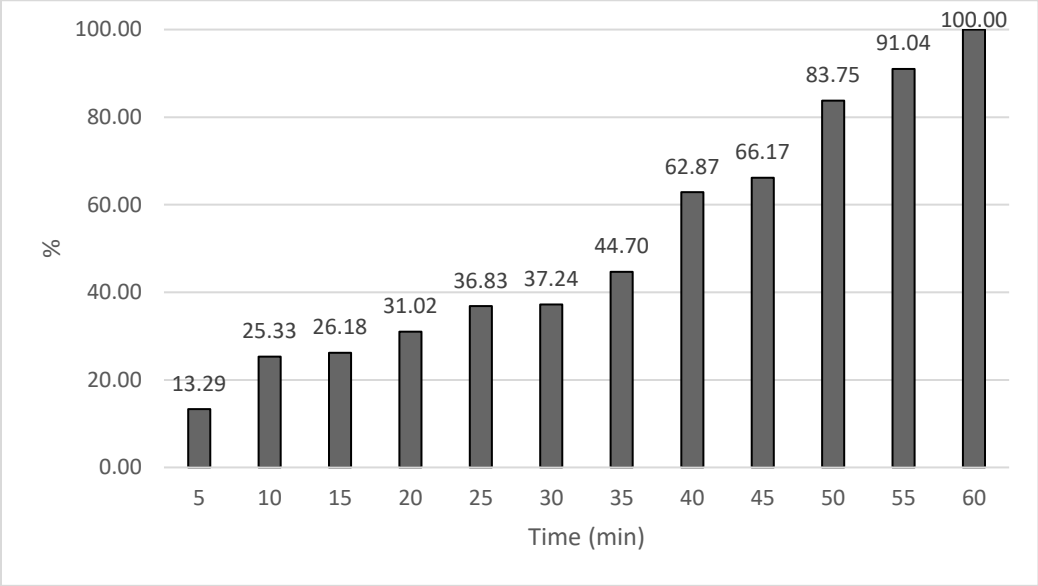

Figure B-5-12: Percentage Iron-Polyphenol Complex Formation in Formulation B (9% WPI, 2.3% Eudraguard®, 7% Fe/Zn loading) in Black Tea. 555nm pH 5.2

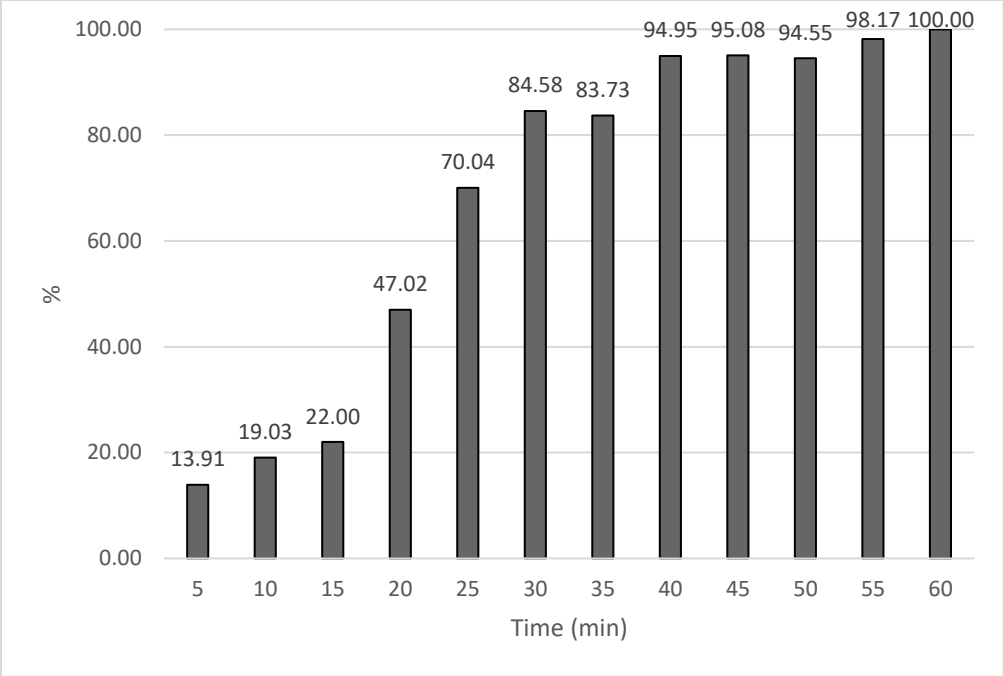

Figure B-5-13: Percentage Iron-Polyphenol Complex Formation in Formulation C (9% WPI, 2.3% Eudraguard®, 7% Fe/Zn loading) in Black Tea. 555nm pH 5.2

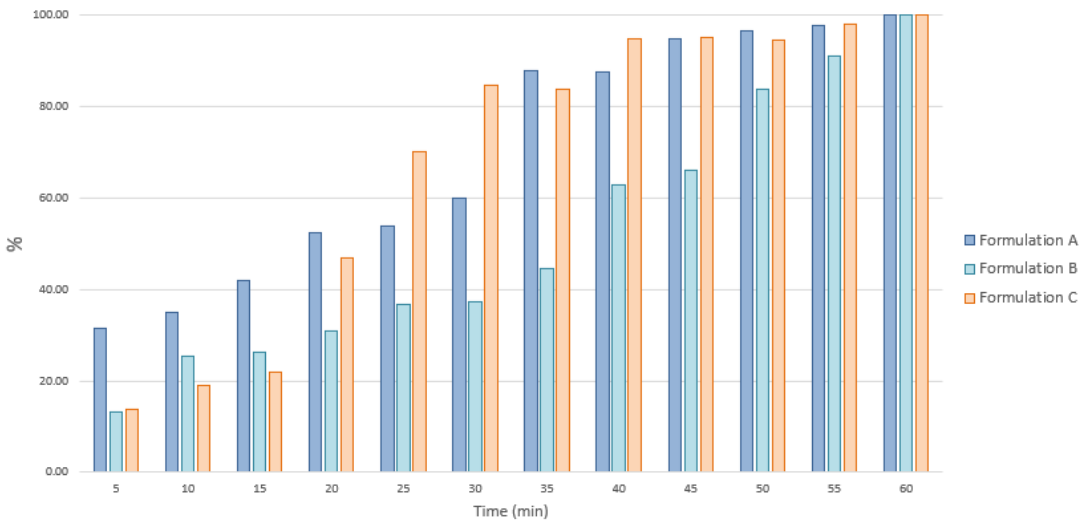

Figure B-5-14: Percentage Iron-Polyphenol Complex Formation in Formulation A, B, and C in Black Tea. 555nm pH 5.2